PERTURBATIVE QCD AND LEPTON PAIR PRODUCTION

A. N. J. J. SCHELLEKENS

PERTURBATIVE QCD AND LEPTON PAIR PRODUCTION

PROMOTOR:

PROF. DR. R. P. VAN ROYEN

PERTURBATIVE QCD AND LEPTON PAIR PRODUCTION

PROEFSCHRIFT

TER VERKRIJGING VAN DE GRAAD VAN DOCTOR IN DE WISKUNDE EN NATUURWETENSCHAPPEN AAN DE KATHOLIEKE UNIVERSITEIT TE NIJMEGEN, OP GEZAG VAN DE RECTOR MAGNIFICUS, PROF. DR. P. G. A. B. WIJDEVELD, VOLGENS BESLUIT VAN HET COLLEGE VAN DECANEN IN HET OPENBAAR TE VERDEDIGEN OP VRIJDAG 12 JUNI 1981 DES NAMIDDAGS TE 4 UUR

door

ADRIANUS NORBERTUS JACOBUS JOZEF SCHELLEKENS

geboren te Nijmegen

krips repro meppel
1981

Graag wil ik iedereen bedanken die aan het tot stand komen van dit proefschrift heeft bijgedragen.

De huidige en voormalige medewerkers van de afdeling Theoretische Hoge-energiefysica zijn mij op velerlei wijze behulpzaam geweest. Met name wil ik Dr. Willy van Neerven noemen, een belangrijk deel van mijn kennis van veldentheorie heb ik aan hem te danken, en in de afgelopen jaren heb ik vele verhelderende discussies met hem gevoerd.

Aan de vormgeving van dit proefschrift is bijgedragen door de afdelingen Illustratie en Fotografie van de Faculteit der Wiskunde en Natuurwetenschappen en door Wilma Lemmers-Vink, die het soms nauwelijks leesbare manuscript met grote zorgvuldigheid heeft getypt. Drs. George Rupp bedank ik voor het nauwkeurig doorlezen van een deel van dit proefschrift.

Dit werk is een gedeelte van het onderzoekprogramma van de "Stichting voor Fundamenteel Onderzoek der Materie" (F.O.M.), welke financieel gesteund wordt door de "Nederlandse Organisatie voor Zuiver Wetenschappelijk Onderzoek" (Z.W.O.).

CONTENTS

1. Introduction

In the last twenty years considerable progress has been made towards the understanding of the fundamental interactions of nature. During that period two theories were developed, which, in combination with general relativity and quantum electrodynamics (QED) offer a complete description of the four basic interactions we know. These theories are the Glashow-Weinberg-Salam (GWS) model [Gla 61, 65, Wei 67, Sal 64, 68], which semi-unifies QED and weak interactions, and quantum-chromodynamics (QCD) which describes the strong interactions. The common feature of general relativity, the GWS-model and QCD is that all three are gauge theories. In a gauge theory the interactions are due to the exchange of an intermediate boson, the coupling of which is prescribed by postulating a local invariance of the lagrangian. For the theories mentioned above these local invariance groups (gauge groups) are the Poincaré-group, SU(2) × U(1) and SU(3).

Despite this attractive picture each of these theories confronts us with some unsolved problems. General relativity is an elegant and beautiful theory on the classical level, but unfortunately up to now no one has been able to quantize it in a consistent way. For the GWS-model the situation is rather the opposite. This theory has been shown to be renormalizable [Hoo 71], and hence quantum corrections are calculable, but on the other hand the structure of the theory is far from attractive. A large number of unexplained parameters (masses, coupling constants and mixing angles) are introduced, and moreover a set of

scalar particles (Higgs bosons) has to be added which have partly unpredictable parameters and which tend to hide themselves in observable processes. Nevertheless the GWS-model, which is the simplest possibility of the ones which have been proposed, is in agreement with all experimental data.

Considered from an optimistic point of view, QCD is plagued by none of the problems mentioned above. Unlike weak interaction theory, QCD is simple and elegant and has only one parameter, the coupling constant. Unlike general relativity QCD is renormalizable. In the case of QCD however, the problems arise when one tries to make verifiable predictions using this theory. Then a number of additional phenomenological parameters (bag model or potential model parameters for spectroscopy, parton distribution functions and fragmentation functions for the description of high energy scattering) have to be introduced, which may be calculable in principle, but which are at most qualitatively understood at present. All these parameters describe the low energy regime of the theory, where the coupling constant becomes large and where nonperturbative effects may be important. The optimistic point of view that QCD is a one-parameter theory is not yet supported by theoretical calculations. To prove it one has to express all phenomenological parameters in terms of the coupling constant, a task which is beyond our technical capacities at present.

Our lack of understanding of these parameters is supposed to be related to our lack of understanding of quark confinement, a property which QCD should have in order to explain the absence of free quarks and gluons. Several ideas about confinement exist at the moment, which are sometimes seemingly unrelated and sometimes even conflicting, but

nevertheless seem to suggest that confinement may be a property of massless non-abelian gauge theories.

The history of QCD is long and many physicists have contributed essential elements to the theory as it exists now. As the starting point one may consider the introduction of SU(3)-symmetry to describe the observed particle multiplets [Gel 61, Nee 61, Gel 62]. A few years later quarks, fundamental fractionally charged constituents of baryons and mesons, were introduced by Gell-Mann and Zweig [Gel 64, Zwe 64]. Baryons were assumed to be three-quark bound states, mesons quark-anti-quark bound states. At that time three quarks were needed to explain the observed particle spectrum, which are nowadays called 'up', 'down' and 'strange'. The SU(3)-symmetry mentioned above was an approximate symmetry among these quarks, and is totally unrelated to the SU(3) color symmetry to be introduced below. A few years ago a fourth and fifth quark were found, and a sixth one is expected but not yet found. These different types of quarks are referred to as 'flavors'.

Soon after the introduction of quarks one was confronted with a problem concerning their fermi-statistics. To explain the baryon spectrum in a simple way the three quarks had to be in a totally symmetrical state. Although solutions were proposed at that time [Gre 64, Han 65], the problem was definitely solved in 1972 by assigning a new degree of freedom called color to each quark [Fri 72, Gel 72]. The quarks were assumed to be a fundamental triplet representation of an SU(3) color-symmetry group. With the additional assumption that only color singlet states can occur as physical particles all the qualitative features of the low-lying baryons and mesons can be understood. The statistics problem is solved because a three quark color singlet

wave function is totally antisymmetric. Further evidence for color is the fact that the color enhancement factors predicted for the $\pi^0 \to \gamma\gamma$ decay width and for the ratio of the cross sections of $e^+e^- \to$ hadrons and $e^+e^- \to \mu^+\mu^-$ are in agreement with experiment.

This global color symmetry is the first ingredient of QCD. The second one is the concept of non-abelian gauge theories, which was formulated already in 1954 by Yang and Mills [Yan 54]. The two ideas can be put together by making the global SU(3) symmetry into a local gauge symmetry. As a consequence eight massless vector bosons emerge, which are coupled to the quarks. These particles, comparable to the photon in QED, are called gluons, and the quantum field theory obtained this way is called Quantum Chromo Dynamics. At that time non-abelian gauge theories were already known to be renormalizable and therefore QCD was a very attractive candidate for a strong interaction theory.

This was of course not sufficient to make QCD an acceptable strong interaction theory. There was however something else which caused interest in this theory. In 1968 the phenomenon of scaling [Bjo 69] in deep inelastic electron-proton scattering was observed at SLAC. Scaling* means that at high energies the dynamics of the process becomes independent of the interaction scale. In field theory scaling can only be understood if the coupling constant becomes small at high energies. For most renormalizable field theories the coupling constant behaves in precisely the opposite way. In 1973, just after the renor-

*The word scaling is often used in a more general sense. In this section it means 'canonical' or 'naive' scaling. A more precise discussion is given in section 3.

malization of non-abelian gauge theories was understood, these theories were shown to be the only exception [Pol 73, Gro 73, Col 73]. For non-abelian gauge theories the coupling constant vanishes logarithmically at high energies, a property which is called asymptotic freedom.

The fact that the coupling constant vanishes logarithmically implies that QCD does not lead to exact scaling. Logarithmic deviations from scaling, which are calculable in perturbation theory, are predicted. To calculate these scaling deviations one needs a method to separate the hadronic bound state effects, which are not understood within QCD, from the high energy scattering part of the cross section. The oldest method used for this purpose was the operator product expansion (OPE) [Wil 69, Bra 71], which limited the application of QCD to deep-inelastic scattering and e^+e^- annihilation. An important step forward was made when it turned out to be possible to use a QCD-improved version of the parton model.

The parton model [Fey 69] gives a description of deep-inelastic scattering processes in terms of incoherent scattering of a photon and a pointlike constituent of the hadron, which is called a parton. With this model the scaling behavior observed in deep-inelastic scattering experiments could be explained. With our present understanding of hadronic structure it is natural to identify these partons with quarks and gluons. Since QCD provides us with a consistent renormalizable theory for the interaction of quarks and gluons, it is possible to calculate corrections to the parton model results, which now become the leading terms in a perturbation expansion. To make this perturbation series convergent the mass singularities, which appear in each order of perturbation theory, must be factorized out of the parton

cross sections. By means of this factorization procedure it turns out to be possible to reobtain the leading parton model results, but with small and calculable non-scaling corrections. In this way the success of the old parton model can be understood, and the model is shown to be consistent with QCD.

It can be shown that this method is completely equivalent to the operator product expansion for deep-inelastic scattering. But with the QCD-improved parton model one can go beyond the OPE and calculate corrections to processes to which the OPE does not apply. An example of such a process is lepton pair production in hadron-hadron scattering. The leading parton model result for the cross section of this process was suggested in 1970 by Drell and Yan [Dre 70].

Much effort has gone into calculations of QCD-corrections to all kinds of processes, and into experiments attempting to measure these corrections. The experimental verification of QCD turns out to be very difficult for several reasons. First of all the information obtained from experiments concerning the quark-gluon interaction is rather indirect because one cannot do experiments with free quarks and gluons.

Moreover the logarithmic scaling deviations are rather small from the phenomenological point of view. Beside the scaling deviations predicted by QCD there are scale breaking effects due to other sources, such as the mass of the target and interactions involving more than one parton from each hadron. These effects are usually somewhat loosely summarized as 'higher twist effects'. Although one can make estimates of these effects using QCD, they are not yet completely under control theoretically, and in any case extra parameters will be needed to describe them. Fortunately all these effects vanish more rapidly with

increasing energy than the logarithmic scaling deviations predicted by QCD in the leading twist approximation, and hence one can minimize their effect by going to higher energies. The price one pays is that the logarithmic scaling deviations will be even smaller, and that more accurate experimental results are needed to measure them.

The scaling deviations may be small phenomenologically, from the theoretical point of view they are sometimes too large. In the accessible energy range the QCD coupling constant is not extremely small (it is an order of magnitude larger then the QED coupling constant), which may afflict perturbation theory. Indeed, in some cases one finds that the QCD-corrections are larger than the leading terms. If it is understood theoretically why these corrections are large one may be able to extract the large terms out of all higher order corrections and sum them. Then one may hope that the remaining terms are sufficiently small to make perturbation theory reliable. One of the problems which is always associated with such a procedure is the appearance of ambiguities in the perturbation series. These ambiguities are related to the fact that the coefficients of the badly convergent perturbation series must be split in an arbitrary way into a large part, which is to be summed, and a small part, which is left as a perturbative correction.

At least one kind of summation is always required to make a perturbative approach to QCD possible, and that is the summation of the logarithms which are the vestiges of the ultraviolet-divergencies or the mass singularities of the theory. The method to sum these logarithms, with the 'renormalization group' equations, dates back to 1953 [Stu 53, Gel 54], when it was used to study the asymptotic behavior of the photon propagator in QED. Where on the previous pages

the words 'perturbation theory' were used, this renormalization group summation was implicitly understood. The ambiguities mentioned above are present in a renormalization group improved perturbation series and have been a source of much confusion in the last years. We will come back to this problem in more detail in chapter II.

Despite these difficulties the experimental evidence in favor of QCD is gradually increasing. The scaling deviations in deep inelastic scattering data are in agreement with QCD, although other explanations cannot be rigorously excluded. The three-jet events, recently observed at DESY, are hard to explain by anything else than QCD. Many other successful applications of QCD exist, although they are less convincing than these two. There are also a few cases where QCD does not work very well, but in those cases the experiments or theoretical calculations are always much more complex and uncertain. Nevertheless it would be premature to conclude that QCD has been confirmed experimentally. To arrive at such a conclusion additional information from as many processes as possible is needed. We will study one of these processes, lepton pair production in hadron-hadron scattering, in chapter III.

In the remainder of this chapter we will discuss briefly a few essential elements of QCD and related topics, in as far as we need them in the subsequent chapters. For more extensive discussions of these topics we refer to [Pol 74], about the operator product expansion, the renormalization group and asymptotic freedom, [Mar 78] about renormalizability, the renormalization group and several approaches to the confinement problem, [Bur 80] about the phenomenology of second order corrections and, [Bjo 80] about the quantization problems for non-abelian gauge theories, the confinement problem and

some other topics.

In chapter II we will give a detailed discussion of the factorization formalism for mass singularities, and the relation with the renormalization group. Much attention will be given to the ambiguities in the procedure.

In chapter III the application of this formalism to lepton pair production is discussed. This includes all first order corrections, and a calculation of a potentially important second order parton subprocess.

The phenomenological quantities, needed to calculate the lepton pair production cross section are all defined and measurable in deep inelastic scattering processes. In section IV we discuss the relation between the two processes, and determine these parameters using deep inelastic scattering data. The results of this analysis are then used to calculate the cross section.

2. Lagrangian, Feynman rules and quantization of QCD

To obtain the lagrangian of QCD one starts with the free lagrangian for N_f quark-flavors, each of which has three colors:

$$\mathcal{L}_f = \sum_{j=1}^{N_f} \sum_{\alpha=1}^{3} [i \bar{\psi}_{j,\alpha}(x)\gamma^\mu \partial_\mu \psi_{j,\alpha}(x) - m_j \bar{\psi}_{j,\alpha}(x)\psi_{j,\alpha}(x)] \quad . \qquad (2.1)$$

The flavor and colorindices are j and α respectively. The lagrangian has a global SU(3) color-symmetry with respect to the index α; the flavor-symmetry is however broken by the quarkmasses m_j. The global symmetry can be realized locally by introducing a gaugefield A_μ and changing the derivative into a covariant one:

$$\partial_\mu \rightarrow D_\mu = \partial_\mu + A_\mu \qquad (2.2)$$

$$A_\mu(x) = - ig A_\mu^a(x)\, T^a \qquad (2.3)$$

where T^a is a generator of the symmetrygroup, and $A^a_\mu(x)$ is the gluonfield. For SU(3) there are eight generators and hence eight gluons. The matrices T^a form a basis for the triplet-representation of the Lie algebra of the gaugegroup SU(3), and they satisfy the following relations:

$$[T^a,T^b] = i\, C^{abc}\, T^c \tag{2.4}$$

$$Tr\ (T^aT^b) = \frac{1}{2}\,\delta^{ab} \tag{2.5}$$

In (2.4) C^{abc} is called the structure constant of the gaugegroup. The second relation fixes the normalization of the generators. The transformation of the gaugefields is completely determined by the requirement that the lagrangian is locally invariant:

$$D_\mu \rightarrow D'_\mu = U(x)\ D_\mu\ U^{-1}(x) \tag{2.6}$$

where U(x) is a local (space-time dependent) gauge transformation, which acts upon the quarkfields in the usual way. This way of introducing a coupling between the fermions and vectorbosons is a generalization to non-abelian groups of the analogous procedure for QED [Yan 54, Abe 73].

To make the gaugefields dynamical variables one introduces an extra term in the lagrangian:

$$\mathcal{L}_g = -\frac{1}{4}\, F^a_{\mu\nu}\ F^{a,\mu\nu} \tag{2.7}$$

where

$$F^{\mu\nu} = [D^\mu,D^\nu] = \partial^\mu A^\nu - \partial^\nu A^\mu + [A^\mu,A^\nu] \tag{2.8}$$

$$F^{\mu\nu} = -\,ig\ F^{a,\mu\nu}\ T^a \tag{2.9}$$

This extra term is of course gauge invariant. Although the expression of the lagrangian in terms of the field strength tensor $F^{\mu\nu}$ is completely

analogous to the expression for QED, there is an important difference in the Feynman rules of a non-abelian gauge theory. This difference is due to the last term of (2.8) which causes the appearance of three and four gluon couplings in the lagrangian.

The fermion lagrangian (2.1), with the derivative replaced by a covariant one, together with the gaugefield lagrangian (2.7) constitute the entire QCD lagrangian. The only free parameter in the lagrangian is the coupling constant g, if parameters describing properties of the sources (e.g. the quarkmasses) are not considered as fundamental parameters of the theory. (This distinction is however not completely justified, because the number of flavors is very important for the asymptotic behavior of a non-abelian gauge theory. In the case of QCD, asymptotic freedom is lost if this number is larger than sixteen.)

The quantization of a gauge theory leads to some complications due to the gauge invariance of the lagrangian. For a non-abelian gauge theory these problems are more serious then for an abelian theory like QED, but they can be solved by means of the path integral formalism. Because of local gauge invariance the action does not have a single minimum but a continuum of minima, which lead to an undefined propagator, when they are not properly taken into account. The method to solve this problem was invented by Faddeev and Popov [Fad 67]. Their approach leads to an additional term in the lagrangian which fixes the gauge and removes the unphysical degrees of freedom so that the propagator becomes well-defined. But in addition to that an auxiliary field has to be introduced, which is called Faddeev-Popov ghost. These ghosts are scalar fields with fermi-statistics, which can only appear in loops of Feynman diagrams, and not as external lines. When these ghost-loop

diagrams are added a gauge invariant and unitary S-matrix is obtained. In some gauges the ghost does not couple to physical particles, and then they can be neglected completely. (This is what happens automatically for QED unless an unusual gauge is chosen.) These gauges are called 'physical gauges'.

The gauges which are most frequently used are the Feynman or the Landau gauge, connected by means of a continuous parameter, and the axial gauge. The difference between these gauges manifests itself in the numerators of the gluon-propagator and in the fact that for the axial gauge no ghost fields are needed. These numerators are

$$D^F_{\mu\nu} = -\left(g_{\mu\nu} - \frac{k_\mu k_\nu}{k^2}\right) - \alpha \frac{k_\mu k_\nu}{k^2} \qquad \text{Feynman/Landau gauge} \qquad (2.10)$$

$$D^A_{\mu\nu} = -g_{\mu\nu} + \frac{k_\mu n_\nu + n_\mu k_\nu}{n\cdot k} - n^2 \frac{k_\mu k_\nu}{(n\cdot k)^2} \qquad \text{Axial gauge} \qquad (2.11)$$

The Feynman gauge is obtained for $\alpha = 1$; the Landau gauge for $\alpha = 0$. The four-vector n^μ in (2.11) can be arbitrarily chosen. Of course all physical results should be independent of α and n^μ. The axial gauge is very often used for theoretical considerations because of the absence of ghosts and the fact that the gluon has physical polarizations. For calculations this gauge is less suitable because of the complicated numerator and the $(n\cdot k)^{-1}$ singularities which cancel not until gauge-invariant sets of diagrams are added together. In other gauges one has additional ghost diagrams, but these are always the simplest ones to be calculated.

When a gauge is fixed the Feynman rules for QCD can be derived by means of the usual methods. We have summarized them in appendix A.

The original gauge symmetry of the lagrangian manifests itself by relations among Feynman diagrams, called Ward-Takahashi identities

[War 50, Tak 57], generalized to non-abelian gauge theories by Slavnov and Taylor [Sla 75, Tay 71] and formulated in a more elegant way by means of the BRS transformation [Bec 75]. These identities must be preserved order by order in perturbation theory, and this puts severe constraints upon the methods one can use to regularize the ultraviolet singularities. A method which satisfies this requirement is dimensional regularization [Hoo 72, Bol 72, Ash 72]: the Feynman-integrals are regularized by continuing them from 4 to n dimensions, and the ultraviolet singularities manifest themselves as poles for $n \to 4$. It can be shown that these poles can be removed from all Green's functions by making suitable redefinitions of the parameters in the lagrangian (i.e. the coupling constant, the quark-masses and the scales of the fields). This means that the theory is renormalizable. The proof of renormalizability was given by 't Hooft [Hoo 71].

As far as ultraviolet divergencies are concerned, a non-abelian gauge theory is not essentially different from an abelian one. No one has however been able to show that the infrared singularities cancel when soft gluon radiation is taken into account, as is the case for QED, according to the Bloch-Nordsieck theorem [Blo 37]. It has been suggested that this problem was related to our lack of understanding of quark confinement, but explicit calculations of higher order corrections showed that the perturbative infrared behavior of QCD was not extremely different from the behavior of QED. In processes with one incoming hadron I.R. divergencies have been shown to cancel [Lib 78]. A proof for the case of two incoming hadrons could not be given and recently a counterexample was found for this case [Dor 80]. This example is the process $q + \bar{q} \to \gamma^* +$ soft gluons, where γ^* is a hard virtual photon.

The noncancelling divergencies are of second order in α_s and of non-leading twist. This means that they do not affect any of the calculations which have been done up to now. Nevertheless the problem should be investigated thoroughly, and new developments can be expected here. Recently a way to avoid this counterexample was suggested [Nel 80].

3. Renormalization group equations

To study the behavior of a theory when certain Lorentz-invariant combinations of the external momenta of Green's functions become large, the renormalization group equations are indispensable. To show how these equations can be derived we consider a renormalizable lagrangian consisting of a set of fields, denoted by the symbol $\phi(x)$, and a coupling constant, denoted by g. Masses can be taken into account, but they cause some confusing complications and moreover we will not use renormalization group equations with nonvanishing masses. Therefore we have omitted them.

When a Green's function is calculated in such a theory one finds ultraviolet divergencies, which must be regulated. In the arguments given below we use dimensional regularization for that purpose. Then a calculation of a Green's function results in an expression of the following form:

$$G_u^m = G_u^m(p,g,\varepsilon) \tag{3.1}$$

Here p denotes all external momenta, m the number of external legs, and $\varepsilon = 4 - n$ where n is the number of space-time dimensions. The subscript 'u' indicates that the Green's function is unrenormalized. This means that the expression will have poles for $\varepsilon \to 0$ (or equivalently $n \to 4$).

A finite result can be obtained by making a redefinition:

$$\phi_u(x) = \sqrt{Z_3(\mu, g_R, \varepsilon)}\ \phi_R(x) \tag{3.2}$$

$$g_u = Z_g(\mu, g_R, \varepsilon)\ g_R \tag{3.3}$$

The index R means renormalized. The quantities ϕ_u and g_u are the ones which appeared in the original lagrangian. The renormalization constants Z_3 and Z_g can be calculated by subtracting the poles order by order by means of counterterms. The physical Green's function is obtained by using the renormalized fields ϕ_R and expressing the result in terms of the renormalized coupling constant g_R. Then Z_3 and Z_g have to meet the requirement that the resulting expression must be finite, i.e.:

$$\lim_{\varepsilon \to 0} G_R^m(p, g_R, \varepsilon, \mu) = \lim_{\varepsilon \to 0} [Z_3(\mu, g_R, \varepsilon)]^{-m/2}\ G_u^m(p, Z_g(\mu, g_R, \varepsilon) g_R, \varepsilon) \tag{3.4}$$

must exist.

A mass-scale μ was introduced in the above equations, because all quantities have to be given the correct physical dimension in n space-time dimensions. Because the action is dimensionless, the lagrangian must have dimension n and the dimensions of the fields and coupling constants must be modified accordingly. This parameter μ is completely arbitrary. Because the unrenormalized parameters do not depend upon this mass-scale one can derive an equation for the Green's function expressed in terms of renormalized parameters. This equation, which is called the renormalization group equation, is:

$$\left[\mu \frac{\partial}{\partial \mu} + \beta(g_R) \frac{\partial}{\partial g_R} + \frac{m}{2} \gamma(g_R)\right]\ G_R^m(p, g_R, \mu) = 0 \ ^* \tag{3.5}$$

*In an arbitrary gauge there is an additional term expressing the fact that the gauge parameter is not renormalized. This term vanishes if the Landau gauge is chosen.

The functions appearing in (3.5) are defined as follows:

$$\beta(g_R) = \lim_{\varepsilon\to 0} \mu \frac{\partial}{\partial\mu} g_R(\mu,\varepsilon,g_u)\Big|_{g_u} \tag{3.6}$$

$$\gamma(g_R) = \lim_{\varepsilon\to 0} \mu \frac{\partial}{\partial\mu} \ln\,(Z_3(\mu,g_R,\varepsilon))\Big|_{g_u} \tag{3.7}$$

$$G_R(p,g_R,\mu) = \lim_{\varepsilon\to 0} G_R(p,g_R,\varepsilon,\mu) \quad . \tag{3.8}$$

The derivation of the equations with the dimensional regularization method was given by several authors [Hoo 73, Hol 74, Col 74]. The beta-function $\beta(g_R)$ and the anomalous dimension $\gamma(g_R)$ are calculable in perturbation theory and finite. In these equations we have left out some extra complications which arise when the lagrangian contains more than one coupling constant or more than one type of field. The generalization to more coupling constants is simple, but since QCD is a theory with only one coupling constant we will not consider this case. When more fields are present one needs a different factor Z_3 for every field, and consequently each field has its own anomalous dimension. The factor m in (2.5) has to be replaced by a sum over the anomalous dimensions of the fields corresponding to the external legs. This procedure is however not correct when two or more fields have the same quantum numbers. Then these fields can be mixed by the renormalization procedure. This means that the renormalization constant Z_3 and the anomalous dimension become matrices. We will discuss a situation like this in section 5.

The task set out at the beginning of this section was to determine the asymptotic behavior of a Green's function. To show how equation (3.5) helps us in that respect we rewrite the Green's function as follows:

$$G_R(p,g_R,\mu) = G'_R(p,g_R,\frac{\mu}{p}) \quad . \tag{3.9}$$

The dependence of G'_R on its first variable is necessarily trivial because this variable has a dimension. Therefore a rescaling $p \to \lambda p$ of this first variable will cause a transformation of the Green's function corresponding to the physical dimension of this function. When renormalization effects were absent this would completely determine the scaling behavior of a Green's function. But because quantum effects introduce an extra scale μ an anomalous scaling behavior of the Green's function is possible. This anomalous behavior is determined by the dependence of G'_R on $\frac{\mu}{p}$, or equivalently by the dependence of G_R on μ, and this is why equation (3.5) is important for the study of the asymptotic behavior of a theory. The relation of the renormalization group equation to broken scale invariance was first discussed by Callan and Symanzik [Cal 70, Sym 70].

These arguments rely upon the assumption that the only mass-scales in the problem are the momenta and μ. When masses are present they remain correct provided that the limit $m \to 0$ yields a finite result. Then deviations from the behavior governed by equation (3.5) are of order (m/p) and vanish in the asymptotic limit. The case in which a singularity is encountered at $m = 0$ will be discussed in chapter II.

To make these arguments more precise we write down the formal solution of equation (3.5). One can easily show that this solution is:

$$G'_R(p,g_R,\frac{\mu}{p}) = G'_R(p,\bar{g}(\ln(\frac{p}{\mu})),1)\ \exp\frac{m}{2}\int_0^{\ln(\frac{p}{\mu})}\gamma(\bar{g}(\tau))\,d\tau \qquad (3.10)$$

$$= G'_R(p,\bar{g}(\ln(\frac{p}{\mu})),1)\ \exp\frac{m}{2}\int_g^{\bar{g}(\ln(\frac{p}{\mu}))}\frac{\gamma(\tau)}{\beta(\tau)}\,d\tau$$

where the function $\bar{g}(t)$ is defined as follows:

$$\frac{d\bar{g}(t)}{dt} = \beta(\bar{g}(t)) \qquad ; \qquad \bar{g}(0) = g \qquad (3.11)$$

We have not given an exact definition of the momentum p used in these equations. When it appears as an argument of a logarithm it has to be a scalar constructed out of the external momenta, but the renormalization group equations do not give a prescription of the way this variable is chosen. Formally this does not make any difference, but in practice it does, because one uses power series in the coupling constant which are truncated at a given order. This ambiguity and related ones will be discussed in chapter II. For the moment we will not bother about the precise definition of p.

To exhibit the behavior of (3.10) we now suppose that $\bar{g}(t)$ approaches a constant g_f for large t. Then the behavior of the Green's function for a momentum rescaling $p \to \lambda p$ is predicted to be $\sim \lambda^{D+\gamma(g_f)}$, where D is the dimension of the Green's function. This is called scaling. Without quantum effects one would expect a scaling behavior $\sim \lambda^D$, which is called naive or canonical scaling. The extra term $\gamma(g_f)$ leads to an anomalous scaling behavior. This explains the name 'anomalous dimension'.

The supposed asymptotic behavior of the 'running coupling constant' g(t) is determined by the β-function. If this function is positive for some value of g, the coupling constant will increase with t until a zero of the β-function is reached. The running coupling constant will then approach this zero asymptotically, and the limit is called a fixed point. If on the other hand $\beta(g)$ is negative the coupling constant will decrease with increasing t, until a fixed point is reached.

The zero's of the β-function fall into two classes. The ones for which the derivative of $\beta(g)$ with respect to g is positive are called infrared stable fixed points. They are reached from both sides for

$t \to -\infty$, which corresponds to $p << \mu$. In practical situations however this limit is never reached because of the presence of masses, which cannot be neglected for small p. The zero's for which $\beta(g)$ has a negative derivative are reached for large p and are called ultraviolet stable fixed points.

Because the perturbation expansion of $\beta(g)$ starts with a term proportional to a non-zero power of g, the origin is always a fixed point. If the first coefficient is negative it is ultraviolet stable, and the coupling constant will vanish asymptotically for large t. This is called asymptotic freedom. The only renormalizable theories which have this property are non-abelian gauge theories, with a limited number of other fields to which the gauge-bosons couple, and $\lambda\phi^4$-theory with a negative coupling constant [Sym 73]. The latter does not have a physical spectrum.

4. Deep-inelastic scattering

The most important source of information about the asymptotic behavior of the strong interactions are deep-inelastic scattering experiments. In a deep-inelastic scattering (D.I.S.) process a hadron is struck by a high energy incoming lepton and fragments into a number of other particles. In present experiments the lepton is an electron, muon or neutrino, and the target is a proton or a nucleus. The process can be represented by figure 4.1. The wavy line represents a photon, a $W^{\pm}$ boson or a Z^0 boson, mediating the electromagnetic, charged current and neutral current weak interactions respectively. The symbol 'X' represents any hadronic state with allowed quantum numbers. The differential cross section for the process can be written in the

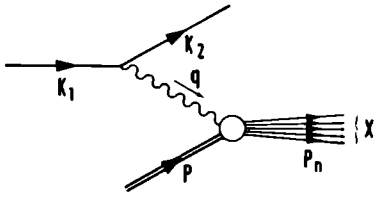

fig. 4.1: deep-inelastic scattering process ; the double line represents the hadron, the single line the lepton.

following way:

$$\frac{d\sigma}{d\Omega dE'} = \frac{1}{2} \frac{\alpha^2}{(q^2)^2} \frac{E'}{E} L_{\mu\nu} W^{\mu\nu} \qquad (4.1)$$

This is the cross section for electromagnetic processes. For weak processes there is a modification due to the mass of the intermediate vectorboson. In (4.1) E and E' are the lab-energies of the in- and outgoing lepton and the solid angle Ω corresponds to the direction of the outgoing lepton; $L_{\mu\nu}$ is the lepton tensor, which depends upon the type of process considered, but which is exactly calculable. The unknown part in the process is the hadron tensor $W^{\mu\nu}$. The known leptonic part of the cross section is used as a probe to obtain information about this tensor. It depends upon the hadronic current $J^{\mu}(x)$:

$$W^{\mu\nu}(P,q) = \frac{1}{4\pi M} \int d^4x \, e^{iqx} \, \langle P | [J^{\mu}(x), J^{\nu +}(0)] | P \rangle_{av} \qquad (4.2)$$

where M is the mass of the target hadron. The subscript 'av' indicates that matrix elements are assumed to be averaged over the degrees of freedom of the particle; in this case it implies that a spin-averaged matrix element is meant.

From Poincaré and time-reversal invariance one can deduce that $W^{\mu\nu}$ can be decomposed into five structure functions. Two of them appear in the cross section multiplied by the lepton mass and can therefore not be measured. Expressed in terms of the remaining three the hadron tensor reads

$$W^{\mu\nu}(P,q) = -\left(g^{\mu\nu} - \frac{q^\mu q^\nu}{q^2}\right) W_1(P,q)$$

$$+ \left(P^\mu - \frac{P\cdot q}{q^2} q^\mu\right)\left(P^\nu - \frac{P\cdot q}{q^2} q^\nu\right) \frac{1}{M^2} W_2(P,q)$$

$$- i\varepsilon^{\mu\nu\alpha\beta} P_\alpha q_\beta \frac{1}{2M^2} W_3(P,q) \quad . \qquad (4.3)$$

The last term is absent in electromagnetic processes because of parity conservation.

The momenta appearing as arguments of the structure functions $W_1 \ldots W_3$ can be combined into a dimensionless Lorentz-scalar $x = \frac{-q^2}{2P\cdot q}$. The structure functions are usually expressed in x and $Q^2 = -q^2$. Another variable which is often used is $\nu = \frac{P\cdot q}{M} = E' - E$, the energy loss of the lepton.

In 1969 Bjõrken [Bjo 69] suggested, on the basis of deep-inelastic scattering data from SLAC, that these structure functions would show a scaling behavior in the limit $Q^2 \to \infty$, x fixed. This can be understood theoretically if one assumes that there are no dynamical mass-scales in the problem, and that the proton mass plays only a kinematical role in the process. Nevertheless, the nonvanishing target mass makes it a priori not obvious which functions can be expected to scale, since dimensional arguments are not sufficient. One can show however, that the following functions will scale for $Q^2 \to \infty$, x fixed:

$$MW_1(x,Q^2) \rightarrow F_1(x)$$
$$\nu W_2(x,Q^2) \rightarrow F_2(x)$$
$$\nu W_3(x,Q^2) \rightarrow F_3(x) \qquad (4.4)$$

In the early SLAC experiments mentioned above this naive scaling behavior was indeed observed for F_1 and F_2. Theoretically scaling can only be expected in the asymptotic region, because any theory describing the structure of hadrons, which predicts naive scaling for large Q^2, also predicts deviations from scaling for smaller Q^2. Of course the approach to scaling depends upon the theory. In 1975 the observation of such deviations was reported [Wat 75, Cha 75] and since then many new experiments have been done. From these experiments one can conclude that scaling deviations are present, but small. More recent data indicate that they become even smaller at higher values of Q^2. This kind of behavior is - at least qualitatively - what can be expected for an asymptotically free interaction.

5. The operator product expansion

The oldest method to study scaling violations in deep-inelastic scattering is the operator product expansion (O.P.E.) [Wil 69, Bra 71]. The O.P.E. is used to describe the behavior of the product of two operators if the difference between their space-time arguments become zero or lightlike. It can be shown that the product of two operators J(x) can be expanded in the following way:

$$J(x)\ J(0) = \sum_i G_i(x)\ O_i(0) \qquad (5.1)$$

where O_i are operators, constructed out of the fundamental fields of the theory, and $G_i(x)$ are functions which are usually singular for

$x^\mu \to 0$ or $x^2 \to 0$.

In the case of deep-inelastic scattering the relevant operator product is:

$$T^{\mu\nu}_{op} = i \int d^4x\, e^{iqx}\, T\, J^\mu(x)\, J^\nu(0) \tag{5.2}$$

The subscript 'op' stands for operator; the operators J^μ are the electromagnetic currents. (The extension to weak currents is straightforward.)

The matrix elements of the operator between hadron states is the forward Compton amplitude, which is related to the hadron tensor $W^{\mu\nu}$ by the optical theorem. The Compton amplitude can be decomposed in the following way:

$$\begin{aligned} T^{\mu\nu} &= \langle P|T^{\mu\nu}_{op}|P\rangle_{av} \\ &= (-g^{\mu\nu} + \frac{q^\mu q^\nu}{q^2})T_1 + (P^\nu - \frac{P\cdot q}{q^2} q^\nu)(P^\mu - \frac{P\cdot q}{q^2} q^\mu)T_2 \quad . \end{aligned} \tag{5.3}$$

The optical theorem leads to the following relation between the structure functions W_i, introduced in the previous section, and T_i:

$$W_i = \frac{1}{2M}\frac{1}{\pi}\, \mathrm{Im}\,(T_i) \tag{5.4}$$

In momentum space, the operator product expansion for $T^{\mu\nu}_{op}$ is:

$$\begin{aligned} T^{\mu\nu}_{op} = \sum_{n,i} \{ & 4\, q_{\mu_1} q_{\mu_2} \left[-g^{\mu\nu} + \frac{q^\mu q^\nu}{q^2}\right] C^n_{i,1}(q^2) \\ & - 2q^2 \left[g^\mu_{\mu_1} g^\nu_{\mu_2} - \frac{q^\mu q_{\mu_1} g^\nu_{\mu_2}}{q^2} - \frac{q^\mu q_{\mu_2} g^\nu_{\mu_1}}{q^2} + \frac{q^\mu q^\nu q_{\mu_1} q_{\mu_2}}{q^4} \right] C^n_{i,2}(q^2)\} \\ & \times q_{\mu_3} \cdots q_{\mu_n} \left(\frac{2}{-q^2}\right)^n O_i^{\mu_1 \cdots \mu_n} \end{aligned} \tag{5.5}$$

In this expression $C^n_{i,\alpha}$ are the coefficient functions, related to the Fourier transforms of the functions $G_i(x)$ in (5.1), and $O_i^{\mu_1 \cdots \mu_n}$ are

the operators, to be given below. The matrix elements of these operators between hadron states, which have to be known to calculate $T^{\mu\nu}$, are tensors of rank n which have to be constructed out of the four-momentum of the hadron:

$$<P|O_1^{\mu_1\cdots\mu_n}|P>_{av} = A_1^n(P^2)\ P^{\mu_1\cdots\mu_n} + B_1^n(P^2)[P^2 g^{\mu_1\mu_2} P^{\mu_3}\cdots P^{\mu_n} + \text{permutations}] + \ldots \tag{5.6}$$

Notice that the terms containing a metric tensor instead of two momenta, are suppressed by powers of $P^2/q^2 = M^2/q^2$ compared to the first term (M is the mass of the hadron). A four-vector P^μ on the other hand is contracted with a four-vector q_μ to give $P\cdot q$, which is of the same order of magnitude as q^2 in the Bjõrken-limit. With exactly the same arguments one can show, that the dominant operators in the expansion are the ones with the smallest value of dimension minus spin, a quantity which is called 'twist'. The operators of lowest twist are the ones with twist 2. For fixed spin a higher twist operator has a higher dimension, which can only be provided by factors P^2 in the matrix element. Therefore their contribution is suppressed by powers of P^2/q^2. The expansion (5.5) is written in such a way that the coefficient functions are dimensionless for twist-2 operators.

The importance of (5.5) is that it makes a separation between the part of the theory which can be calculated in perturbation theory and the part which is supposed to contain non-perturbative effects and which cannot be calculated with standard techniques. This uncalculable part consists of the hadron matrix elements of the operators. These are treated as parameters which have to be determined from experiment. The coefficient functions however, are calculable. To calculate them

one simply takes the matrix elements of (5.5) between states for which we do know the operator matrix elements, i.e. quarks and gluons. Then the coefficient functions are obtained by making an expansion in $\frac{p\cdot q}{q^2}$ of the lefthand side and comparing the coefficients in this expansion with those appearing at the righthand side of (5.5). Since (5.5) is a relation among operators the coefficient functions should be the same for matrix elements of physical hadrons.

Then, using (5.4), one can find the relation between the deep inelastic structure functions and the coefficient functions and operator matrix elements. For the moments of the structure function the following relations can be derived [Chr 72]:

$$\int_0^1 MW_1(x,Q^2)\, x^{n-1}\, dx = \sum_i C^n_{i,1}(Q^2)\, A^n_i$$
$$\int_0^1 \nu W_2(x,Q^2)\, x^{n-1}\, dx = \sum_i C^n_{i,2}(Q^2)\, A^n_i \qquad (5.7)$$

where $Q^2 = -q^2$.

When loop-corrections to the Wilson-coefficients $C^n_{i,\alpha}$ are calculated according to the procedure described above, one finds that beside the usual mass, wave function and coupling constant renormalizations, also the operators have to be renormalized. The infinities subtracted in this renormalization procedure manifest themselves in the Q^2-dependence of the coefficient functions in a way which is determined by a renormalization group equation. With this equation the moments of the structure functions can be calculated at any value of Q^2 once they are known at one point Q_0^2. This explains how (5.7) should be interpreted: the uncalculable parameters A^n_i are determined at some point, and are used as boundary conditions for a differential equation which predicts the moments at all other values of Q^2. The parameters appearing in the

renormalization group equation are the β-function and the anomalous dimensions of the operators, which are all calculable in perturbation theory.

The only gauge invariant twist-2 operators with nonvanishing expectation values which one can construct out of the quark and gluon fields in the lagrangian are:

$$O_a^{\mu_1\cdots\mu_n} = \frac{1}{2} S\, \bar{\psi}_\alpha \lambda^a_{\alpha\beta} \gamma^{\mu_1} D^{\mu_2}\cdots D^{\mu_n} \psi_\beta - \text{traces} \qquad (5.8)$$

$$O_Q^{\mu_1\cdots\mu_n} = \frac{1}{2} S\, \bar{\psi}_\alpha \gamma^{\mu_1} D^{\mu_2}\cdots D^{\mu_n} \psi_\alpha \quad - \text{traces} \qquad (5.9)$$

$$O_G^{\mu_1\cdots\mu_n} = S\, F^{\mu_1\nu} D^{\mu_2}\cdots D^{\mu_{n-1}} F^{\mu_n}{}_\nu \quad - \text{traces} \qquad (5.10)$$

Here S means that a symmetrization with respect to the indices $\mu_1\ldots\mu_n$ has to be performed; $\lambda^a_{\alpha\beta}$ is a traceless matrix in flavor space, and α and β are flavor-indices. The operators can always be chosen traceless, because trace terms give a contribution of higher twist.

The second and third operator are both flavor singlets and have exactly the same quantum numbers. Therefore they are mixed by quantum corrections and the Q^2-dependence of the Wilson coefficients corresponding to these operators is described by a set of coupled renormalization group equations. The anomalous dimension for these two operators is a 2x2 matrix. The first operator is not a flavor singlet and does not mix with the others. A discussion of operator mixing and a calculation of the one-loop contributions to the anomalous dimensions is given by [Gro 73, Gro 74, Pol 74, Geo 74]. The two-loop contributions to the anomalous dimension have also been calculated [Flo 77, Flo 79]. These two-loop contributions have to be combined with one-loop results for the coefficient functions in order to get a consistent result.

These one-loop corrections have been calculated too [Bar 78, Flo 79, Cal 77, DeR 77b]. (The results of the first two references are obtained in the same renormalization scheme as the two-loop anomalous dimensions. The other two however, use a different scheme and should not be used in combination with these anomalous dimensions.) Finally one needs the two-loop β-function, which has been calculated by [Cas 74, Jon 74]. These results make an analysis of deep-inelastic scattering beyond the leading order possible.

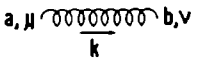

gluon propagator $\dfrac{i\, D_{\mu\nu}}{k^2+i\varepsilon}\ \delta_{ab}$

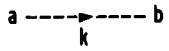

ghost propagator $\dfrac{i}{k^2+i\varepsilon}\ \delta_{ab}$

fermion propagator $\dfrac{i\,(\not{k}+m)}{k^2-m^2+i\varepsilon}\ \delta_{ij}$

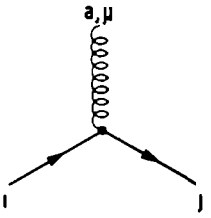

$i\, g\, \gamma_\mu\, T^a_{ij}$

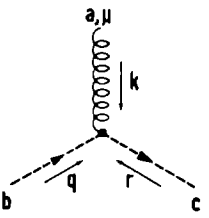

$g\, C_{abc}\, r_\mu$

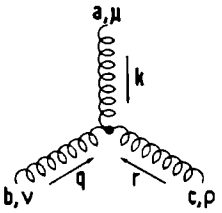

$$g\, C_{abc}\, [g_{\mu\nu}(k-q)_\rho + g_{\nu\rho}(q-r)_\mu + g_{\mu\rho}(r-k)_\nu]$$

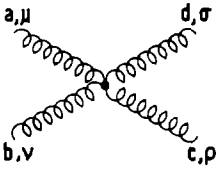

$$\begin{aligned} -i\, g^2\, [&C_{abe}\, C_{cde}\, (g_{\mu\rho}g_{\nu\sigma} - g_{\mu\sigma}g_{\nu\rho}) \\ &+ C_{ace}\, C_{bde}\, (g_{\mu\nu}g_{\rho\sigma} - g_{\mu\sigma}g_{\nu\rho}) \\ &+ C_{ade}\, C_{cbe}\, (g_{\mu\rho}g_{\nu\sigma} - g_{\mu\nu}g_{\sigma\rho})] \end{aligned}$$

Indices: μ, ν, ρ, σ Lorentz

a, b, c, d SU(3) adjoint representation

i, j SU(3) triplet representation

metric and related conventions according to Björken and Drell.

1. The parton model [Fey 69]

In section I.5 we have discussed the operator product expansion as a method to calculate the Q^2-dependence of deep-inelastic structure functions. In the last four years a different approach was developed, which was based on the parton model. For deep-inelastic scattering this approach gives the same results as the O.P.E., but it is intuitively more appealing. Moreover the parton model can be applied to processes other than deep-inelastic scattering, for which the operator product expansion does not work. Such an application will be the subject of chapter III. In this chapter we discuss the formalism which is needed to calculate corrections to the parton model.

According to the parton model an interacting hadron is described by a set of distribution functions $f_i(x)$, which measure the probability for finding in the hadron a constituent ('parton') of type i, which carries a momentum fraction x. Nowadays these partons are supposed to be quarks and gluons. The scattering process is assumed to be an incoherent sum of scattering processes for individual partons. This is illustrated by fig. 1.1.

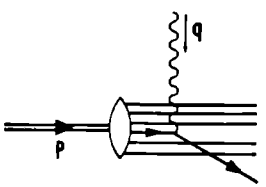

fig. 1.1: parton picture of deep-inelastic scattering.

The expression which relates the parton processes to the hadronic process is, according to the definition of the distribution functions given above:

$$\sigma_H(x) = \sum_j \int_0^1 d\xi \int_x^1 dx_p \; \xi \; f_j(\xi) \; \sigma_j(x_p) \; \delta(x-\xi x_p) \qquad (1.1)$$

where:

σ_j is a differential or total cross section for a parton of type j

σ_H is the corresponding hadron cross section

x_p is $-q^2/2p_1q$, where p_1 is the parton four-momentum, and q the photon four-momentum

x is $-q^2/2Pq$, where P is the four-momentum of the hadron

ξ is the momentum fraction of the parton, $p_1 = \xi P$ (transverse momentum is neglected here).

The integral is over all momentum fractions and all possible values of x_p, restricted to $x = \xi x_p$. The parton cross section has to be calculated as if the partons are free incoming particles, and the usual flux factor has to be included in this cross section. The factor ξ in (1.1) converts this parton flux factor into a flux factor for the incoming hadron. An expression analogous to (1.1) can be written down for other processes, e.g. for processes with two incoming hadrons, but in the remainder of this section we restrict ourselves to deep-inelastic scattering processes.

The cross section for unpolarized lepton-parton scattering is given by:

$$d\sigma = \frac{1}{4} \frac{1}{2\sqrt{\lambda(\hat{s},k^2,p_1^2)}} \frac{d^3k'}{2E'(2\pi)^3} \sum_{\{n\}} \left[\prod_{j\in\{n\}} \frac{d^3P_j}{2E_j(2\pi)^3} \right] \times$$

$$\sum_{spin} |M_{in}|^2 \; (2\pi)^4 \delta^4(k+p_1 - \sum_{j\in\{n\}} P_j) \qquad (1.2)$$

where

k^μ, k'^μ are the four-momenta of the in- and outgoing leptons

E, E' are the energies of these leptons

p_j^μ, E_j are the four-momenta and energies of the outgoing partons

$\hat{s}$ is the lepton-parton cm energy, $\hat{s} = (k+p_1)^2$.

The first summation is over all possible parton final states $\{n\}$, consisting of a number of partons with four-momenta P_j. Further the process is summed over the spins of the outgoing partons and averaged over the spins of the incoming particles (the factor $\frac{1}{4}$ should be $\frac{1}{2}$ for an incoming neutrino). The same procedure is applied to the color degree of freedom of the partons, although this is not explicitly indicated in (1.2). For notational convenience we will introduce the following symbol for the phase space integration for state $\{n\}$:

$$d\mathcal{P}_n = \prod_{j\in\{n\}} \frac{d^3P_j}{2E_j(2\pi)^3} \quad (2\pi)^4 \delta^4(k+p_1 - \sum_{j\in\{n\}} P_j) \tag{1.3}$$

The matrix element in (1.2) can be written as the product of a lepton and a parton tensor. The latter is defined as follows:

$$W^j_{\mu\nu}(x_p, Q^2) = \frac{1}{2\pi} \sum_{\{n\}} d\mathcal{P}_n \langle j|J_\mu(0)|\{n\}\rangle\langle\{n\}|J^+_\nu(0)|j\rangle_{av} \tag{1.4}$$

We want to express the hadron tensor in terms of the parton tensors and the distribution functions. This relation is specified by (1.1), and therefore we can use the expression for the parton cross section corresponding to (I.4.1):

$$\frac{d\sigma^j}{d\Omega dE'} = \frac{1}{2M\xi} \frac{1}{2} \frac{E'}{E} \frac{\alpha^2}{Q^4} L_{\mu\nu} W^{\mu\nu,j}(x_p, Q^2) \tag{1.5}$$

This result can be derived from (1.2) and (1.4). Comparing (1.5) and (I.4.1) and using (1.1) we obtain:

$$W_{\mu\nu}(x,Q^2) = \frac{1}{2M} \sum_j \int_x^1 d\xi \frac{f_j(\xi)}{\xi} W^j_{\mu\nu}\left(\frac{x}{\xi}, Q^2\right) \tag{1.6}$$

To find the corresponding relations for the structure functions we make two projections. For the parton tensor these projections are:

$$\nu W_2^j(x_p,Q^2) = -\frac{1}{2} x_p \left(g^{\mu\nu} - 12 \frac{x_p^2}{Q^2} p_1^\mu p_1^\nu\right) W_{\mu\nu}^j(x_p,Q^2)$$

$$W_1^j(x_p,Q^2) = -\frac{1}{4} \left(g^{\mu\nu} - \frac{4x_p^2}{Q^2} p_1^\mu p_1^\nu\right) W_{\mu\nu}^j(x_p,Q^2) \qquad (1.7)$$

Using these definitions we find:

$$\nu W_2(x,Q^2) = \sum_j \int_x^1 d\xi\ f_j(\xi)\ \nu W_2^j\left(\frac{x}{\xi},Q^2\right) \qquad (1.8)$$

$$MW_1(x,Q^2) = \sum_j \int_x^1 d\xi\ \frac{f_j(\xi)}{\xi}\ W_1^j\left(\frac{x}{\xi},Q^2\right) \qquad (1.9)$$

These relations enable us to calculate the hadronic structure functions from the parton structure functions.

If the leading parton cross sections are substituted in (1.8) and (1.9), and if QCD corrections are neglected, one obtains the old parton model results. For electron scattering the lowest order contribution is given by the Born diagram (fig. 1.2). Using (1.3) one finds:

$$W_{\mu\nu}^1(x_p,Q^2) = \frac{2e_1^2}{Q^2} \delta(1-x_p) \left[2p_{1\mu}p_{1\nu} + p_{1\mu}q_\nu + p_{1\nu}q_\mu - g_{\mu\nu}p_1\cdot q\right] \qquad (1.10)$$

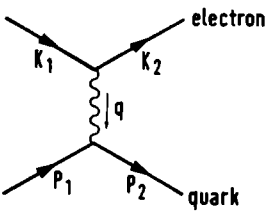

fig. 1.2: lowest order parton process contributing to electron-hadron scattering.

Substituting (1.10) in (1.7) and using (1.8) and (1.9) we get the well

known parton model expressions for the structure functions:

$$\nu W_2(x) = \sum_i e_i^2 \, x \, f_i(x)$$
$$MW_1(x) = \sum_i \frac{1}{2} e_i^2 \, f_i(x) \qquad (1.11)$$

where e_i is the charge (in units e) of the parton. These results are derived under the assumption that the charged partons are spin - $\frac{1}{2}$ particles. An immediate consequence of that assumption is the Callan-Gross relation:

$$\nu W_2 = 2x \, MW_1 \qquad (1.12)$$

This relation is, however, broken by QCD-corrections.

The important property of the leading parton model results (1.11) is that exact scaling is predicted. The distribution functions in (1.1) describe properties of a hadron, and can only depend upon variables belonging to that hadron. In particular they must be independent of the interaction scale Q^2. This remains true when higher order corrections are included; then the parton distributions appearing in (1.1) will still be independent of Q^2. It will turn out to be convenient however, to absorb part of the interaction in the parton distributions. It is by that procedure that the distributions get a scale dependence, but that is not in contradiction to the arguments given above.

2. Mass singularities

Assuming that partons are quarks and gluons, and that QCD describes the coupling of particles correctly, one can calculate corrections to the leading parton model expressions given in the previous section. In first order such corrections are due to diagrams like the ones in fig.

2.1. The solid lines in these diagrams can be quarks or gluons, as far as the Feynman rules allow it. The contribution of these diagrams is singular in the large Q^2 limit, for the following reason. In the

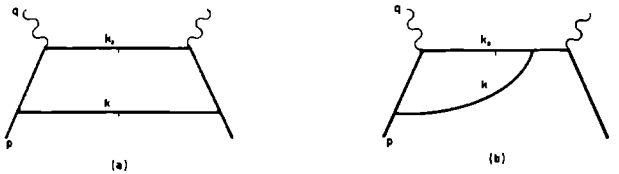

fig. 2.1: examples of cut diagrams which yield first order corrections to the parton model.

expressions for these diagrams a propagator $[(p-k_1)^2]^{-1}$ appears at least once. This propagator diverges if the angle θ between the vectors $\vec{p}$ and $\vec{k}_1$ vanishes, and if p^μ and k_1^μ correspond to massless, on-shell particles:

$$(p-k_1)^2 = -2\,|\vec{p}|\,|\vec{k}_1|\,(1-\cos\theta) \sim -\,|\vec{p}|\,|\vec{k}_1|\,\theta^2 \quad .$$

The phase space integral has the following angular part:

$$\int_0^\pi \sin\theta\, d\theta \sim \int \theta\, d\theta$$

and therefore one can expect a logarithmic and a quadratic singularity for diagrams with the topology of fig. 2.1b and 2.1a respectively. (The other propagator in fig. 2.1b does not have a singularity.) We have, however, not yet considered the numerator factors. It can be shown easily, that for each vertex at which two partons are emitted almost parallel to each other, one gets a factor θ (the angle between the directions of the two partons), as long as only the physical polarizations of the gluons are taken into account. This is true both for the

quark-gluon vertex and the three-gluon vertex of appendix I-A. The restriction to physical polarizations can be made by choosing the axial gauge. In that gauge one obtains an additional factor θ^2 for diagram 2.1a and θ for diagram 2.1b, so that the latter is finite and the first has a logarithmic singularity. This singularity can be regularized by giving the partons a mass or taking the incoming parton off mass shell. Due to these singularities, which are called mass singularities, the series expansion of the parton cross section becomes essentially:

$$\sigma = \sigma^{(0)} + \alpha_s(Q^2) \left[\sigma_0^{(1)} + \sigma_1^{(1)} \ln (p^2/Q^2)\right] + \ldots \qquad (2.1)$$

where p^2 is the variable which cuts off the mass singularity and $\alpha_s = \frac{g^2}{4\pi}$, where g is the QCD coupling constant. When the renormalization group is used to sum up the logarithms coming from the vertex corrections, α_s is replaced by a Q^2 dependent coupling variable, which, for a non-abelian gauge theory, becomes small for large Q^2. But according to (2.1) perturbation theory is spoiled in that limit by the mass singularity.

In field theory, the appearance of mass singularities is controlled by the Lee-Nauenberg-Kinoshita (LNK) theorem [Lee 64, Kin 62]. According to this theorem the cross section for a process is finite when the mass of one of the particles goes to zero, provided that one sums over all initial and final states which are degenerate. Two states are called degenerate if they cannot be distinguished experimentally. A well known example is the cancellation of I.R divergencies in QED. If the mass of the photon goes to zero the electron becomes degenerate with states consisting of an electron plus a number of infinitesimally soft photons. If one sums over all these states in the calculation of the cross

section, the result is finite for vanishing photon mass. In the example discussed above we have a different kind of degeneracy, which is due to the fact that the quarks become effectively massless for large Q^2. Such a quark can emit a gluon parallel to its direction of motion without violating energy momentum conservation. Therefore a single quark is degenerate with states containing a quark plus parallel gluons and, according to the LNK theorem, a physically meaningful and finite cross section is obtained only if one sums over all these states. This is done for jet cross sections in e^+e^- annihilation, where degenerate states contribute to the same jet. When one sums over all particles in a jet, the resulting cross section is finite. In the case of initial quarks, as in deep-inelastic scattering, the cancellation of mass singularities will only occur if beside a summation over final state degeneracies (which is always made in an inclusive process) also a summation over initial state degeneracies is made. When this is not done a mass singularity belonging to each initial parton remains.

To discuss the solution to this problem we will first consider the appearance of mass singularities in higher orders. According to the arguments given above such singularities will appear for each double occurrence of a divergent propagator in a cut diagram. Therefore the leading singularities in each order in α_s are due to ladder diagrams as in fig. 2.2. When for example two of the rungs of the ladder are crossed two propagators will be different in the left and right half of the diagram and the singularity will be reduced.

To simplify the discussion we consider the moments of the parton cross sections. For a cross section $\sigma_j(x)$, as introduced in (1.1), the moments are defined as follows:

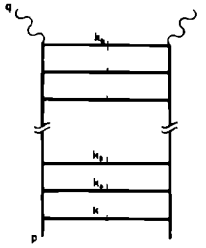

fig. 2.2: ladder diagram contributing to the leading mass singularity.

$$\sigma_j^n = \int_0^1 dx\, x^{n-1}\, \sigma_j(x) \qquad (2.2)$$

The advantage of these moments is that the leading mass singularities coming from the ladder diagrams can be summed to all orders and are found to exponentiate:

$$\sigma_i^n\ (\ln p^2/Q^2) = \sum_j \tilde{\sigma}_j^n\ (\ln p^2/Q^2)\ [\exp \frac{\alpha_s}{4\pi}\, \gamma_0^n\, \ln p^2/Q^2]_{ji} \qquad (2.3)$$

The remainder, $\tilde{\sigma}_j^n$ is free of leading singularities, but it still contains non-leading ones. The matrix γ_0^n turns out to be the anomalous dimension matrix of the operators in the O.P.E.

The next step is the generalization of this factorization to non-leading mass singularities. This can be done by replacing the rungs of the ladder by two particle irreducible scattering kernels. It can be shown that the following relation holds for deep-inelastic scattering

$$\sigma_j^n\ (\ln p^2/Q^2) = \sum_j \sigma_j^n(0)\ \Gamma_{ji}^n(\ln p^2/Q^2) \qquad (2.4)$$

In this case the remainder, $\sigma_j^n(0)$, is finite; all singularities have been factorized into Γ^n.

The relation between the parton cross sections and the hadron cross section is given by (1.1). In terms of moments this relation reads:

$$\sigma_H^n = \sum_j \sigma_j^n(\ln p^2/Q^2)\ f_j^n \tag{2.5}$$

where

$$f_j^n = \int_0^1 dx\ x^{n-1}\ f_j(x) \tag{2.6}$$

Substituting the factorized expression (2.4) into (2.5) we get:

$$\sigma_H^n = \sum_j \sigma_j^n(0)\ \tilde{f}_j^n(Q^2) \tag{2.7}$$

where

$$\tilde{f}_j^n(Q^2) = \sum_i \Gamma_{ji}^n(\ln p^2/Q^2)\ f_i^n \tag{2.8}$$

This last relation can be interpreted as a renormalization of the moments of the distribution functions. When theoretical results are compared with experiment, one uses (2.7), which resembles the leading parton formula if only the first term on the perturbation expansion of $\sigma_j^n(0)$ is kept. That should be a good approximation, because $\sigma_j^n(0)$ is a well-behaved power series in α_s, and for large enough Q^2 the corrections should be small. When these higher orders are neglected (2.7) differs from the naive parton model formula only because the distributions depend upon the interaction scale Q^2. What is measured is clearly $\tilde{f}_j^n(Q^2)$, and not f_j^n, which, by analogy to charge or mass renormalization, may be called the moments of the bare parton distributions.

This procedure is in fact nothing else than a translation of the operator product expansion into parton language. The factors $\sigma_j^n(0)$ appearing in (2.7) are the equivalent of the coefficient functions and the moments of the distribution functions correspond to the operator matrix elements. The Q^2-dependence of the distribution functions is governed by equations involving the anomalous dimensions of the operators [Alt 77]. As we will show in the next section, one can

derive a renormalization group equation for the Γ-factors using the factorization property (2.4).

The main advantage of this factorization formalism, beside the nice intuitive picture of scaling deviations which it offers, is the fact that it can also be applied to some processes with two incoming hadrons, for which the OPE does not work. The ladder diagram which yields the leading logarithms for such processes is shown in fig. 2.3. An example

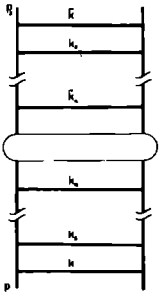

fig. 2.3: ladder diagram for two incoming hadrons. The blob corresponds to some parton interaction, e.g. annihilation into a virtual photon.

of such a process is the production of lepton pairs in hadron-hadron scattering. As we will show in the next chapter the parton model leads to the following relation between the moments of the cross sections and the parton distributions for this process:

$$\sigma^n = \sum_{i,j} \sigma^n_{ij} f^n_i f^n_j \qquad (2.9)$$

where σ^n is the hadron cross section and σ^n_{ij} the corresponding one for partons i and j. It can be shown that the mass singularities, produced by diagrams like that of fig. 2.3, factorize in the following way:

$$\sigma^n_{ij}(\ln p_1^2/Q^2,\ \ln p_2^2/Q^2) = \sum_{\ell k} \sigma^n_{\ell k}(0,0)\ \Gamma^n_{\ell i}(\ln p_1^2/Q^2)\ \Gamma^n_{kj}(\ln p_2^2/Q^2) \qquad (2.10)$$

where p_1^2 and p_2^2 are the cut off parameters for the mass singularities belonging to the two incoming partons. The factors Γ^n are the same as the one which appears in (2.4). This can be understood by noticing that the same ladder structures appear for each incoming hadron in all processes.

The statements made above have all been proven rigorously in perturbation theory. The ideas were first formulated and tested at the leading logarithm level [Gri 72, Par 76, Alt 77, Pol 77, Sac 78]. The general proof is considered by [Mue 78, Ell 78, Ell 79, Ama 78, Lib 78, Dok 78, Mue 79, Hum 80]. More extensive references can be found in these papers.

3. Factorization and the renormalization group

In this section we will derive the renormalization group equations for the transition functions. These equations are a consequence of the factorization of mass singularities discussed in the previous section. We will consider processes with one or two incoming hadrons, for which the moments of the hadron and the parton cross sections are related as follows:

$$\sigma_H^n = \sum_i \sigma_i^n f_{i,H}^n \tag{3.1}$$

$$\sigma_{H_1H_2}^n = \sum_{i,j} \sigma_{ij}^n f_{i,H_1}^n f_{j,H_2}^n \tag{3.2}$$

where f_{i,H_k}^n is the n^{th} moment of the distribution function for parton type i in hadron H_k, σ_H^n and $\sigma_{H_1H_2}^n$ are moments of cross sections or structure functions for a process with one and two incoming hadrons respectively, and σ_i^n and σ_{ij}^n the corresponding quantities for partons. For some processes with two incoming hadrons it is convenient to introduce double moments:

$$\sigma_{H_1H_2}^{nm} = \sum_{i,j} \sigma_{ij}^{nm} f_{i,H_1}^n f_{j,H_2}^m \tag{3.3}$$

This does not alter any of the arguments given below. To simplify the notation we will leave out the moment indices and the indices H_k in the following.

To arrive at a renormalization group equation for the scale dependent distribution functions we consider first the parton cross sections. These cross sections, calculated with properly normalized external lines, satisfy a renormalization group equation governing the asymptotic behavior of the vertex corrections:

$$\left[\mu \frac{\partial}{\partial \mu} + \beta(g) \frac{\partial}{\partial g}\right] \sigma_{ij} = 0 \tag{3.4}$$

Here μ is the scale parameter associated with the renormalization of the coupling constant. The cross section depends upon some interaction scale Q^2, regulators p_i^2 for the mass singularity belonging to incoming parton i (p_i^2 can be the square of a mass or the square of one of the incoming four-momenta), and the renormalization scale μ. Further there may be other Lorentz-invariants, which we assume to have a fixed ratio with Q^2 if Q^2 becomes large. When cases are considered where such a ratio is close to a limiting value, one may find a kinematical singularity in that limit, which spoils perturbation theory. We will not consider that situation here, and restrict ourselves to singularities appearing for $Q^2 \to \infty$, with all dimensionless ratio's except p_1^2/Q^2 and μ^2/Q^2 kept fixed.

Neglecting the irrelevant kinematical variables we can write the parton cross section in the following way:

$$\sigma_{ij} = \sigma_{ij}\ (g,\ u,\ v_1,\ v_2) \tag{3.5}$$

where

$$\begin{aligned} u &= \frac{1}{2}\ \ln\ (\mu^2/Q^2) \\ v_1 &= \frac{1}{2}\ \ln\ (\mu^2/p_1^2) \\ v_2 &= \frac{1}{2}\ \ln\ (\mu^2/p_2^2) \end{aligned} \tag{3.6}$$

Expressing (3.4) in terms of these variables we obtain:

$$\left[\frac{\partial}{\partial u} + \frac{\partial}{\partial v_1} + \frac{\partial}{\partial v_2} + \beta(g)\ \frac{\partial}{\partial g}\right]\ \sigma_{ij}(g,\ u,\ v_1,\ v_2) = 0 \tag{3.7}$$

Factorization implies that matrix functions $\Gamma(g,v)$ exist with:

$$\sigma_{ij}(g,u,v_1,v_2) = \sum_{k,\ell}\ \sigma_{k\ell}(g,u,0,0)\ \Gamma_{ki}(g,v_1)\Gamma_{\ell j}(g,v_2) \tag{3.8}$$

$$\sigma_i(g,u,v) = \sum_k\ \sigma_k(g,u,0)\ \Gamma_{ki}(g,v) \tag{3.9}$$

These Γ's are the same for all processes. In particular this means that the same Γ appears in (3.8) and (3.9). This is called universality of mass singularities.

Now we substitute the factorized expressions (3.8) or (3.9) into (3.7). After some rearrangement we find that the transition functions Γ have to satisfy the following equation:

$$\sum_{\ell} \{[\mu \frac{\partial}{\partial \mu} + \beta(g) \frac{\partial}{\partial g}] \delta_{k\ell} + \gamma_{k\ell}(g)\} \Gamma_{\ell i}(g,v) = 0 \qquad (3.10)$$

where

$$\gamma_{k\ell} = - \frac{\partial}{\partial v} \Gamma_{k\ell}(g,v) \Big|_{v=0} \qquad (3.11)$$

This renormalization group equation can be used to study the behavior of the transition function for variations of μ. Notice that the transition function does not only depend upon μ via its second argument, but also via the coupling constant, which is defined at μ^2. This implicit μ-dependence is taken into account by $\beta(g) \frac{\partial}{\partial g}$. To examine the scale dependence of the transition function in a more convenient way we choose μ^2 equal to Q^2 and we introduce a parameter μ_0^2 as a fixed scale, at which we define the coupling constant. The consequence of choosing the a priori arbitrary variable μ^2 equal to Q^2 is that the variable u in the righthand side of (3.8) and (3.9) is set equal to zero, so that the remainder of the parton cross section after factorization depends upon Q^2 only through $g(Q^2)$. In perturbation theory it becomes a power series in $g(Q^2)$, which is the equivalent of the coefficient function in the O.P.E. formalism.

Introducing the variables

$$t = \frac{1}{2} \ln (Q^2/\mu_0^2) \qquad (3.12)$$

$$t_1 = \frac{1}{2} \ln (p_1^2/\mu_0^2) \tag{3.12}$$

we can write (3.10) as follows:

$$\left[\frac{\partial}{\partial t} + \beta(g) \frac{\partial}{\partial g} + \gamma(g) \right] \Gamma(g, t-t_1) \tag{3.13}$$

where γ and Γ are matrices.

As remarked above, the implicit t-dependence of Γ via g is taken into account by the second term in (3.13). This implies:

$$\begin{aligned} \frac{d}{dt} g(t) &= \beta(g(t)) \\ g(0) &= g_0 \end{aligned} \tag{3.14}$$

The second condition ensures that the coupling constant for $Q^2 = \mu_0^2$ is equal to an experimental value g_0, determined at that point. Now we can make the implicit t-dependence explicit by introducing a new distribution function:

$$\tilde{\Gamma}(t, t_1) = \Gamma(g(t), t-t_1) \tag{3.15}$$

If g(t) depends upon t as required by (3.14) the renormalization group equation becomes:

$$\frac{\partial}{\partial t} \tilde{\Gamma}(t, t_1) + \gamma(g(t)) \tilde{\Gamma}(t, t_1) = 0 \tag{3.16}$$

This equation has the following formal solution:

$$\tilde{\Gamma}(t, t_1) = T \exp - \int_{t_1}^{t} \gamma(g(\tau)) \, d\tau \tag{3.17}$$

where 'T' denotes t-ordering of the expansion of the exponent, completely analogous to the time ordered product used in the expression for the time evolution operator in quantum mechanics.

The transition functions have a similar behavior with respect to their second argument t_1. The following relation determines the t_1 dependence:

$$\frac{\partial}{\partial t_1} \tilde{\Gamma}(t,t_1) = \tilde{\Gamma}(t,t_1)\gamma(g(t_1)) \tag{3.18}$$

Using (3.17) we can derive the following product rule:

$$\tilde{\Gamma}(t,t_1) = \tilde{\Gamma}(t,t_2)\ \tilde{\Gamma}(t_2,t_1) \qquad t > t_2 > t_1 \tag{3.19}$$

Because of (3.16) and (3.18) the righthand side is independent of t_2.

The transition functions can be considered as operators, changing the scale of the distribution functions from t_1 to t. If we substitute the factorization relations (3.8) and (3.9) into (3.1) and (3.2) we get:

$$\sigma_H^n = \sum_{i,j} \sigma_i^n\ (g,u,0)\ \Gamma_{ij}^n\ (g,v_1)\ f_j^n(t_1) \tag{3.20}$$

and a corresponding relation for two incoming hadrons. For convenience we consider the 'bare' distribution function in (3.20) as a function of t_1. Choosing $\mu^2 = Q^2$ we get:

$$\sigma_H^n = \sum_{i,j} \sigma_i^n\ (g(t),0,0)\ \tilde{\Gamma}_{ij}^n\ (t,t_1)\ f_j^n(t_1) \tag{3.21}$$

Now we can define a new set of distribution functions, which are functions of t:

$$f_i^n(t) = \sum_j \tilde{\Gamma}_{ij}^n\ (t,t_1)\ f_j^n(t_1) \tag{3.22}$$

The dependence of the new distribution functions upon t is governed by the renormalization group equation (3.16):

$$\frac{df^n(t)}{dt} = -\ \gamma^n\ (g(t))\ f^n(t) \tag{3.23}$$

This equation is called the Altarelli-Parisi equation [Alt 77]. Notice that because of (3.23) and (3.18) the distributions do not depend upon t_1.

The final result of the entire procedure is the following relation between hadron and parton cross sections:

$$\sigma_H^n(t) = \sum_i \sigma_i^n(g(t))\ f_{i,H}^n(t) \tag{3.24}$$

$$\sigma_{H_1H_2}^n(t) = \sum_{i,j} \sigma_{ij}^{nm}(g(t))\ f_{i,H_1}^n(t)\ f_{j,H_2}^n(t) \tag{3.25}$$

The functions $\sigma(g(t))$ are calculable power series in the 'running coupling constant' $g(t)$. The t-dependence of the distribution functions is calculable as well, but because their scale dependence is given by a differential equation one has to know the boundary condition at some point t_0. These values can, at least at this stage of development of QCD, only be determined from experimental data.

We conclude this section by giving the conventions we will use for the notation of these equations in the case of QCD. In terms of the coupling constant g one finds for the β-function and the γ-function expressions of the following type:

$$\begin{aligned}\beta(g) &= -\beta_0 \frac{g^3}{16\pi^2} - \beta_1 \frac{g^5}{(16\pi^2)^2} - \beta_2 \frac{g^7}{(16\pi^2)^3} \cdots \\ \gamma(g) &= \gamma_0 \frac{g^2}{16\pi^2} + \gamma_1 \frac{g^4}{(16\pi^2)^2} + \gamma_2 \frac{g^6}{(16\pi^2)^3} \cdots\end{aligned} \tag{3.26}$$

Some trivial factors (a π^2 for each loop integral and a $(2\pi)^{-4}$ from the Fourier transforms) have been extracted out of the coefficients. The renormalization group equation is, as before:

$$\left[\frac{\partial}{\partial s} + \beta(g)\ \frac{\partial}{\partial g}\right]\ \Gamma(g, s-s_1) = -\gamma(g)\ \Gamma(g, s-s_1)$$

where t and t_1 are now called s and s_1. For gauge theories the effective expansion parameter is g^2 rather than g, and therefore it is convenient to introduce a new set of variables:

$$\begin{aligned} t &= 2s \quad ; \quad t_1 = 2s_1 \\ \lambda &= \frac{\alpha_s}{4\pi} = \frac{g^2}{16\pi^2} \end{aligned} \tag{3.27}$$

Then the equations are:

$$\left[\frac{\partial}{\partial t} + \beta(\lambda)\,\frac{\partial}{\partial \lambda}\right] \Gamma(\lambda, t-t_1) = -\frac{1}{2}\,\gamma(\lambda)\;\Gamma(\lambda, t-t_1) \tag{3.28}$$

where

$$\begin{aligned} \beta(\lambda) &= -\beta_0\,\lambda^2 - \beta_1\,\lambda^3 - \beta_2\,\lambda^4 + \ldots \\ \gamma(\lambda) &= \quad \gamma_0\,\lambda \;+ \gamma_1\,\lambda^2 + \gamma_2\,\lambda^3 \end{aligned} \tag{3.29}$$

with the same coefficients as in (3.26).

4. Diagonalization of the transition matrix

The transition matrix Γ_{ij}, introduced in the previous sections, mixes the various types of partons. Because QCD has the same coupling to all quark flavors, it can be partly diagonalized, at least as long as we neglect the masses of the quarks. At high enough energies this is of course certainly allowed, but for heavy quarks there will be non-negligible threshold effects at lower energies.

The partons we will consider are gluons, indicated by 'g' and N_f flavors of quarks and antiquarks, indicated by q_i and $\bar{q}_i$. Then the matrix elements of the transition matrix fall in the following categories:

$$\begin{aligned} \Gamma_{gg} &= \Gamma^S_{gg} \\ \Gamma_{q_i g} &= \Gamma^S_{qg} \\ \Gamma_{g q_i} = \Gamma_{g \bar{q}_i} &= \Gamma^S_{gq} \\ \Gamma_{q_i q_j} = \Gamma_{\bar{q}_i \bar{q}_j} &= \Gamma^S_{qq} + \Gamma^{NS}_{qq}\,\delta_{ij} \\ \Gamma_{q_i \bar{q}_j} = \Gamma_{\bar{q}_i q_j} &= \Gamma^S_{qq} + \Gamma^{NS}_{q\bar{q}}\,\delta_{ij} \end{aligned} \tag{4.1}$$

The superscript S means 'singlet', NS means 'non-singlet'. This terminology refers to the operator product expansion, where one has

flavor singlet and flavor non-singlet operators. The first three transition functions can only be singlets, because the gluon has a universal coupling to all quarks. In the case of transitions among quarks however, one has to make a distinction between transitions to the same flavor and transitions to different flavors. The latter is possible only in diagrams with separate quarklines, coupled by gluons. Due to the necessity of having an intermediate gluon such transition functions are singlets. From the diagrams of this type Γ^S_{qq} can be determined. In the case of a transition from a quark to a quark with the same flavor there are additional diagrams, in which the initial and final quarks are the begin and end of the same quarkline. These extra diagrams determine Γ^{NS}_{qq}. A transition from a quark to its own antiquark is different from a transition to a different antiquark because of identicle particle effects in the final state. This will be discussed in detail in section III.7. In figure 4.1 these arguments are illustrated by means of examples of transitions as described above. (In each case there are more diagrams than the ones shown in fig. 4.1. The dot's indicate the partons between which a transition occurs. In a physical process, the left dot in each diagram corresponds to an incoming hadron, the right dot to a parton interaction. The transitions shown here are: I: Γ^{NS}_{qq}, II: Γ^S_{gq}, III: Γ^S_{qg}, IV: Γ^S_{gg}, V: Γ^S_{qq}, VI: $\Gamma^{NS}_{q\bar{q}}$. The arrow in VI indicates that the contribution to $\Gamma^{NS}_{q\bar{q}}$ comes from the interference of this diagram with the one without crossed quark lines.)

The diagrams shown are the ones of lowest non-trivial order in each class. Therefore we may conclude:

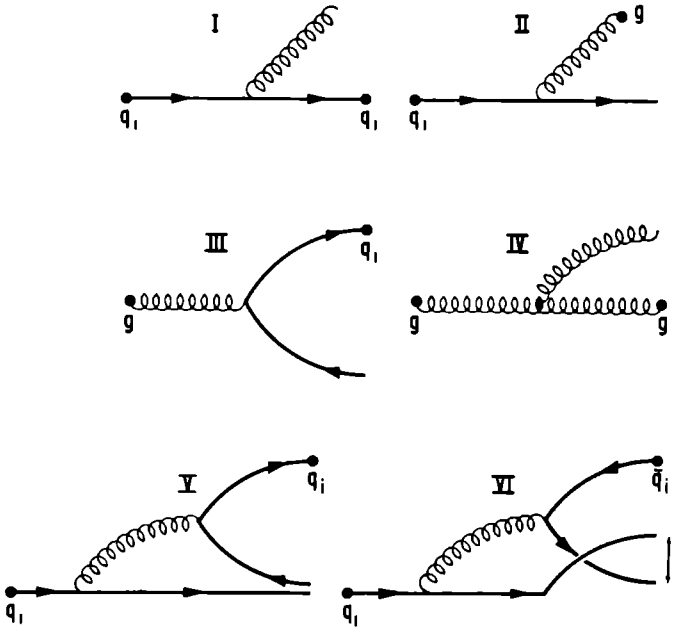

Fig. 4.1: Examples of diagrams contributing to the transition functions.

$$
\begin{aligned}
\Gamma^{S}_{gg} &= 1 + O(\alpha_s) \\
\Gamma^{S}_{qg} &= O(\alpha_s) \\
\Gamma^{S}_{gq} &= O(\alpha_s) \\
\Gamma^{NS}_{qq} &= 1 + O(\alpha_s) \\
\Gamma^{S}_{qq} &= O(\alpha_s^2) \\
\Gamma^{NS}_{q\bar{q}} &= O(\alpha_s^2)
\end{aligned}
\tag{4.2}
$$

Substituting (4.1) into (3.22) we find that the distribution functions transform in the following way:

$$
\begin{aligned}
f_g &= \Gamma^{S}_{gq} \sum_i (f^0_{q_i} + f^0_{\bar{q}_i}) + \Gamma^{S}_{gg} f^0_g \\
f_{q_i} &= \Gamma^{S}_{qg} f^0_g + \Gamma^{NS}_{qq} f^0_{q_i} + \Gamma^{NS}_{q\bar{q}} f^0_{\bar{q}_i} + \Gamma^{S}_{qq} \sum_i (f^0_{q_i} + f^0_{\bar{q}_i})
\end{aligned}
\tag{4.3}
$$

$$f_{\bar{q}_i} = \Gamma^S_{qg} f^0_g + \Gamma^{NS}_{qq} f^0_{\bar{q}_i} + \Gamma^{NS}_{q\bar{q}} f^0_{\bar{q}_i} + \Gamma^S_{qq} \sum_i (f^0_{q_i} + f^0_{\bar{q}_i})$$

The superscript '0' indicates that the corresponding distribution function is defined at $Q^2 = Q_0^2$. These input distributions are transformed to scale dependent distributions by (4.3). We can simplify these relations by introducing the following linear combinations:

$$\begin{aligned} Q &= \sum_i (f_{q_i} + f_{\bar{q}_i}) \\ V_i &= f_{q_i} - f_{\bar{q}_i} \\ \Delta_{ij} &= f_{q_i} + f_{\bar{q}_i} - f_{q_j} - f_{\bar{q}_j} \\ G &= f_g \end{aligned} \tag{4.5}$$

Then the equations become:

$$\begin{aligned} G &= \Gamma^S_{gq} Q^0 + \Gamma^S_{gg} G^0 \\ Q &= 2 N_f \Gamma^S_{qg} G^0 + (\Gamma^{NS}_{qq} + \Gamma^{NS}_{q\bar{q}} + 2 N_f \Gamma^S_{qq}) Q^0 \\ V_i &= (\Gamma^{NS}_{qq} - \Gamma^{NS}_{q\bar{q}}) V^0_i \\ \Delta_{ij} &= (\Gamma^{NS}_{qq} + \Gamma^{NS}_{q\bar{q}}) \Delta^0_{ij} \end{aligned} \tag{4.6}$$

The first two equations are equivalent to the operator mixing relations obtained in the operator product expansion approach. The four coefficients appearing in these two equations yield, when substituted into (3.11), the singlet anomalous dimension matrix. The last two equations are purely non-singlet. The distributions, evolving according to these relations are the valence distributions and the difference between the total (quark plus antiquark) distributions of two flavors.

5. First order contributions to the structure function νW_2

In this section we summarize some contributions to the transition functions up to first order in α_s. As we will discuss in section 6, the definition of the transition function is not unique, because constants can be subtracted together with the logarithms. For the calculations presented in chapter III we will choose the convention adopted by most other authors (e.g. [Alt 78, 79, Kub 79]).

According to this convention the distribution functions are redefined in such a way that all higher order corrections to the structure function νW_2 vanish. Then the only modification which QCD makes compared to the leading order result is to make the distribution functions scale dependent. Of course all other structure functions will be modified by powers of α_s. The convention described above is not sufficient to fix all arbitrariness completely; it does not determine the quark-gluon and gluon-gluon transition functions. We will come back to that problem in the next chapters.

In order to calculate the transition function according to this convention one has to calculate the first order QCD-corrections to the leading parton model result for νW_2. There are two kinds of corrections. The first consists of radiative corrections to photon-quark scattering. The diagrams are given in fig. 5.1. Diagram I interferes with the zeroth order diagram to give a contribution of order α_s. We have omitted two other diagrams which should be added to I. These are the self-energy corrections for the external quark lines. When these diagrams are added to I and the wave function renormalization constants for the external lines are taken into account, they cancel the ultraviolet singularity of I because of the QED Ward-Identity $Z_1 = Z_2$. A

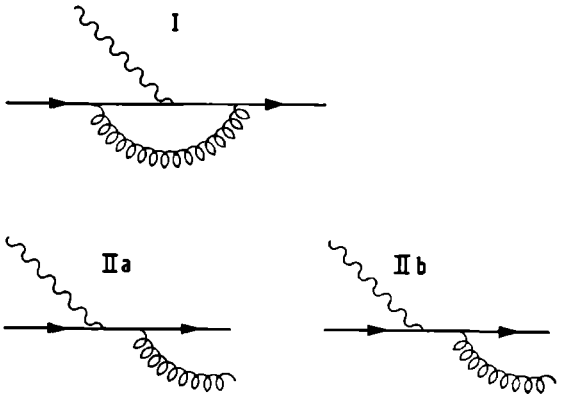

Fig. 5.1: Radiative corrections to photon-quark scattering.

simpler way to arrive at the same result is to subtract the electromagnetic form factor at $q^2 = 0$. As in QED, the infrared divergencies of diagram I are cancelled by the soft gluon parts of IIa and IIb.

To obtain the transition functions one has to do the following. First the diagrams of fig. 5.1 have to be calculated. The result is a structure function νW_2 for quark-photon scattering. This structure function is then convoluted with quark distributions according to (1.8), and the result is added to the leading order result (1.11). Now, to satisfy the requirement that νW_2 should not have perturbative corrections the distributions in the leading order term are modified in such a way that the perturbative correction is entirely absorbed. This determines the transition function. According to [Kub 79] the result is (see also [Alt 79]):

$$f_q(x,Q^2) = f_q(x) + \frac{N^2-1}{N}\,\frac{\alpha_s}{4\pi}\int_x^1 \Bigg\{ \frac{d\xi}{\xi}\, f_q(\xi) \Big[\delta(1-\eta)\left(2\ln\varepsilon + \frac{3}{2}\right) + \theta(\xi - (1+\varepsilon)x)\,\frac{1+\eta^2}{1-\eta}\Big]\ln(Q^2/m^2) + \delta(1-\eta)\left[-\frac{\pi^2}{3} - \ln^2(\varepsilon) - \frac{5}{2} - \frac{7}{2}\ln\varepsilon\right] + \theta(\xi - (1+\varepsilon)x)\left[-\frac{1+\eta^2}{1-\eta}\ln(\eta(1-\eta)) + \frac{1}{2}\,\frac{1-8\eta}{1-\eta} + 3\eta\right]\Bigg\} \tag{5.1}$$

where $\eta = \frac{x}{\xi}$. Here ε is an infrared cut-off parameter. One can easily check that the result is independent of ε apart from terms which vanish for $\varepsilon \to 0$. In (5.1) the mass m of the quark was used to regularize the mass singularity, which now appears for $m \to 0$. Alternatively one could have taken the incoming quarks off-shell and use the 'off-shell-ness' of this quark in a regulator. This method would have led to a different transition function, but exactly the same deep-inelastic scattering results. The coefficient $\frac{N^2-1}{N}$ in (5.1) is the color factor for the group SU(N). We will give all color factors for arbitrary N so that they can be easily identified. Of course QCD corresponds to N = 3.

The transition function is implicitly defined by (5.1):

$$f_q(x,Q^2) = f_q(x) + \int_x^1 \frac{f_q(\xi)}{\xi}\,\Gamma_{qq}\left(\frac{x}{\xi}, \ln(Q^2/m^2)\right) d\xi \quad . \tag{5.2}$$

A second contribution to νW_2 is given by the diagrams of fig. 5.2.

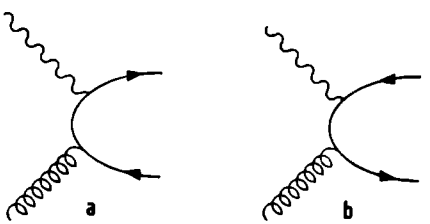

fig. 5.2: gluon-photon scattering diagrams.

In this case we have a new subprocess, which was not possible in leading order because of the absence of a photon-gluon coupling. The incoming gluon requires some care, especially when an off-shell regularization method is used, because the gluon has both transverse and longitudinal polarizations in that case. This problem can be solved by introducing separate distributions for transverse and longitudinal gluons [Sch 80a]. Then one finds the following transition function:

$$f_q(x,Q^2) = \frac{\alpha_s}{4\pi}\int_x^1 d\xi\,\frac{f_g^T(\xi)}{\xi}\left\{-[(1-\eta)^2+\eta^2]\,\ln\left[\left(\frac{m^2\eta^2}{1-\eta}-p^2\eta^2\right)/Q^2\right]\right.$$
$$\left.+6\eta-6\eta^2-1-\eta(1-\eta)\left[\frac{p^2-2p^2\eta(1-\eta)+2m^2}{p^2\eta(1-\eta)-m^2}\right]\right\} \qquad (5.3)$$
$$+\frac{\alpha_s}{4\pi}\int_x^1\frac{f_g^L(\xi)}{\xi}\left[\frac{-4p^2\eta^2(1-\eta)^2}{p^2\eta(1-\eta)-m^2}\right]$$

Here we used two regulators, a quark mass m, and a gluon which is off-shell by an amount p^2. Expression (5.3) contains the results of [Kub 79, Alt 79, Con 79b] as special cases. We will use this expression in chapter III to show explicitly that a physical result does not depend upon the regularization method. As a consequence the longitudinal gluon distributions decouple from the physical results.

6. Ambiguities in the perturbation expansion

In the previous section we discussed the one-loop QCD-corrections to the parton model. If higher orders are calculated one finds that the subtraction of singularities is not unambiguous. By subtraction we mean here either the subtraction of ultra-violet divergencies in a renormalization procedure, or the absorption of mass singularities into parton distributions. In fact the two procedures are closely related, and they are the same for the operator product expansion.

Before we discuss the ambiguities we want to make a few general remarks about their physical relevance. First of all the results are not really undetermined. The differences between two subtraction procedures are always within the theoretical uncertainty. This means that if a calculation is performed up to a certain order in the coupling constant, and if a consistent procedure is used, the subtraction ambiguities have an effect of higher order in the coupling constant. Unfortunately such an order of magnitude argument does not give any information about the coefficients of these neglected higher order terms. When a calculation is done a choice has to be made for the subtraction scheme, and clearly the best choice is the one which minimizes the higher order effects. But without a calculation of these higher order effects the best one can do is to make a reasonable choice on the basis of the known corrections. This problem is the subject of several recent investigations [Cel 80, Ste 80].

To discuss subtraction ambiguities we go back to the results of section I.3. There a set of renormalization constants Z_3 and Z_g was introduced in order to cancel poles in the calculated Green's functions. For a given choice of these renormalization constants the anomalous dimension and β-function are given by (I.3.6) and (I.3.7). The renormalization constants have to meet the requirement that they lead to a finite Green's function. But if $G_R^m(p,g_R,\varepsilon,\mu)$ is finite for $\varepsilon \to 0$, then that is also the case for:

$$G_R^{m*}(p,g_R^*,\varepsilon,\mu) = [X_3^m(g_R^*,\varepsilon)]^{-m/2}\, G_R^m(p,g_R^*\, X_g(g_R^*,\varepsilon),\varepsilon,\mu) \qquad (6.1)$$

provided

$$\lim_{\varepsilon\to 0} X(g_R^*,\varepsilon) = X(g_R^*) \qquad \text{exists.} \qquad (6.2)$$

Comparing (6.1) and (I.3.4) we can determine the modified renormalization constants:

$$Z_3^*(\mu,g_R^*,\varepsilon) = X_3(g_R^*,\varepsilon)\ Z_3(\mu,g_R^*\ X_g(g_R^*,\varepsilon),\varepsilon)$$
$$Z_g^*(\mu,g_R^*,\varepsilon) = X_g(g_R^*,\varepsilon)\ Z_g(\mu,g_R^*\ X_g(g_R^*,\varepsilon),\varepsilon) \tag{6.3}$$

The effect of a change in the subtraction procedure upon $\beta(g)$ and $\gamma(g)$ can now be calculated with (I.3.6) and (I.3.7):

$$\begin{aligned}\beta^*(g_R^*) &= \lim_{\varepsilon\to 0} \mu\frac{\partial}{\partial\mu}\, g_R^*(\mu,\varepsilon,g_u)\Big|_{g_u} \\ &= \beta(g_R^*\ X_g(g_R^*))\left[\frac{d}{dg_R^*}\left[g_R^*\ X_g(g_R^*)\right]\right]^{-1}\end{aligned} \tag{6.4}$$

$$\begin{aligned}\gamma^*(g_R^*) &= \lim_{\varepsilon\to 0} \mu\frac{\partial}{\partial\mu} \ln Z_3^*(\mu,g_R^*,\varepsilon)\Big|_{g_u} \\ &= \gamma(g_R^*\ X_g(g_R^*)) + \beta^*(g_R^*)\frac{d}{dg_R^*}\ln X_3(g_R^*)\end{aligned} \tag{6.5}$$

Of course with these modifications G_R^* satisfies the equation:

$$\left[\mu\frac{\partial}{\partial\mu} + \beta(g_R^*)\frac{\partial}{\partial g_R^*} + \frac{m}{2}\gamma^*(g_R^*)\right]\ G_R^{m*}(p,g_R^*,\mu) = 0 \tag{6.6}$$

Next we will consider the analogous situation for factorization ambiguities. Relation (3.21) can be rewritten in the following way:

$$\begin{aligned}\sigma_H &= \sigma_i(g(t))\ \Gamma_{ij}\ (g(t),t-t_1)\ f_j(t_1) \\ &= \sigma_i^*(g(t))\ \Gamma_{ij}^*\ (g(t),t,t_1)\ f_j^*(t_1)\end{aligned} \tag{6.7}$$

where

$$\sigma_i^*(g(t)) = \sigma_i(g(t))\ X_{ij}(g(t)) \tag{6.8}$$

$$\Gamma_{ij}^*(g(t),t,t_1) = X_{i\ell}^{-1}(g(t))\ \Gamma_{\ell m}(g(t),t-t_1)\ X_{mj}(g(t)) \tag{6.9}$$

$$f_i^*(t_1) = X_{ij}^{-1}(g(t_1))\ f_j(t_1) \tag{6.10}$$

Clearly the finite renormalization matrices X cancel in the final result. Therefore the difference between the old and the new quantities

is physically irrelevant. Only the product of the three factors, summed over all parton-indices can be measured experimentally. This may raise some questions concerning the physical interpretation which one would like to give to the parton distributions. This freedom of definition shows that this interpretation should not be taken too seriously. If one still wants to use this concept, care must be taken that at least some of the basic properties of the distribution functions, like the normalization of valence distributions, momentum conservation and positivity are preserved by the QCD corrections. We will come back to some of these points in chapter IV. We would like to emphasize, however, that such an intuitive physical interpretation is not really needed, when the parton distributions are used only to transfer information about the structure of a hadron from one process to another. Then a change of definition does not make any difference, apart from higher order effects. Of course one has to take care that the same definition is used in all processes.

Now we will show that the transformed transition functions have exactly the same properties as the ones introduced in section 3. First of all, they are functions of $t-t_1$ instead of t and t_1 separately. This can be shown by expressing $g(t_1)$, appearing in one of the factors multiplying Γ, in terms of g(t). The relation between the two coupling constants is a double expansion in g(t) and $t-t_1$.

One can derive a renormalization group equation for the modified transition function by calculating the effect of the operator $\mu \frac{\partial}{\partial \mu} + \beta(g) \frac{\partial}{\partial g}$ (modifications of the coupling constant will not be considered again here; they have the same effect as discussed above). Using the known behavior of the original transition function we find:

$$\left[\mu \frac{\partial}{\partial \mu} + \beta(g) \frac{\partial}{\partial g} \right] \Gamma^*(g,t-t_1) = - \gamma^*(g) \Gamma^*(g,t-t_1) \qquad (6.11)$$

where Γ and γ are matrices. The modified anomalous dimension matrix is:

$$\gamma^*(g) = - \frac{\partial}{\partial v} \Gamma^*(g,v) \Big|_v$$

$$= X^{-1}(g) \gamma(g) X(g) + \beta(g) X^{-1}(g) \frac{\partial}{\partial g} X(g) \qquad (6.12)$$

This is the same relation as (6.5), but it includes the possibility of operator mixing.

The modified transition function can be expressed as formal solutions of the renormalization group equations, like (3.17), but with different anomalous dimension and β-function. The product rule (3.19) remains valid. The new transition function is clearly completely equivalent to the old one.

We will now compare two different parametrizations. The changes occur in the parton cross sections (corresponding to the coefficient functions in the operator product expansion) and the scale-dependent distributions. Formally we have different expressions for the measured cross-section

$$\sigma_H = \sigma(g(t)) \left[T \exp - \int_{t_1}^{t} \gamma(g(\tau)) \, d\tau \right] f(t_1) \qquad (6.13)$$

$$\sigma_H = \sigma^*(g^*(t)) \left[T \exp - \int_{t_1}^{t} \gamma^*(g^*(\tau)) \, d\tau \right] f^*(t_1) \qquad (6.14)$$

we have taken into account the possibility of coupling constant redefinition in (6.14). The scale-dependent couplings are defined by:

$$\frac{dg(t)}{dt} = \beta(g(t)) \quad ; \quad g(0) = g \qquad (6.15)$$

$$\frac{dg^*(t)}{dt} = \beta^*(g^*(t)) \quad ; \quad g^*(0) = g^* \qquad (6.16)$$

The values at the definition point $t = 0$ are related by the finite renormalization:

$$g = g^* \, X_g(g^*) \tag{6.17}$$

Formally there is no problem associated with these different results, because they are equivalent if we use the expressions to all orders in the coupling constant. Using (6.12) one can show:

$$T \exp - \int_{t_1}^{t} \gamma^*(g^*(\tau))\, d\tau = X^{-1}(g^*(t))\; T \exp - \int_{t_1}^{t} \gamma(g^*(\tau)) d\tau \; X(g^*(t_1)) \tag{6.18}$$

The X-factors reappear and cancel the ones in the parton cross section and the disctribution function. This is not surprising, since they were introduced that way. The problem is, however, that in practical situations one does not use the formal solution of the renormalization group equation, nor a complete expression for the parton cross sections.

Relation (6.18) can be applied to obtain an often used approximation to the exact solution of the renormalization group equations. To derive it we expand the relevant functions in the coupling constant:

$$\begin{aligned} X &= 1 + \sum_{n=1}^{\infty} X^{(n)} g^n \quad ; \quad X_g = 1 + \sum_{n=1}^{\infty} X_g^{(n)} g^n \\ \gamma &= \sum_{n=1}^{\infty} \gamma^{(n-1)} g^n \quad ; \quad \beta = - \sum_{n=2}^{\infty} \beta^{(n-2)} g^n \end{aligned} \tag{6.19}$$

where X, $X^{(n)}$, γ and $\gamma^{(n)}$ are matrices and 1 is a unit matrix. For gauge theories these expansions are correct if the squared coupling constant is used as expansion parameter.

Using (6.4), (6.5) and (6.12) one can easily show that $\gamma^{(0)}$, $\beta^{(0)}$ and $\beta^{(1)}$ are not modified for any choice of $X^{(n)}$ and $X_g^{(n)}$. All other coefficients, however, are arbitrary. One can use this freedom to redefine the anomalous dimension matrix, by choosing suitable matrices $X^{(n)}$, in such a way that only the first coefficient remains. Then (6.18) can be applied for a non-trivial γ^*, but with $\gamma = \gamma^{(0)} g$. Whereas for γ^* the T-ordering is non-trivial, the matrices γ commute for all

values of g(t), and therefore T-ordering can be omitted. The solution is then:

$$\Gamma_0(t,t_1) = \exp\left\{ \frac{\gamma^{(0)}}{\beta^{(0)}} \ln\left[\frac{g(t)\,(1+bg(t_1))}{g(t_1)\,(1+bg(t))}\right]\right\} \qquad (6.20)$$

where $b = \frac{\beta^{(1)}}{\beta^{(0)}}$. This is an exact solution of the renormalization group equations if g(t) is an exact solution to (6.15). We have truncated the β-function after the second coefficient to obtain (6.20); effects of coupling constant redefinition will be discussed later in this section. In (6.20) $\gamma^{(0)}$ is a matrix, which can be diagonalized and subsequently exponentiated. The higher order contributions to the anomalous dimension matrix can be taken into account by calculating the finite renormalization matrix X which makes these higher orders disappear. Then (6.18) gives the approximated solution:

$$\Gamma(t,t_1) = X^{-1}(g(t))\ \Gamma_0(t,t_1)\ X(g(t_1)) \qquad (6.21)$$

The approximation made is the truncation of the expansions for the X-factor. The equation for the first coefficient is:

$$[\gamma^{(0)}, X^{(1)}] + X^{(1)}\ \beta^{(0)} = \gamma^{(1)} \qquad (6.22)$$

Similar, but more and more complicated equations can be derived for the higher order coefficients.

When results, obtained with different conventions, are compared and when perturbative approximation (6.21) is used, they will be exactly the same, without any small corrections. This is due to the fact that both results are truncated power series in the coupling constant, multiplied by the same expression $\Gamma_0(t,t_1)$. The results can only be identical up to a given order in the coupling constant when these power series are identical up to that order.

This exact cancellation of arbitrary constants does not occur when the renormalization group equations for the transition functions are solved in a different way. An example of such a different method is numerical integration of the equations. With that method one finds numerical differences between two definitions of the subtraction procedure. This is due to incomplete cancellations of arbitrary constants beyond the order up to which one has included correction terms, as was discussed in the beginning of this section. These factorization ambiguities have not played a very important role in deep inelastic scattering phenomenology up to now, because most analyses use (6.20) and (6.21). Therefore, even if different subtraction schemes are chosen initially, all results are finally calculated in the same scheme, namely the one in which the renormalization group equations are most easily solved. For a determination of parton distributions or a comparison of different processes, however, these ambiguities are important, and care must be taken that consistent definitions are used everywhere.

The definition of the coupling constant is a more serious source of problems and confusion. In any field theory one can define the coupling constant by means of the vertex diagram with external momenta which are kept fixed to certain values. All ultra-violet divergencies due to loop corrections are subtracted in such a way that the renormalized coupling constant at that subtraction point keeps that value. This value has to be determined experimentally. In this respect there is no difference between QED and QCD. But in QED there is a natural choice for this definition: the electron-photon vertex with on-shell electrons at $q^2 = 0$. This definition is useless for QCD, because

perturbation theory does not make sense in that limit. Therefore the coupling constant is defined at some arbitrary point $q^2 = \mu^2$ (preferably with $\mu^2 < 0$ to avoid threshold effects), or, which is just as arbitrary, one uses the minimal subtraction scheme*. For any definition one obtains perturbation expansions which can be compared to the experimental data in order to determine the coupling constant corresponding to that definition. Because there is no natural definition, several possibilities are used in the literature, related to each other by finite renormalizations.

The coupling constant is usually expressed in terms of a parameter Λ, which has the dimension of a mass. To define it we consider the formal solution of equation (6.15):

$$g(t) = F_\delta^{-1}(t + F_\delta(g)) \tag{6.23}$$

where

$$F_\delta(g) = \int_\delta^g \frac{1}{\beta(\tau)}\, d\tau \tag{6.24}$$

The QCD scale parameter is defined as follows:

$$\Lambda_\delta = \mu \exp\,[-F_\delta(g)] \tag{6.25}$$

Here μ is either the subtraction point defined above, or, when minimal subtraction is used, it is the scale parameter introduced in the dimensional regularization procedure. In either case the 'constant' g depends upon the choice of μ. This dependence is determined by (6.23), and it is such that Λ_δ, as defined by (6.25) is independent of the choice one makes for μ. To get the coupling constant at a different

*This means that dimensional regularization is used and that only the poles in $\epsilon = 4 - n$ are subtracted.

subtraction point μ' one can substitute $t = \frac{1}{2} \ln (\mu'^2/\mu^2)$ in (6.23). This can also be stated as follows QCD predicts the scale dependence of the coupling constant, but not the magnitude. The scale dependence is determined by a first order differential equation, and the solutions to that equation form a one-parameter class of curves; Λ can be used to label these curves. To determine which curve is the physical one, the coupling constant must be determined at some point μ. But irrespective of that point one will always find the same curve, and hence the same value for Λ.

According to (6.25) there is, however, a problem with the definition of this scale parameter, because it depends upon the arbitrary integration constant δ. Notice that this parameter δ cancels in (6.23).

The appearance of this ambiguity is related to the subtraction scheme dependence of the coupling constant. When a different subtraction scheme is used one obtains a different β-function, given by (6.4), and therefore a different scale dependence of the coupling constant. Using (6.4), (6.16) and (6.17) one can show explicitly [Sch 79]:

$$g(t) = g^*(t)\ X_g(g^*(t)) \tag{6.26}$$

as expected. We have already mentioned the fact, that not only the first, but also the second coefficient of the β-function is unique. This is at first sight surprising, because this second coefficient depends upon the non-leading ultra-violet divergence in two loops, which is affected by the subtraction made at the one-loop level. This subtraction determines the first non-trivial coefficient of $X_g(g)$. For two different subtractions one obtains different expansions in different

coupling constants g(t) and g*(t). But these expansions can be expressed into each other by means of (6.26) and therefore the physical result is the same. The one-loop subtraction constant does not affect the scale dependent coupling constant via the β-function, but via the boundary condition of the differential equation.

To show that this is related to the definition of Λ we consider the following perturbative solution of equations (6.14):

$$g(t) = F_{\delta}^{-1}(y) = \sum_{n=1}^{\infty} \sum_{m=0}^{n-1} a_{nm}\, y^{-n} [\ln (y)]^m \qquad (6.27)$$

where $y = \frac{1}{2} \ln (Q^2/\Lambda^2)$.

This is the expression for the coupling constant which is most often used. To prove that it is indeed a solution one can substitute it into (6.14) and expand it in n up to a certain power. This expansion is justified if y^{-1} is small, which is the case for large Q^2. When (6.27) is substituted into the equation one finds that a_{20} remains undetermined. All other coefficients can be expressed in terms of a_{20} and the coefficients of the β-function. Notice, however, that this coefficient can be absorbed in Λ by making a redefinition:

$$y^{-1} = \tilde{y}^{-1} \left[1 + \sum_{k=1}^{\infty} \left(- \frac{\ln \gamma}{\tilde{y}}\right)^k\right]$$

where $\tilde{y} = \ln \frac{Q}{\gamma\Lambda}$.

The arbitrary factor γ can be chosen in such a way that a_{20} is cancelled. This factor corresponds to the arbitrary constant δ in (6.25), which also modifies Λ in a multiplicative way. This ambiguity in expansion (6.27) was first noticed by [Bac 78]. To give a proper definition of the parameter Λ, which is often used in phenomenological considerations, one has to fix a_{20} for instance by choosing it equal to zero. In any case the value of Λ is meaningless if only the first

term in the perturbation expansion is used.

When a_{20} is fixed, a finite renormalization of g into g* changes it. It can be reset to its conventional value by making a change in Λ. This shows that the one-loop subtraction scheme dependence of the coupling constant appears as a subtraction scheme dependence of Λ.

To investigate the dependence of Λ upon the definition we have plotted $\alpha_s(Q^2) = \frac{g^2(Q^2)}{4\pi}$ for QCD, with different definitions of Λ (fig. 6.1). The plotted function is:

$$\alpha_s(Q^2) = \frac{4\pi}{\beta_0} \frac{1}{\ln \frac{Q^2}{\gamma^2\Lambda^2}} - \frac{4\pi}{\beta_0} \frac{\ln \gamma^2}{\ln^2 \frac{Q^2}{\gamma^2\Lambda^2}} - \frac{4\pi\beta_1}{\beta_0^3} \frac{\ln(\ln(Q^2/\gamma^2\Lambda^2))}{\ln^2(Q^2/\gamma^2\Lambda^2)} \qquad (6.28)$$

The dependence upon γ vanishes up to this order in the expansion. We have plotted this function for Λ = 500 MeV and several values of γ. As expected there is not much difference in α_s for large values of Q^2 although $\Lambda_\gamma = \gamma\Lambda$ ranges from 0.01 GeV to 2 GeV. This shows that much care is needed in comparing values of Λ obtained in different analyses.

Finally we should mention still another ambiguity in the perturbation expansion: the definition of the scale variable. When the renormalization group equations are solved, the logarithms $\ln(Q^2/\mu^2)$ are summed to all orders and appear as modifications of the coupling constant into a 'running coupling constant' and of scaling parton distributions into scale dependent ones. The renormalization group does not determine which scale variable Q^2 one should use; the procedure works for any choice one makes. A change in Q^2 is identical to a change in μ^2. This allows us to trace the effects of such a change in a simple way. For that purpose we consider a dimensionally regularized and renormalized expression like (3.4). The μ-dependence of the renormalized result can be attributed completely to the renormalization

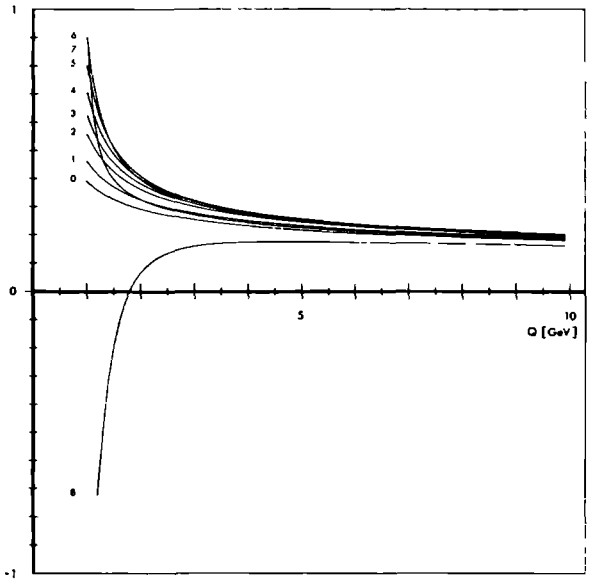

fig. 6.1: plot of (6.28). Λ = 0.5 GeV; $\beta_0 = 11 - \frac{8}{3}$; $\beta_1 = 102 - \frac{152}{3}$ (four flavors); γ^2 = .01;.032;.1;.178;.316;.562;1.0;1.78 and 3.16 for curve 0 - 8 respectively.

constants. For dimensional reasons these constants depend upon μ in the following way:

$$Z_3(\mu,g_R,\varepsilon) = \mu^{-\varepsilon}\ (1 + \sum_{n=1}^{\infty} \frac{c_n(g_R)}{\varepsilon^n})$$
$$Z_g(\mu,g_R,\varepsilon) = \mu^{\varepsilon}\ (1 + \sum_{n=1}^{\infty} \frac{a_n(g_R)}{\varepsilon^n}) \qquad (6.30)$$

where c_n and a_n are power series in g_R. A change of μ by a factor λ changes the renormalization constants by a power series in $\varepsilon \ln \lambda$ which multiplies them. Such a power series can be treated in the same way as the factors X_3 and X_g introduced in (6.1). But because these factors are equal to 1 for $\varepsilon \to 0$ they do no affect the β-function

and the anomalous dimension, according to (6.4) and (6.5). Nevertheless such a change does affect the perturbation expansion when it is 'renormalization group improved', as discussed above.

In the analysis of deep-inelastic scattering data this ambiguity has never lead to any problems, because all analyses use the natural scale variable Q^2. When information, obtained from deep-inelastic scattering data - the coupling constant or parton distributions - is transfered to other processes it is a serious problem. Notice that all other ambiguities can be fixed by means of definitions, made in deep inelastic scattering alone. One is not allowed to choose a different subtraction for another process, because this affects either the anomalous dimensions, the β-function or Λ, and then it would not be consistent to use deep-inelastic scattering parameters in that process. But it is still allowed to change the scale variable, which appears as argument of the running coupling constant or the parton distributions. Even when all definitions are fixed in deep-inelastic scattering processes, this freedom remains. As usual, the effect of this ambiguity is formally only of higher order, and is compensated by terms in the calculated perturbative corrections. When these corrections are large, that may indicate that an inappropriate choice was made for the scale variable. When no perturbative corrections have been calculated, there is clearly no such criterion, and then one has to resort to an intuitive guess about the most suitable variable. A large perturbative correction may also be due to an inappropriate definition of the coupling constant or the parton distributions. It is very well possible that a definition which leads to a well-behaved perturbation series for deep-inelastic scattering results leads to poor convergence in another process. It

should be clear that one can only have confidence in a QCD-prediction, when higher order corrections have been calculated, and when definitions can be found for which these are sufficiently small, and can be expected to remain small in still higher orders. Without higher orders corrections the determination of distribution functions, but in particular of the Λ-parameter, is meaningless.

1. Introduction

In this chapter we will consider processes in which a lepton pair is produced in a collision between two hadrons, i.e. processes of the type

$$H_1 + H_2 \rightarrow \ell_1 + \ell_2 + \text{'anything'}$$

Here H_1 and H_2 are hadrons, ℓ_1 and ℓ_2 leptons and 'anything' can be any hadronic final state. The leptons can be electrons, muons, τ-leptons and neutrino's, but only in combinations which can be pair-produced by a photon or the intermediate bosons of the weak interactions. This vector boson is then supposed to be produced in $q\bar{q}$ annihilation or radiated from one of the quarks in the hadrons.

Lepton pair production is of interest for several reasons. First of all it offers a test of the parton model. In principle one can calculate lepton pair production cross sections using parameters (parton distribution functions and the QCD coupling constant) which are determined in other processes, like deep-inelastic scattering, at least if the parton model is correct. In processes which are expected to be dominated by valence quark annihilation, like lepton pair production in proton-antiproton scattering, the cross section can be accurately predicted and compared with experiment. In processes where valence-sea annihilation is important the cross section is sensitive to the sea distributions, which cannot be determined very well in deep-inelastic scattering processes. This kind of processes - proton-proton scattering is an example - can be used to measure the sea distributions, provided that one finds agreement with experimental data for the valence-valence

processes - otherwise the parton model would not be applicable - and that the background due to other parton subprocesses is known.

More important than testing the parton model would be to test QCD. There are several ways in which QCD and color can manifest themselves in the cross sections. Evidence for color can be found because the $q\bar{q}$ annihilation cross section is suppressed by 1/N, where N is the number of colors. This is because annihilation into a colorless vector boson is only possible for a quark and an antiquark with opposite color, and the probability that these particles have opposite colors is 1/N. If one could measure this factor it would give information about the number of colors, in addition to the 'R' ratio in e^+e^- annihilation, the $\pi^0 \to \gamma\gamma$ decay width, and the branching ratio's for the decay of the τ-lepton. Unfortunately this color suppression factor may be almost cancelled by QCD-corrections to the $q\bar{q}$ process. The radiative corrections to this process turn out to be as large as the lowest order contribution. One expects that these large corrections can be summed to all orders of perturbation theory. Then they will give rise to an enhancement factor in the order of two or three, which by itself would be interesting to measure.

The obvious QCD-test is to look for deviations from scaling. As we will discuss below, the parton model predicts a scaling behavior for the lepton pair production cross section, which is slightly violated by QCD corrections. The predicted scaling deviations are within the errors of current experiments, and much better data are needed to test QCD in this way. The fact that the data show a scaling behavior within the experimental errors is however by itself a non-trivial and encouraging result.

Because it is difficult to observe scaling deviations the main effort in this field has gone into attempts to calculate the normalization of the process, including higher order corrections, as accurately as possible. This is necessary if one wants to use lepton pair production data to determine parton distributions.

Knowledge of the effects of QCD corrections upon the normalization is also very important for the calculation of $W^{\pm}$ and Z_0 production rates in $p\bar{p}$ collisions. At this moment experiments are prepared at CERN in which one hopes to find evidence for these heavy intermediate bosons by means of a high energy proton-antiproton collider. The mechanism for the production of these bosons is the same as for the production of virtual photons, and therefore it should be possible to make reliable predictions for heavy vector boson production. The expectation that the intermediate boson will be seen is based upon such predictions.

The kinematics of a lepton pair production process is shown in fig. 1.1. The symbol P_n denotes the sum of the momenta of the outgoing

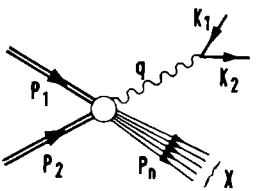

fig. 1.1: lepton pair production.

hadrons. The following variables are often used:

$$Q = \sqrt{q^2} \quad ; \quad s = (P_1 + P_2)^2$$

$$\tau = Q^2/s \quad ; \quad x_1 = Q^2/2P_1q \quad .$$

The matrix-element is the product of a lepton and a hadron current. When the phase-space integral for the lepton part is performed one obtains the following formula for the unpolarized cross section

$$d\sigma = \frac{1}{2\sqrt{\lambda(s,M_1^2,M_2^2)}} \frac{1}{(2S_1+1)} \frac{1}{(2S_2+1)} \sum_{\{n\}} \int d\mathcal{P}_n \int \frac{d^4q}{(2\pi)^4} 2\pi\delta(q^2-Q^2)$$

$$\times \frac{e^4}{6\pi Q^2} P(Q^2) \left[-g^{\mu\nu} + \frac{q^\mu q^\nu}{q^2} \right] \sum_{\text{spin}} \langle P_1 S_1, P_2 S_2 | J_\mu(0) | \{n\} \rangle$$

$$\times \langle \{n\} | J_\nu(0) | P_1 S_1, P_2 S_2 \rangle \qquad (1.1)$$

where M_i and S_i are the masses and spins of the incoming hadrons. The symbol $d\mathcal{P}_n$, introduced in section II.1, denotes the phase space integral for the hadronic final state $\{n\}$. The factor $P(Q^2)$ comes from the lepton phase-space integral. For a lepton-antilepton pair with mass m it is:

$$P(Q^2) = (1 + \frac{2m^2}{Q^2}) \sqrt{1 - 4m^2/Q^2} \qquad (1.2)$$

We will only consider cases for which $m^2/Q^2 << 1$, so that $P(Q^2)$ can be approximated by 1. These formulae are only valid for electromagnetic processes; the generalization to weak processes is simple.

In the remainder of this chapter we will restrict ourselves mainly to the differential cross section $\frac{d\sigma}{dQ^2}$. To calculate that cross section one uses the parton model. According to the intuitive definition of parton distributions the relation between the hadron cross section and the parton cross sections is:

$$\frac{d\sigma^{H_1H_2}}{dQ^2}(\tau,Q^2) = \sum_{i,j} \int_0^1 d\xi_1 \, d\xi_2 \int_\tau^1 d\tau_p \, \delta(\tau - \xi_1\xi_2\tau_p)$$

$$\times \xi_1 f_{i,H_1}(\xi_1) \, \xi_2 f_{j,H_2}(\xi_2) \frac{d\sigma^{ij}}{dQ^2}(\tau_p,Q^2) \qquad (1.3)$$

The subscript 'p' denotes the kinematical variables for the parton subprocess. The C.M. energy for the two incoming partons is:

$$s_p = (p_1 + p_2)^2 \sim 2p_1p_2 = 2\,\xi_1\xi_2P_1P_2 \sim \xi_1\xi_2\,s \tag{1.4}$$

where masses are neglected. Capital P denotes hadron momenta, small p parton momenta. Because of (1.4) one gets:

$$\tau_p = \frac{\tau}{\xi_1\xi_2} \tag{1.5}$$

This condition is imposed by the δ-function.

The parton cross sections in (1.3) are calculated with formula (1.1), where now matrix elements of the currents between gluon and quark states have to be used. When the lowest order term, the $q\bar{q}$ annihilation cross section (fig. 1.2) is substituted into (1.3) one obtains the Drell-Yan formula [Dre 70]:

$$\frac{d\sigma}{dQ^2} = \frac{4\pi\alpha^2}{3sQ^2}\,\frac{1}{N}\int_0^1 dx_1\,dx_2\,\delta(x_1x_2 - \tau)\sum_i e_i^2\left(f_i(x_1)\bar{f}_i(x_2) + \bar{f}_i(x_1)f_i(x_2)\right)$$

$$= \frac{4\pi\alpha^2}{3sQ^2}\,F(\tau,Q^2) \tag{1.6}$$

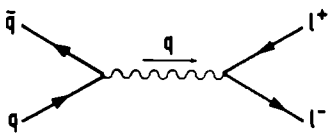

fig. 1.2: lowest order contribution to lepton pair production.

Notice that $F(\tau,Q^2)$ does not depend upon Q^2 in this approximation. This is called Drell-Yan scaling. To calculate higher order corrections which cause deviations from Drell-Yan scaling, one must apply the factorization formalism, discussed in the previous chapter. The moments, which

simplify this factorization formally, are defined as follows:

$$\sigma^n = \int_0^1 \tau^{n-2}\, \sigma(\tau)\, d\tau$$
$$f_1^n = \int_0^1 x^{n-1}\, f_1(x)\, dx \qquad (1.7)$$

where σ is a short notation for $\frac{d\sigma}{dQ^2}$. Now (1.3) reduces to (II.3.2). We will discuss some of the higher order corrections in the subsequent sections.

2. QCD-corrections to the Drell-Yan formula

When non-leading terms are taken into account formula (1.6) is modified in two ways. First of all the distribution functions are replaced by scale dependent ones. The Q^2-dependence is predicted to be the same as in deep-inelastic scattering, and does not require additional calculations. The second modification is the appearance of extra terms, which are suppressed by powers of the strong coupling constant α_s. There are two kinds of extra terms which will appear in (1.6). The first kind is due to new parton subprocesses, which are absent in zeroth order. The second kind consists of radiative corrections to processes already present in lower order. A new process distinguishes itself by a different initial or a different final state. The latter distinction is not very relevant, since the details of the hadronic final state remain unobserved for inclusive processes. As far as the initial state is concerned, four subprocesses can be distinguished: quark-antiquark annihilation, possible in zeroth order, quark-gluon scattering, possible in first order and quark-quark and gluon-gluon scattering, which appear first in order α_s^2.

The power corrections are terms which remain after the factoriza-

tion of mass-singularities. As was remarked in chapter II it is possible to absorb all power corrections into the distribution functions, at least for one deep-inelastic structure function. But when this definition is chosen in one process it fixes the factorization for all other processes, and power corrections will appear there. When a choice is made for the scale variable these corrections are unambiguous. In the case of lepton pair production the natural choice for this scale variable is Q^2. To fix the factorization procedure we will choose the convention of absorbing all perturbative corrections to the deep inelastic structure function F_2 in the transition functions. This convention is adopted in most other calculations of corrections to the Drell-Yan process (e.g. [Alt 78, Kub 79, Alt 79]). This choice implies that to all orders in α_s the expression for F_2 will be:

$$F_2(x,Q^2) = \sum_i e_i^2 \; x \; f_i(x,Q^2) \qquad (i = q_i, \bar{q}_i) \qquad (2.1)$$

The corrections of order α_s consists of the new subprocess quark-gluon scattering, and of radiative corrections to the leading order process. The first contribution is due to the diagrams of fig. 1.

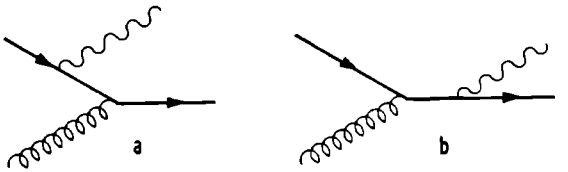

fig. 2.1: quark-gluon contribution to lepton-pair production.
(the lepton pair created by the virtual photon is omitted)

These diagrams are the lepton-pair production counterpart of those of fig. II.5.2. As we remarked in section II.5 one should make a distinction between transversal and longitudinal gluons. If this is done one obtains

a cross section for both polarizations

$$\frac{d\sigma^L_{qg}(\tau)}{dQ^2} = \frac{4\pi\alpha^2}{3sQ^2}\frac{\alpha_s}{4\pi}\frac{1}{N}e_q^2\left[\frac{4p^2\tau^2(1-\tau)^2}{m^2-p^2\tau(1-\tau)}\right] \tag{2.2}$$

$$\frac{d\sigma^T_{qg}(\tau)}{dQ^2} = \frac{4\pi\alpha^2}{3sQ^2}\frac{\alpha_s}{4\pi}\frac{1}{N}e_q^2\left[-[(1-\tau)^2+\tau^2]\ln\left(\frac{m_1^2\tau}{Q^2(1-\tau)^2}-\frac{p^2}{Q^2}\frac{\tau^2}{1-\tau}\right)\right.$$
$$\left.+\frac{1}{2}(1-\tau)(1+3\tau+\frac{2p^2\tau-4p^2\tau^2(1-\tau)+4m^2\tau}{m^2-p^2\tau(1-\tau)})\right] \tag{2.3}$$

where m is the quark mass and p^μ the four-momentum of the gluon. As in section 5 two regularization methods were used. By taking either m^2 or p^2 equal to zero these formulae reduce to the ones obtained by other authors. The parton cross sections contribute in the following way to the hadron cross section:

$$\frac{d\sigma^H(\tau)}{dQ^2} = \frac{d\sigma_{DY}(\tau)}{dQ^2} + \int_0^1 dx_1dx_2\,\theta(x_1x_2-\tau)\left\{\sum_i (f_i(x_1)f_g^L(x_2)\frac{d\sigma^L_{qg}}{dQ^2}(\frac{\tau}{x_1x_2})\right.$$
$$\left.+\sum_i f_i(x_1)f_g^T(x_2)\frac{d\sigma^T_{qg}}{dQ^2}(\frac{\tau}{x_1x_2})+x_1\leftrightarrow x_2\right\} \tag{2.4}$$

where σ_{DY} is the Drell-Yan term. The variable τ used in (2.4) is the one for the hadron process; in (2.2) and (2.3) however, τ and s are the variables for the parton subprocess. The summation is over all quark flavors, including antiquarks.

The result diverges for large Q^2 because of the mass singularities in the parton cross section. These can be absorbed in the distribution functions by making a redefinition according to (II.5.2), replacing the distribution functions in the Drell-Yan term by scale dependent ones. Then the result becomes [Kub 79, Alt 79, Aba 79, Con 79]:

$$\frac{d\sigma^H(\tau)}{dQ^2} = \frac{d\sigma_{DY}}{dQ^2}(\tau,Q^2) + \int_0^1 dx_1dx_2\theta(x_1x_2-\tau)$$
$$\sum_i [f_i(x_1)f_g^T(x_2)+f_g^T(x_1)f_i(x_2)]\frac{d\sigma^0_{qg}}{dQ^2}(\frac{\tau}{x_1x_2}) \tag{2.5}$$

where

$$\frac{d\sigma^0_{qg}(\tau)}{dQ^2} = \frac{4\pi\alpha^2}{3Q^4}\frac{\alpha_s}{4\pi}\frac{e_q^2}{N}\,\tau\left\{\left[(1-\tau)^2+\tau^2\right]\ln(1-\tau) + \frac{3}{2} - 5\tau + \frac{9}{2}\tau^2\right\}$$

$$= \frac{4\pi\alpha^2}{3Q^4}\frac{\alpha_s}{4\pi}\frac{e_q^2}{N}\,\tau\,\Sigma^{qg}(\tau) \qquad (2.6)$$

A few important observations can be made concerning this result. First of all, the longitudinal gluon contribution has disappeared completely. Further, not only the mass singularity disappears, but also the other terms depending upon p^2 or m^2. This means that we could have started with either $p^2 = 0$ or $m^2 = 0$ (but not both) and still would have found the same result. In other words, the final result does not depend upon the way we regularize the mass singularities, at least not in the example considered here. This is crucial for the consistency of the procedure.

When we subtracted the mass singularity we assumed that Q^2 is the scale variable which appears as argument of the distribution function. However, when we would have used λQ^2 instead of Q^2, where λ is an arbitrary factor, then we would have arrived at a result differing from (2.6) by terms proportional ln (λ). The effect of such a rearrangement upon the complete result is of the order of magnitude of α_s^2.

The second contribution of order α_s is given by the diagrams of fig. 2.2. Diagram I interferes with the Drell-Yan term to give a result of order α_s. These diagrams correspond to the deep inelastic scattering diagrams of fig. II.5.1. They give the following contribution to the hadron cross section:

$$\frac{d\sigma^H(\tau)}{dQ^2} = \frac{d\sigma_{DY}(\tau)}{dQ^2} + \frac{4\pi\alpha^2}{3Q^4}\frac{N^2-1}{N^2}\frac{\alpha_s}{4\pi}\;2\sum_q e_q^2$$

$$\times \int_0^1 dx_1 dx_2 \, [f_q(x_1) f_{\bar{q}}(x_2) + f_q(x_2) f_{\bar{q}}(x_1)]$$

$$\times \left\{ \delta(x_1 x_2 - \tau)\tau \left[(2\ln \varepsilon + \frac{3}{2}) \ln(Q^2/m^2) - 2\ln \varepsilon + \frac{\pi^2}{3} - 2 \right] \right.$$

$$\left. + \theta(x_1 x_2 - (1+\varepsilon)\tau)\eta \left[\frac{\eta^2+1}{\eta-1} \ln \left(\frac{m^2}{Q^2} \eta \right) + \frac{\eta^2+1}{\eta-1} \right] \right\} \qquad (2.7)$$

where $\eta = \tau/x_1 x_2$.

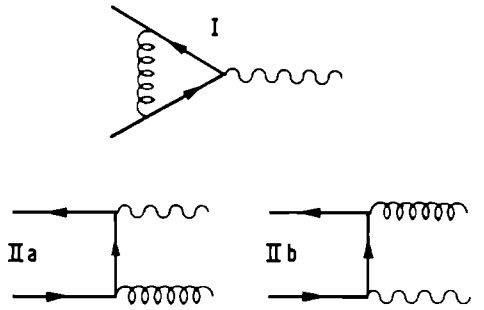

fig. 2.2: Radiative corrections to the Drell-Yan process.

To obtain this result one can give the gluon in all diagrams a mass λ to regularize the infrared singularities. To cancel the infrared divergencies the soft gluon part of IIa and IIb has to be added to I. Notice that when the gluon becomes soft, the photon carries away all the energy, and hence $\tau \sim x_1 x_2$. The separation between the soft and the hard part is made by a parameter ε. The hard gluon part gives the second term in (2.7), the soft part with $\tau \sim x_1 x_2$, together with diagram I gives the first term. Although ε still appears in (2.7), one can show by partial integration that the limit $\varepsilon \to 0$ yields a finite result, which means that the infrared singularities have cancelled completely. It is obvious that this cancellation occurs, because the

diagrams are the same ones as in a QED calculation to this order. The only difference is a group-theoretical factor, which is the same for these three diagrams.

Beside the infrared divergency there are two other sources of singularities, the ultraviolet divergence and the mass singularity. The first disappears by renormalizing the QED vertex function or by adding the selfenergy diagrams for the external quarks and normalizing the external lines. This was already mentioned in section II.5.

The mass singularity is cancelled by the factorization procedure. To achieve that the distribution functions in the Drell-Yan term are modified according to (II.5.1). Apart from scaling deviations in the Drell-Yan term the effect is an extra contribution of order α_s:

$$\frac{d\sigma^0_{q\bar{q}}}{dQ^2} = \lim_{\varepsilon\to 0} \frac{4\pi\alpha^2}{3Q^4} \frac{N^2-1}{N^2} \frac{\alpha_s}{4\pi} 2e_q^2 \int_0^1 dx_1 dx_2 \sum_q e_q^2 \left[f_q(x_1) f_{\bar{q}}(x_2) + f_q(x_2) f_{\bar{q}}(x_1)\right]$$

$$\times \left\{ \theta(x_1 x_2 - \tau(1+\varepsilon))\, \eta \left[\frac{1+\eta^2}{1-\eta}\left[\ln(1-\eta) - 1\right] - \frac{1}{2}\left(\frac{1-8\eta}{1-\eta}\right) - 3\eta\right] \right.$$

$$\left. + \delta(x_1 x_2 - \tau)\, \tau \left[\frac{2\pi^2}{3} + \frac{1}{2} + \frac{3}{2}\ln\varepsilon + \ln^2\varepsilon\right] \right\} \qquad (2.8)$$

This result or analogous ones has been obtained by [Kub 79, Alt 79, Hum 79a, Aba 78, Har 79]. Again, the limit $\varepsilon \to 0$ is finite.

In the calculation of (2.4) and (II.5.1) the mass of the quark was used to regularize the mass singularity. One might expect that the same result can be obtained by taking the incoming quarks off-shell and neglecting their masses, as was the case for the quark-gluon result. This is, however, not the case. If the off-shell method is used one finds a different (larger) constant instead of the $2\pi^2/3$ appearing in (2.8). This problem was noticed and solved by [Hum 79b]. The key to the

solution is the fact that the diagrams of fig. 2.2 and fig. II.5.1 are intimately related. They can be obtained by making different final and initial state cuts of the same vacuum bubble diagram. One finds that an unambiguous answer is obtained only if the regularization methods used in lepton pair production and deep-inelastic scattering calculations are related to each other via the double cut graph. The on-shell regularization method meets that requirement because all lines in the double cut graph will have a mass. However, when processes with one and two incoming partons are regularized with the off-shell method, then this will correspond to either one or two off-shell lines in the double cut graph, and hence these graphs are different for lepton pair production and deep-inelastic scattering. When a more subtle definition of the off-shell regularization method is given, which satisfies the requirement mentioned above, one obtains the on-shell result.

The effect of (2.8) upon the lepton pair production cross section is rather large, in contrast to (2.6) which gives a very small effect. This large correction is due to the factor $2\pi^2/3$ and the kinematical singularity $\frac{1}{\eta-1} \ln (1-\eta)$. The first factor originates from the analytical continuation of the electromagnetic vertex (diagram I) from deep-inelastic scattering (space-like q^2) to lepton pair production (time-like q^2). The singular term is the quark-quark anomalous dimension multiplied by a factor $\ln (1-\eta)$. Such a logarithmic term is found in all corrections calculated up to now, and it is a remainder of the mass singularity. Notice the appearance of a $\ln (1-\tau)$ in (2.6). Since the origin of the large effect is understood it may be possible to determine the large contributions which can be expected in higher order corrections, and sum them to all orders. This has indeed been suggested

[Par 80, Cur 80a]. If such a procedure fails perturbation theory may run into serious problems.

This summarizes the results up to first order in α_s. In the next order there are several contributions, some of which may be important. First of all there are the two-loop radiative corrections to the Drell-Yan process, which are expected to give a large result just as the one loop corrections did. It is certainly important to calculate these diagrams, either to improve the perturbation expansion or to show that the summation procedure described above really works. The one-loop corrections to the quark-gluon process appearing in this order may be large as well - but large compared to the quark-gluon process, which itself is small compared to the Drell-Yan term. Therefore, there is probably no need to calculate these diagrams.

Beside these radiative corrections two new subprocesses will appear. The gluon-gluon process might give a large contribution due to the fact that about 45% of the momentum of the proton is carried by gluons. The quark-quark process can be expected to be important in proton-proton scattering, because in that case the leading Drell-Yan process is suppressed. For this leading process one needs a sea-quark, and the sea-quark distributions are much smaller than the valence-quark distributions, especially near $x = 1$. This implies that despite the α_s^2-suppression the valence-valence process will dominate at large values of τ, and will give a smaller value near $\tau = 0$. To determine the exact region where each of the processes is the dominant one, one has to calculate the quark-quark contribution. Without a reliable estimate of the effect of this process all attempts to extract the sea-quark distributions out of lepton pair production data are unjustified

[Geo 78]. The calculation of this subprocess will be the subject of the subsequent sections. On the basis of the results we can also give a rough estimate of the contribution of the gluon-gluon process.

3. The quark-quark contribution for nonidentical quarks

In this section we will calculate the contribution to lepton pair production of non-identical quark-quark scattering. When the quarks are identical there are additional 'crossed' diagrams which interfere with the other ones. The calculation of these interference terms will be postponed to section 5.

There are four diagrams which contribute to the amplitude for non-identical quark-quark scattering. They are drawn in fig. 3.1.

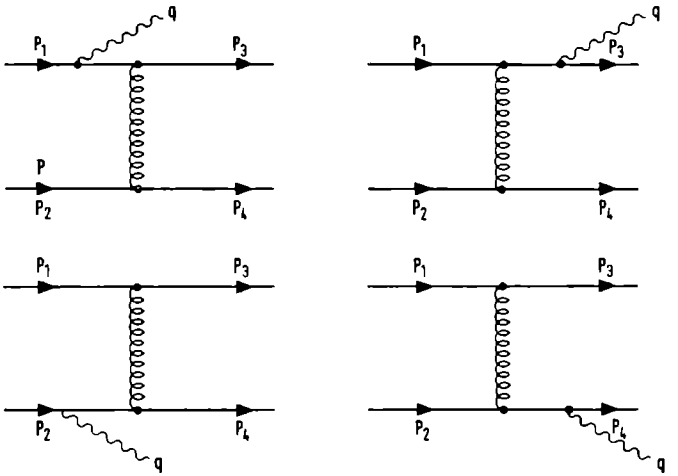

fig. 3.1: quark-quark contribution to lepton pair production.

The squared amplitude consists of sixteen terms which can be divided into two classes. First of all there are eight terms proportional to the squares of the quark-charges. This class consists of the square of

the two upper diagrams in fig. 3.1 plus the square of the two lower ones. The second class is formed by the interference terms, and consists of products of one of the upper and one of the lower diagrams. These terms distinguish themselves from the other ones because they are proportional to the product of the charges of the two quarks. In particular that implies that these classes are gauge-invariant sets of diagrams.

The mass singularities in these diagrams are due to the gluon propagator and the quark propagators belonging to the diagrams in which the photon is emitted from an incoming line. The denominators of the gluon propagators ($(p_1-p_3)^2$ or $(p_2-p_4)^2$) vanish when the four-momenta p_1, p_3 or p_2, p_4 are parallel and light-like. A quark-propagator belonging to an incoming line has a denominator $(p_1-q)^2 = (p_2-p_3-p_4)^2$ which vanishes if the two outgoing quarks are parallel to the incoming one. A quark propagator belonging to an outgoing line has a denominator like $(p_3+q)^2$. This is the C.M. energy of the virtual photon and a quark, and therefore this variable is bounded from below.

As was explained in section II.2 in the axial gauge a mass singularity can only occur if a potentially singular propagator appears twice in the squared amplitude. Since we have two such propagators, we can expect a double logarithmic singularity. This singularity will appear in the first class of the two described above. The interference terms can not have a double propagator and therefore this class has to be finite. The only change in this argument for other gauge choices is that the mass singularity can no longer be attributed to a single term, but is distributed over the other diagrams in a gauge-invariant class. For the interference terms this implies that individual terms are no

longer finite, but that the singularities cancel when all diagrams are added.

A consequence of the mass singularities is that the non-leading singularities and the finite terms will depend upon the regularization method one chooses. The interference terms, however, are singularity-free and therefore the result should be unambiguous in this case.

For these calculations we have chosen two regularization methods. The first one is to take all quarks on-shell, and use their mass to regularize the singularities. The masses are used only as a regulator and are not supposed to have a physical meaning; the final result will be independent of them. Therefore we are allowed to choose these masses in a convenient way. We will find that it is always possible to take one of them equal to zero, which simplifies the intermediate results. The second method is to take one of the quarks off-shell; then the masses can be neglected. Again the 'off-shell-ness' of the incoming quarks is not supposed to have a physical meaning, and final results will be independent of it.

To calculate the cross section we have used two methods. One of them can only be used for the calculation of the squared terms, the second one is very general, but more complicated. We will first discuss a relatively simple calculation of the squared terms using the first method.

With the momenta defined as in fig. 3.1, the squared amplitude, summed over the polarizations of the virtual photon and the spins of the quarks, can be written as follows:

$$\Sigma \, |M|^2 = A^{\mu\nu}(p_1,p_3) \; B_{\mu\nu}(p_2,p_4,q) \qquad (3.1)$$

The summation symbol denotes both spin and color summation. Only the four terms coming from the upper diagrams of fig. 3.1 are given here. The tensor $A^{\mu\nu}$ is the trace of the γ-matrices of the lower quark line:

$$A^{\mu\nu} = \frac{4}{(p^2)^2}\,(p_3^{\mu}p_1^{\nu} + p_3^{\nu}p_1^{\mu} - g^{\mu\nu}(p_1p_3 - m^2)) \tag{3.2}$$

where $p^{\mu} = p_1^{\mu} - p_3^{\mu}$ and m is the quark mass. The second tensor is the squared matrix element for the process:

$$g^*(p^{\mu}) + q(p_2^{\mu}) \rightarrow \gamma^*(q^{\mu}) + q(p^{\mu})$$

where g^* denotes an off-shell gluon.

For this process one can define the following tensor:

$$T_{\mu\nu} = \int \frac{d^3p_4}{(2\pi)^3 2p_4^0}\,\frac{d^3q}{(2\pi)^3 2q^0}\,(2\pi)^4\delta^4(p+p_2-p_4-q)\,B_{\mu\nu}(p_2,p_4,q) \tag{3.3}$$

This tensor depends only on the four-vectors p_2 and p and has to be contracted with the symmetric tensor $A^{\mu\nu}$. Therefore the most general expression for $T_{\mu\nu}$ is:

$$T_{\mu\nu} = T_1\left[-g_{\mu\nu} + \frac{p_{\mu}p_{\nu}}{p^2}\right] + \frac{T_2}{p_2^2}\left[p_{2\mu} - \frac{p_2p}{p^2}\,p_{\mu}\right]\left[p_{2\nu} - \frac{p_2p}{p^2}\,p_{\nu}\right]$$
$$+ T_3\,p_{\mu}p_{\nu} + T_4[p_{\mu}p_{2\nu} + p_{\nu}p_{2\mu}] \tag{3.4}$$

The coefficients $T_1 \ldots T_4$ are scalar functions of the two Lorentz-invariants p^2 and $s_2 = (p + p_2)^2$. In the case of on-shell regularization $T_{\mu\nu}$ is conserved (i.e. $p^{\mu}T_{\mu\nu} = p^{\nu}T_{\mu\nu} = 0$) and hence T_3 and T_4 vanish. The structure functions $T_1 \ldots T_4$ can be calculated by making the following projections:

$$\begin{aligned} C &= g^{\mu\nu}T_{\mu\nu} \\ D &= p_2^{\mu}p_2^{\nu}T_{\mu\nu} \\ E &= p^{\mu}p^{\nu}T_{\mu\nu} \\ F &= (p_2^{\mu}p^{\nu} + p_2^{\nu}p^{\mu})T_{\mu\nu} \end{aligned} \tag{3.5}$$

This gives C..F as a linear combination of $T_1..T_4$ and by inverting this relation one obtains the structure functions. These projections are most easily calculable in the C.M.-frame of the momenta p_2 and p. Then only a one-dimensional integral remains to be calculated.

When the structure functions are known we can contract $T_{\mu\nu}$ with $A_{\mu\nu}$ and add the remaining phase-space integral. For off-shell quarks one obtains the following result:

$$\int d\mathcal{P}_\Sigma \, |M|^2 = \frac{1}{4s} \frac{1}{(2\pi)^2} Q^2 \int^{s} ds_2 \int_{(s_2-s)}^{p^2_{max}} dp^2$$

$$\times \left\{ \left[1 + \frac{(p_2k)^2}{\beta} - \frac{2p_1^2}{p^2} \frac{(p_2k)(p_2p)}{\beta} \right] \frac{C}{p^2} \right.$$

$$- \left[1 - \frac{3(p_2k)^2}{\beta} + 6 \frac{p_1^2}{p^2} \frac{(p_2k)(p_2p)}{\beta} - \frac{2p_1^2}{p^2} - \frac{2p_1^4}{p^4} \right] \frac{D}{\beta}$$

$$\left. + \left[-2 + \frac{2(p_2k)^2}{\beta} \right] \frac{E}{p^4} \right\} \qquad (3.6)$$

where $k^\mu = p_1^\mu + p_3^\mu$

$$\beta = \frac{1}{4} \left[(s_2+p^2-p_2^2)^2 - 4s_2p^2 \right]$$

$$p^2_{max} = p_1^2 s_2 / s$$

For on-shell regularization the result is:

$$\int d\mathcal{P}_\Sigma \, |M|^2 = \frac{1}{4s} \frac{1}{(2\pi)^2} Q^2 \int^{s} ds_2 \int_{(s_2-s)}^{p^2_{max}} dp^2$$

$$\times \left\{ \left[1 + \frac{(p_2k)^2}{\beta} + \frac{4m_1^2}{p^2} \right] \frac{C}{p^2} \right.$$

$$\left. - \left[1 - \frac{3(p_2k)^2}{\beta} - \frac{4m_1^2}{p^2} \right] \frac{D}{\beta} \right\} \qquad (3.7)$$

where $k^\mu = p_1^\mu + p_3^\mu$

$$\beta = \frac{1}{4} \left[(s_2+p^2-m_2^2)^2 - 4s_2p^2 \right]$$

$$p^2_{max} = (-m_1^2 s_2^2) / ((s_2-s)s)$$

The singular behavior of these integrals is completely determined by the upper boundary of the p^2 integral. Near $p^2 = 0$ the coefficient C is logarithmically divergent, D diverges as $\frac{1}{2}$ and E is finite. Since the off-shell result is gauge-invariant for $p_2^2 = 0$, E is proportional to p_2^2. The terms originating from E contain ratios of p_2^2 and p_1^2. Such terms are unacceptable, because they do not have a well-defined value. They can, however, be absorbed in the distribution functions when the same terms appear in the calculation of the deep-inelastic scattering diagrams, fig. 4.1. This cancellation can only be expected to occur when exactly the same regularization method is used, i.e. the outgoing quark-line with momentum p_2 must be taken off-shell in the diagrams of fig. 4.1. When the unacceptable terms are not identical in both results, such terms will remain either in the deep-inelastic scattering, or in the Drell-Yan result. The easiest method to avoid these complications is to take p_2 on-shell. This can be done because only p_1^2 is needed as a regulator for the mass singularities. If p_2 is taken on-shell, T_3 and T_4 vanish and the result becomes gauge-invariant. Gauge-invariance is not required for the result of this section, because it is not yet the physical cross section. Gauge-dependent terms should cancel when the mass singularities are subtracted, and therefore the final results of section 6 must be gauge independent. (Notice however that we are not calculating S-matrix elements in the usual way. It has not been proven that for any choice of the regularization procedure the final result is gauge-invariant. The diagrams of fig. 2.2, combined with those of fig. II.5.1 for example, yield a gauge-invariant final result for covariant gauges, but a different result is obtained in the axial gauge [Nee 80]. Of course, such problems can only occur for an off-shell regularization

method, which in this example is inconsistent for other reasons (see section 2). If an on-shell method is used the results are already gauge-invariant before the mass-singularities are subtracted.)

Although terms proportional to m_2^2 appear in (3.7), which may be expected to give rise to factors m_2^2/m_1^2, a remarkable cancellation occurs, and all such terms disappear. This does not mean that the result is independent of this ratio, because it also appears in arguments of logarithms. The limit $m_2^2 \to 0$ yields however a finite result. This choice simplifies the results of this section, but as discussed above we expect the unwanted terms to cancel in the final result. Therefore nothing is lost by taking this limit already in this stage of the calculation.

The integrand which is obtained when C and D are substituted into (3.6) and (3.7) contains a large number of terms, which can be relatively easily integrated individually. To handle these integrals we used the algebraic manipulation program SCHOONSCHIP [Vel 67, Str 74]. The p^2-integrals were calculated by hand, checked numerically and substituted into the expression. Then an analytical expression for the s_2 integrand is obtained. At this point the intermediate result should be equal to the one obtained by means of the second method, and therefore we postpone the discussion of the s_2 integral until we have described that method.

The other method was needed mainly because the simple calculation outlined above does not work for the interference diagrams, nor for the crossed diagrams. This is because the first method uses the topology of the squared terms in an essential way. Therefore we developed a series of algorithms to evaluate a three-particle phase-space integral for

second order tree diagrams analytically, independent of the topology. In principle this method can be extended to any diagram of that type, but we have only extended it as far as we need it.

To perform these algorithms an extensive use of SCHOONSCHIP is made, because already at early stages of the calculation a huge number of terms is generated. In fact the complete calculation was finally done by a set of SCHOONSCHIP instructions to calculate the traces of the γ-matrices and perform the four-dimensional phase-space integral. In intermediate steps several thousands of terms were generated, but the final result turns out to be relatively simple. We have used the 1-1-1978 IBM-version of SCHOONSCHIP. With this program the calculation of one of the contributions took 5 to 12 minutes CPU-time. The program based upon the first method, including the s_2-integral, takes not more than two minutes.

To do the integrations we introduce a set of angular variables and a set of energy variables. For the latter we choose the center of mass energies of all pairs of outgoing particles:

$$\begin{aligned} s_1 &= (p_3 + p_4)^2 \\ s_3 &= (p_4 + q)^2 \\ s_4 &= (p_3 + q)^2 \end{aligned} \tag{3.8}$$

These variables are not independent:

$$s_1 + s_3 + s_4 = s + Q^2 + m_1^2 + m_2^2 \tag{3.9}$$

As angular variables we use polar angles θ and ϕ, specifying the direction of $\vec{p}_3$ with respect to the direction of incoming quarks in the CM-frame, and polar angles χ and ξ which specify the direction of $\vec{p}_4$ with respect to $\vec{p}_3$. (For some terms in the integration it turned out to be advantageous to interchange the role of $\vec{p}_3$ and $\vec{p}_4$.) In terms of these

new variables the integration volume becomes.

$$\int \frac{d^4p_3}{(2\pi)^4}\frac{d^4p_4}{(2\pi)^4}\frac{d^4q}{(2\pi)^4} 2\pi\delta(p_3^2-m_1^2)\,2\pi\delta(p_4^2-m_2^2)\,2\pi\delta(q^2-Q^2)\,(2\pi)^4\delta^4(p_1+p_2-p_3-p_4-q)$$

$$\times\ \theta(p_3^0)\,\theta(p_4^0)\,\theta(q^0) = \frac{1}{(2\pi)^4}\frac{1}{32\ s}\int ds_3\ ds_4\ d\cos\theta\ d\xi \qquad (3.10)$$

where $s = (p_1+p_2)^2$. In (3.10) the trivial integration over the azimuthal angle ϕ is already performed. The angle χ between $\vec{p}_3$ and $\vec{p}_4$ is restricted by the constraint:

$$\cos\chi = \frac{1}{2|\vec{p}_3||\vec{p}_4|}\left[s - 2\sqrt{s}\,(E_3+E_4) + m_1^2 + m_2^2 + 2\,E_3E_4 - Q^2\right] \qquad (3.11)$$

where $E_3 = p_3^0$ and $E_4 = p_4^0$. The boundaries for $\cos\theta$ and ξ are as usual $-1 \leq \cos\theta \leq 1$ and $0 \leq \xi < 2\pi$. The allowed region for the variables s_3 and s_4 is scetched in fig. 3.2.

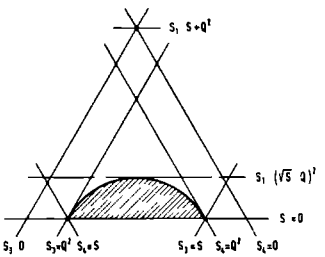

fig. 3.2: Boundaries of the integration region (for massless quarks).

In terms of the variable s_1 the boundary lines are given by:

$$m_1^2\,\frac{s-Q^2}{s-s_3} + m_2^2\,\frac{s-Q^2}{s_3-Q^2} \leq s_1 \leq s+Q^2-s_3-\frac{sQ^2}{s_3} + m_1^2\,\frac{sQ^2-s_3^2}{s_3(s-s_3)} + m_2^2\,\frac{s_3^2-sQ^2}{s_3(s_3-Q^2)} \qquad (3.12)$$

where we have neglected terms of higher order in the masses.

The complications in integrations like the ones discussed here are mainly due to the denominators of the propagators. In the diagrams

discussed in this section six different denominators appear:

$$
\begin{aligned}
N_1 &= (p_1-p_3)^2 \\
N_2 &= (p_2-p_4)^2 \\
N_3 &= (p_2-q)^2 - m_2^2 \\
N_4 &= (p_3+q)^2 - m_1^2 \\
N_5 &= (p_1-q)^2 - m_1^2 \\
N_6 &= (p_4+q)^2 - m_2^2
\end{aligned}
\tag{3.13}
$$

We will first calculate the double angular integral, and therefore we have to know the dependence of these denominators upon the angles θ and ξ. This dependence can be reduced to two independent Lorentz-invariants:

$$
\begin{aligned}
p_1 \cdot p_3 &= E_1 E_3 - |\vec{p}|\,|\vec{p}_3| \cos\theta \\
p_2 \cdot p_4 &= E_2 E_4 + |\vec{p}|\,|\vec{p}_4| \,(\cos\theta\cos\chi + \sin\theta\sin\chi\cos\xi)
\end{aligned}
\tag{3.14}
$$

where $|\vec{p}|$ is the CM-momentum of the incoming quarks. The denominators N_4 and N_6 turn out to be independent of the angles. The others depend upon these variables in the following way:

$$
\begin{aligned}
N_1 &= -\,2\,(p_1 \cdot p_3 + R_1) \\
N_2 &= -\,2\,(p_2 \cdot p_4 + R_2) \\
N_3 &= +\,2\,(p_2 \cdot p_4 - p_1 \cdot p_3 + R_3) \\
N_5 &= -\,2\,(p_2 \cdot p_4 - p_1 \cdot p_3 + R_4)
\end{aligned}
\tag{3.15}
$$

where $R_1 \ldots R_4$ are functions of s_3 and s_4. The numerator of the integrand can also be expressed in terms of $p_1 \cdot p_3$, $p_2 \cdot p_4$ and angular independent Lorentz-invariants. By means of fractional decomposition with respect to $p_1 \cdot p_3$ and $p_2 \cdot p_4$ the integrand can now be reduced to a sum of terms containing at most two different angle-dependent factors. The angular integral for each of these terms can then be calculated. The necessary integrals are listed in appendix A. These results do not apply to

combinations like $N_2^{-1}N_5^{-1}$, but in this case one can interchange the role of p_3 and p_4 in the definition of the angles.

The terms obtained after the angular integration are rather complicated when they are completely expressed in terms of the variables s_3, s_4 and s_1. To simplify the remaining double integral as much as possible we choose for each term the most suitable pair of variables. This choice is made in such a way that the final one dimensional integral is always over s_3 or s_4. This enables us to calculate this integral for all terms together. But first the other one dimensional integral has to be calculated.

To do that we apply again a set of fractional decompositions to reduce the number of factors per term as much as possible. Because we neglect terms which vanish for large Q^2 (terms proportional to p^2/Q^2 or m^2/Q^2) some approximations can be made at this stage. Great care is needed however, because several integrals have a power-singularity rather than a logarithmic one for p^2 or $m^2 \to 0$. Combined with a numerator term such a power-singularity may yield a non-negligible contribution. The power-singularities themselves are found to cancel in the final result.

Most of the integrals which have to be calculated can by suitable substitution be written in the following way:

$$\int \frac{dx}{\sqrt{ax^2+bx+c}} \ln \frac{ex+f+\sqrt{ax^2+bx+c}}{ex+f-\sqrt{ax^2+bx+c}} \quad .$$

Apart from this expression there may be a factor $[gx+h]^{-n}$ multiplying it. When there is more than one such factor their number can be reduced to one by fractional decomposition. There is a well-known and successful substitution for integrals of this type:

$$y = \frac{1}{2}\left[x\sqrt{a} + \frac{b}{2\sqrt{a}} + \sqrt{ax^2 + bx + c}\right] \quad .$$

This reduces the argument of the logarithm to a ratio of monomials of y and makes the square root vanish. Most of the integrals can be calculated by means of this substitution. We have listed these integrals in appendix B. The results are given for arbitrary p_1^2 and p_2^2 respectively m_1^2 and m_2^2, but depending on the diagrams considered one can always put one of these variables equal to zero. Notice that for the off-shell regularization method complete factorization occurs, i.e. there is no dependence upon a linear combination of p_1^2 and p_2^2. This is not the case for on-shell regularization, which yields arguments of logarithms depending on ratios of m_1 and m_2. We have already discussed this fact above.

The integrand of the final integral consists of a few hundreds of terms, depending on the variables λ, τ and μ^2 defined in appendix B. The integration variable is λ. Fortunately the individual terms are not very complicated and, apart from a few exceptions, the following types can be distinguished:

(i) $\int_\tau^1 A^n \, d\lambda$

(ii) $\int_\tau^1 A^n \ln(B_1) \, d\lambda$

(iii) $\int_\tau^1 A^n \ln(B_1) \ln(B_2) \, d\lambda$

(iv) $\int_\tau^1 A^n \, Li_2(D) \, d\lambda$

where A, B_1 and B_2 are monomials in λ and D is a ratio of products of such monomials. To evaluate these integrals one can first integrate (iv) by parts. Then this type reduces to type (ii) or, for n = -1, to type (iii). Next one can apply the same procedure to type (iii), which reduces to (ii) except for n = -1. Finally one can reduce (ii) to (i)

in exactly the same way, again with the exception of n = -1. The integrals of type (i) are trivial.

The integrals of type (ii) and (iii) with n = -1 yield generalized Spence functions. For type (ii) there is only one such function, the dilog:

$$Li_2(z) = -\int_0^z \frac{\ln(1-x)}{x}\,dx \tag{3.16}$$

For type (iii) one can in general expect two kinds of Spence functions, but due to some mysterious cancellations we need only one of these for all our results, the trilog:

$$Li_3(z) = \int_0^z \frac{Li_2(x)}{x}\,dx \tag{3.17}$$

It can in some cases be rather complicated to find the analytical expressions for these integrals, and therefore we have listed them in appendix C. Useful relations for dilog and trilog functions (which are special cases of Euler n-logarithms) can be found in [Gro 50].
The algorithms discussed above have been performed by means of SCHOONSCHIP, and the results have been checked numerically. An additional check for the squared terms is obtained from the comparison of the two methods discussed above.

The final result of this section is:

$$\frac{d\tilde{\sigma}^{q_1q_2}}{dQ^2}(\tau) = \frac{4\pi\alpha^2}{3Q^4}\left(\frac{\alpha_s}{4\pi}\right)^2 \frac{N^2-1}{N^2}\,\tau\,\{\, e_1^2\,\tilde{\Sigma}^{qq}(\tau,\mu_2^2) + e_2^2\,\tilde{\Sigma}^{qq}(\tau,\mu_1^2) + 2\,e_1e_2\,\Sigma_I^{qq}(\tau)\,\} \tag{3.18}$$

The ~ symbols indicate that these quantities still contain mass-singularities which have to be subtracted. The color factor is obtained in the following way:

$$\frac{1}{N^2}\,\mathrm{Tr}\,(T^a T^b)\,\mathrm{Tr}\,(T^a T^b) = \frac{N^2-1}{4N^2} \tag{3.19}$$

The factor $\frac{1}{N^2}$ is needed to average over the colors of the quarks in the initial state.

The function $\tilde{\Sigma}^{qq}$ depends upon the regularization scheme. For the off-shell method it can be parametrized as follows:

$$\tilde{\Sigma}^{qq}\left(\tau, \frac{-p^2}{Q^2}\right) = \Sigma^{(1)}(\tau)\,\ln^2\frac{-p^2\tau^2}{Q^2(1-\tau)} + \Sigma^{(2)}_{OFF}(\tau)\,\ln\frac{-p^2\tau^2}{Q^2(1-\tau)} + \Sigma^{(3)}_{OFF}(\tau) \tag{3.20}$$

For the on-shell method:

$$\tilde{\Sigma}^{qq}\left(\tau, \frac{m^2}{Q^2}\right) = \Sigma^{(1)}(\tau)\,\ln^2\frac{m^2\tau}{Q^2(1-\tau)^2} + \Sigma^{(2)}_{ON}(\tau)\,\ln\frac{m^2\tau}{Q^2(1-\tau)^2} + \Sigma^{(3)}_{ON}(\tau) \tag{3.21}$$

The arguments of the logarithms have been chosen in such a way that they are identical to those of formula (2.3). There is a good reason for making this choice, as far as the dependence upon $\ln(1-\tau)$ is concerned. If these logarithms are combined with the mass-singularities in this way one finds that the functions $\Sigma^{(i)}(\tau)$ do not contain any $\ln(1-\tau)$ terms, and can be expanded in a Taylor series in the neighborhood of $\tau = 1$. The $\ln(1-\tau)$ terms are clearly related to the mass-singularities.

The functions $\Sigma^{(i)}(\tau)$ are different for the on-shell and the off-shell method, with the exception of $\Sigma^{(1)}$ which is unique. This is due to the fact that the coefficient of the leading logarithm is related to the first coefficient of the anomalous dimension, which is not affected by finite renormalizations. The functions introduced in (3.20) and (3.21) are ([Sch 80a]; see also [Con 79b]):

$$\Sigma^{(1)}(\tau) = (1+\tau)\ \ln\tau + \frac{1}{2} - \frac{1}{2}\tau + \frac{2}{3}\tau^{-1} - \frac{2}{3}\tau^2 \tag{3.22}$$

$$\Sigma^{(2)}_{OFF}(\tau) = -(1+\tau)\ \ln^2\tau + (\tau - \frac{4}{3}\tau^{-1})\ln\tau - 2(1+\tau)\ Li_2(1-\tau)$$
$$+ \frac{14}{3} - \frac{11}{3}\tau - \frac{4}{3}\tau^2 + \frac{1}{3}\tau^{-1} \tag{3.23}$$

$$\Sigma^{(2)}_{ON}(\tau) = 2(1+\tau)\ \ln^2\tau + (2 - \tau - \frac{8}{3}\tau^2 + \frac{4}{3}\tau^{-1})\ln\tau - 4(1+\tau)\ Li_2(1-\tau)$$
$$+ \frac{16}{3} - \frac{16}{3}\tau - \frac{16}{9}\tau^2 + \frac{16}{9}\tau^{-1} \tag{3.24}$$

$$\Sigma^{(3)}_{OFF}(\tau) = (1+\tau)[6\ Li_3(1 - \frac{1}{\tau}) + 4\ Li_3(1-\tau) - 2\ Li_2(1-\tau)\ \ln\tau$$
$$- \frac{1}{3}\ln^3\tau] + (3 - 4\tau + \frac{4}{3}\tau^{-1})\ Li_2(1-\tau)$$
$$+ (\frac{3}{2} - 2\tau + \frac{2}{3}\tau^{-1})\ln^2\tau + (\frac{15}{2} + 5\tau - \frac{1}{3}\tau^{-1})\ln\tau$$
$$+ \frac{79}{4} - \frac{115}{6}\tau - \frac{13}{12}\tau^2 + \frac{1}{2}\tau^{-1} \tag{3.25}$$

$$\Sigma^{(3)}_{ON}(\tau) = (1+\tau)[8\ Li_3(1 - \frac{1}{\tau}) - 8\ Li_2(1-\tau)\ \ln\tau - \frac{\pi^2}{3}\ln\tau]$$
$$+ (2 - 4\tau + \frac{4}{3}\tau^2 + \frac{4}{3}\tau^{-1})Li_2(1-\tau) + \frac{\pi^2}{6}(\tau - \frac{4}{3}\tau^{-1} + \frac{4}{3}\tau^2 - 1)$$
$$+ (3 - 2\tau - 2\tau^2 + \frac{2}{3}\tau^{-1})\ln^2\tau + \ln\tau\ (\frac{31}{2} - 7\tau - \frac{32}{9}\tau^2$$
$$+ \frac{16}{9}\tau^{-1}) + \frac{757}{36} - \frac{205}{9}\tau - \frac{163}{108}\tau^2 + \frac{88}{27}\tau^{-1} \tag{3.26}$$

Finally we give the explicit expression for the interference term introduced in (3.18). This term does not have any mass-singularities, and according to our conjecture, that ln (1-τ) terms will only occur in combination with such singularities, we do not expect any ln (1-τ) terms. Moreover the result should be independent of the regularization method, at least after the summation of all diagrams. This is indeed the case, and we obtain the following expression:

$$\Sigma_1^{qq}(\tau) = \tau^{-1}\,[1 + (1+\tau)^2][2\ln^3(1+\tau) - \pi^2 \ln(1+\tau) - 5\ln^2\tau \ln(1+\tau)$$

$$- 4\,\mathrm{Li}_3\left(1 - \frac{1}{\tau}\right) - 12\,\mathrm{Li}_3\,\frac{1}{1+\tau}\,]$$

$$+ (1+\tau)\,[-10\,\mathrm{Li}_2(-\tau) - \frac{5}{6}\pi^2 - 10 \ln\tau \ln(1+\tau)]$$

$$+ \frac{4}{3}(1+\tau+\tau^{-1})\ln^3\tau + (10 + 8\tau - \frac{1}{6}\pi^2\tau - \frac{5}{3}\pi^2)\ln\tau$$

$$+ (-8\tau-20\tau^{-1})\ln\tau\,\mathrm{Li}_2(-\tau) + (4\tau-5)\mathrm{Li}_2(1-\tau)$$

$$+ (-20+6\tau+20\tau^{-1})\mathrm{Li}_3(-\tau)$$

$$+ \frac{13}{2}\tau\ln^2\tau + (-2-7\tau-12\tau^{-1})\mathrm{Li}_3(1-\tau) + (6+15\tau+36\tau^{-1})\mathrm{Li}_3(1)$$

$$+ (-2+5\tau+8\tau^{-1})\ln\tau\,\mathrm{Li}_2(1-\tau) + 20(1-\tau) \qquad (3.27)$$

4. Deep-inelastic scattering diagrams

To obtain a physically meaningful result we have to subtract the singularities in (3.20) and (3.21) in a well-determined way. This implies that we have to make a decision about the definition of the parton distribution functions, and in particular about the absorption of non-singular terms in these functions. We will choose the convention introduced in section 2 and used for most of the first order results. For this convention the perturbative corrections to the structure function F_2 vanish.

In order to calculate the finite terms remaining after the subtraction of the singularities in (3.20) and (3.21) we have to calculate the deep-inelastic scattering diagrams shown in fig. 4.1. There is only one class of diagrams in this case; there are no contributions proportional to the product of two charges as in section 3.

In the calculation of these diagrams we must choose the same regularization method and the same gauge as we used for those of

fig. 3.1 (as explained in the previous section the gauge-choice is however irrelevant for the regularization methods we use). Therefore we have to calculate the deep-inelastic scattering diagrams both with an on-shell massive quark and with an off-shell, massless quark. From a comparison of fig. 4.1 and fig. 3.1 (which can be made by means of a double cut diagram) we deduce that the incoming quark in fig. 4.1 has to be the massive or off-shell one.

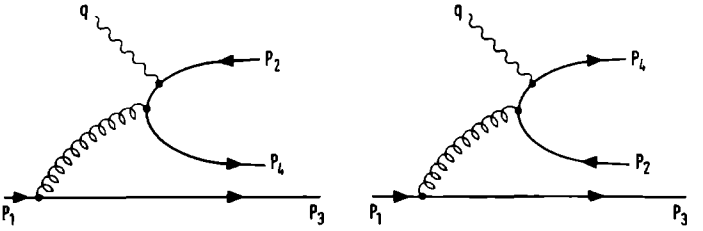

fig. 4.1: deep-inelastic scattering diagrams corresponding to fig. 3.1.

For the calculation we can use both of the methods described in section 3. The first method is to consider first the subprocess

$$g(p) + \gamma^*(q) \to q(p_4) + \bar{q}(p_2) \quad .$$

The four terms contributing to this process add up to a tensor $B_{\mu\nu\rho\sigma}$, where μ, ν are photon-indices and ρ, σ gluon-indices. The contribution to the parton structure function may be written as follows:

$$\nu W_2^J(x_p,Q^2) = C \int d\mathcal{P}\Big[-\frac{1}{2} x_p \Big[g^{\mu\nu} - \frac{12\, x_p^2}{Q^2} p_1^\mu p_1^\nu\Big] A^{\rho\sigma}(p_1,p_3)$$

$$B_{\mu\nu\rho\sigma}(p,q,p_2,p_4)\Big] \qquad (4.1)$$

where C contains all trivial factors. The first tensor in (4.1) projects out the structure function νW_2, and the second one is defined by (3.2); $d\mathcal{P}$ denotes the phase-space integral; x_p is the scaling variable for

the parton subprocess, $x_p = \frac{Q^2}{2p_1q}$.

As in section 3 we now perform the phase-space integral for the subprocess. This integral yields a tensor $T_{\mu\nu\rho\sigma}(p,q)$, which is conserved both with respect to its photon-indices and its gluon-indices:

$$\begin{aligned} q^\mu T_{\mu\nu\rho\sigma} &= q^\nu T_{\mu\nu\rho\sigma} = 0 \\ p^\rho T_{\mu\nu\rho\sigma} &= p^\sigma T_{\mu\nu\rho\sigma} = 0 \end{aligned} \tag{4.2}$$

In (4.1) only the symmetric part of the tensor contributes. Because of (4.2) this part must be a linear combination of the following six tensors:

$$\begin{aligned} T^1_{\mu\nu\rho\sigma} &= G_{\mu\nu}H_{\rho\sigma} \\ T^2_{\mu\nu\rho\sigma} &= G_{\mu\nu}P_\rho P_\sigma \\ T^3_{\mu\nu\rho\sigma} &= Q_\mu Q_\nu H_{\rho\sigma} \\ T^4_{\mu\nu\rho\sigma} &= Q_\mu Q_\nu P_\rho P_\sigma \\ T^5_{\mu\nu\rho\sigma} &= F_{\mu\rho}F_{\nu\sigma} + F_{\nu\rho}F_{\mu\sigma} \\ T^6_{\mu\nu\rho\sigma} &= F_{\mu\rho}Q_\nu P_\sigma + F_{\nu\rho}Q_\mu P_\sigma + F_{\mu\sigma}Q_\nu P_\rho + F_{\nu\sigma}Q_\mu P_\rho \end{aligned} \tag{4.3}$$

where

$$G_{\mu\nu} = g_{\mu\nu} - \frac{q_\mu q_\nu}{q^2} \qquad H_{\mu\nu} = g_{\mu\nu} - \frac{p_\mu p_\nu}{p^2}$$

$$P_\mu = q_\mu - \frac{p\cdot q}{p^2}p_\mu \qquad Q_\mu = p_\mu - \frac{p\cdot q}{q^2}q_\mu$$

$$F_{\mu\nu} = g_{\mu\nu} - \frac{p_\mu q_\nu}{p\cdot q}$$

Now we have to find six projection operators to determine the coefficients of these six basis tensors in a given tensor $T_{\mu\nu\rho\sigma}$. This problem can be solved by choosing six arbitrary but linearly independent operators, contracting them with $T_{\mu\nu\rho\sigma}$ and inverting the six by six matrix which relates the contractions to the coefficients. With these

operators we can then calculate the coefficients by performing the phase-space integral for the subprocess. Now a formula analogous to (3.6) or (3.7) can be derived for the remaining two dimensional integral:

$$\nu W_2^J(x) = 2\pi \left(\frac{\alpha_s}{4\pi}\right)^2 \frac{N^2-1}{N} \frac{x^4}{Q^4} \left[12\, p_1^\mu p_1^\nu - \frac{Q^2}{x^2} g^{\mu\nu}\right]$$

$$\times \int ds_1\, dp^2\, \frac{1}{p^4} \left[p_1^\rho p_3^\sigma + p_1^\sigma p_3^\rho - g^{\rho\sigma}(p_1 p_3 - m^2)\right] T_{\mu\nu\rho\sigma} \qquad (4.4)$$

where $p^2 = (p_1-p_3)^2$ and $s_1 = 2p\cdot q$. These integration variables have boundaries as shown in fig. 4.2.

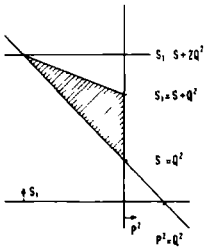

fig. 4.2: integration boundaries.

The upper limit of p^2 is not exactly zero, since that would cause (4.4) to be divergent. The upper limit depends upon the regularization method:

$$p^2_{max} = -m_1^2 \frac{x s_1^2}{Q^2\left(\frac{Q^2}{x} - s_1\right)} \quad ; \quad p^2_{max} = p_1^2 \frac{s_1 x}{Q^2} \qquad (4.5)$$

for the on-shell and off-shell method respectively. The integration area is now divided into two parts; the part with $s_1 < s + Q^2$ gives the mass singularity and the rest of the integral gives a finite contribution. The integrals are all relatively easy to calculate, and the major problem is to handle the large number of terms. For that purpose,

and for all other algebraic manipulations described in this section we used SCHOONSCHIP.

Before we present the result we will briefly discuss the second method we used. In contrast to section 3 we do not really need that method, because all diagrams can be handled by the first one, but nevertheless we used it as an independent check of our results.

We introduce the following variables:

$$s_3 = (p_1 + q - p_3)^2$$
$$s_4 = (p_1 + q - p_4)^2 \qquad (4.6)$$
$$s_2 = (p_1 + q - p_2)^2$$

where $s_3 + s_4 + s_2 = s$.

The angular variables are chosen as in section 3, but we interchange the role of the three outgoing quarks in the definitions of these variables at our convenience, thus reducing the number of integrals. The expression for the phase-space integral is as given by (3.10), but the boundaries of the integration are different. These are given by the well-known relation for a completely massless* three particle final state:

$$s_2 s_3 s_4 = 0 \qquad (4.7)$$

which yields a triangle in the plane defined by two of these variables.

The angular integral is completely analogous to the corresponding one in the calculations of section 3, and the results of appendix A can be used without modification. The double integral which remains to

---

*Only the off-shell regularization method, with massless quarks will be considered here.

be calculated can be written in a more convenient way by making a change of variables:

$$s_3 = Q^2\left(\frac{1}{\lambda} - 1\right) \tag{4.8}$$

which yields

$$\int_0^s ds_3 \int_0^{s-s_3} ds_4 \to Q^2 \int_x^1 \frac{d\lambda}{\lambda^2} \int_0^{\frac{Q^2}{\lambda x}(1-x)} ds_4$$

where we have used the relation $s = Q^2\left(\frac{1}{x} - 1\right)$.

The advantage of this change is that the λ-integral is identical to the one described in the previous section, and can be calculated by means of the same set of SCHOONSCHIP instructions. This reduces all the work that remains to be done to the s_4 integral. By using the three particle symmetry of the final state one can reduce the number of combinations of denominators to two, and therefore there are essentially two types of s_4 integrals to be calculated. One of these types can be integrated easily by applying the methods of appendix B. The other combination leads to a much more complicated integral. Since we have used this method only as a check of our results we leave out the details of that calculation. The most complicated integral will be discussed in more detail in section 7.

The calculation yields the following result:

$$\nu\tilde{W}_2^q(x) = e_q^2 \frac{N^2-1}{N}\left(\frac{\alpha_s}{4\pi}\right)^2 2x\,\tilde{\Omega}(x,\mu^2) \tag{4.9}$$

where $\mu^2 = -p_1^2/Q^2$ or m_1^2/Q^2.

The function $\tilde{\Omega}$ contains mass singularities and can be parametrized as follows:

$$\tilde{\Omega}(x,-\frac{p^2}{Q^2}) = \Omega^{(1)}(x)\,\ln^2(-\frac{p^2}{Q^2}) + \Omega^{(2)}_{OFF}(x)\,\ln(-\frac{p^2}{Q^2}) + \Omega^{(3)}_{OFF}(x) \tag{4.10}$$

$$\tilde{\Omega}(x, \frac{m^2}{Q^2}) = \Omega^{(1)}(x) \ln^2 \left(\frac{m^2}{Q^2(1-x)} \right) + \Omega^{(2)}_{ON}(x) \ln \left(\frac{m^2}{Q^2(1-x)} \right) + \Omega^{(3)}_{ON}(x) \tag{4.11}$$

The coefficient of the leading logarithm equals the one obtained in section 3:

$$\Omega^{(1)}(x) = \Sigma^{(1)}(x) \tag{4.12}$$

About the other coefficients the same remarks can be made as in section 3. The explicit expressions are:

$$\Omega^{(2)}_{OFF}(x) = 3(1+x)\ln^2 x + (5 + 5x - \frac{8}{3}x^2 + \frac{4}{3}x^{-1})\ln x + 9 - 6x - \frac{26}{9}x^2 - \frac{1}{9}x^{-1} \tag{4.13}$$

$$\Omega^{(2)}_{ON}(x) = 4(1+x)\ln^2 x + (6 + 4x - 4x^2 + \frac{8}{3}x^{-1})\ln x + \frac{29}{3} - \frac{23}{3}x - \frac{10}{3}x^2 + \frac{4}{3}x^{-1} - 2(1+x)\,Li_2(1-x) \tag{4.14}$$

$$\Omega^{(3)}_{OFF}(x) = 2(1+x)\ln^3 x + (8 + 13x - \frac{4}{3}x^2 + \frac{4}{3}x^{-1})\ln^2 x + (\frac{58}{3} + \frac{4}{3}x - \frac{52}{9}x^2 - \frac{1}{9}x^{-1})\ln x + \frac{38}{3} - \frac{23}{3}x - \frac{163}{27}x^2 + \frac{28}{27}x^{-1} + (\frac{4}{3}x^2 + 4)\frac{\pi^2}{6} + \frac{4}{3}(1+x)^3 x^{-1}\,[Li_2(-\frac{1}{x}) - \ln(1+x)\ln x] \tag{4.15}$$

$$\Omega^{(3)}_{ON}(x) = (1+x)[-2\,Li_3(1-x) - 4\,Li_2(1-x)\ln x + \frac{11}{3}\ln^3 x] + (\frac{23}{2} + \frac{29}{2}x - 4x^2 + \frac{10}{3}x^{-1})\ln^2 x - (4 + 6x - \frac{4}{3}x^2)Li_2(1-x) + (\frac{83}{3} - 11x - 10x^2 + \frac{8}{3}x^{-1})\ln x + (\frac{4}{3}x^2 + 4)\frac{\pi^2}{6} + \frac{52}{3} - \frac{44}{3}x - \frac{16}{3}x^2 + \frac{8}{3}x^{-1} + \frac{4}{3}(1+x)^3 x^{-1}\,[Li_3(-\frac{1}{x}) - \ln(1+x)\ln x] \tag{4.16}$$

5. The quark-gluon transition function

As we shall see in the next section we need for the subtraction of the mass singularities in the lepton pair production result not only a quark-antiquark transition function, which can be derived from (4.9), but also a quark-gluon transition function. This corresponds to the intuitive picture of a quark emitting a gluon, which subsequently scatters off the other quark, which emits the virtual photon producing the lepton pair. The quark-gluon transition cannot be obtained from a first order deep-inelastic scattering calculation, simply because the weak or electromagnetic probe does not couple to the gluon. The mass singularity of this transition can nevertheless be obtained in many ways. The coefficient of this singularity is by Mellin inversion related to the quark-gluon entry of the singlet anomalous dimension matrix. The mass singularity alone is however not sufficient for our purpose, because the final result will also depend upon the nonsingular terms in the transition function. These terms can only be fixed by giving a proper definition of the gluon distribution beyond the leading order.

For the quark distributions we used a definition in terms of the structure function $F_2(x)$, measured in deep-inelastic scattering processes. Such a definition is preferable, because it is closely related to experiment. An equivalent process which measures directly the gluon distribution is much harder to find. In any case such a process is at least of order α_s, and therefore it is in general screened by leading order processes. Only when, in some kinematical region, the leading processes are suppressed one may be able to measure the gluon distribution directly. Several candidates for such processes exist (e.g.

lepton pair or photon production at large transverse momentum). None of these candidates is very attractive for our purpose, because one has to do a second order calculation to take into account the effect of a definition. This is due to the fact that the leading process is of first order in α_s. Moreover the quality of the experimental information about these processes is incomparable to that of the measurement of the structure function F_2.

Since there is no compelling reason for choosing a particular definition, we will choose it in an arbitrary way. This does not lead to ambiguities in physical cross sections as long as one uses the same definition everywhere. The gluon distribution function, however, does depend upon this definition.

Beside the determination of the gluon distribution there is another reason why we need the finite terms in the quark-gluon transition function. As was the $q\bar{q}$ transition function, the qg transition function will depend upon the regularization method. If one wants to show that the final result is independent of this method one has to calculate the difference of these finite terms.

To achieve that we couple a scalar particle to the gluon, which probes the gluon distribution in the same way as the weak and electromagnetic vector bosons probe the quark distributions. We choose this coupling in such a way that the contribution of the longitudinal and the transverse gluon can be distinguished easily. The universality (process-independence) of the transition functions allows us to choose this coupling at our convenience. Instead of introducing a scalar-gluon vertex we give directly the expression for the absorptive part of the "Compton-amplitude" (fig. 5.1).

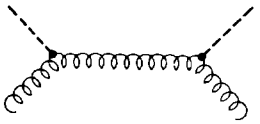

fig. 5.1: scalar-gluon scattering amplitude ; the dashed line represents the scalar particle.

$$T_{\mu\nu,ab}(p,q) = 2\pi\ \delta(p+q)^2\ \delta_{ab}\ \{A^T\ (\frac{q^2p^2-(q\cdot p)^2}{q^2}\ G_{\mu\nu} + \frac{p^2}{q^2}\ H_{\mu\nu}) - A^L\ \frac{p^2}{q^2}\ H_{\mu\nu}\} \qquad (5.1)$$

The external gluon lines in fig. 5.1 have an incoming momentum p and their Lorentz and color-indices are (μ,a) and (ν,b) respectively. The scalar lines have an incoming momentum q. The two tensors introduced in (5.1) are:

$$G_{\mu\nu} = -\ g_{\mu\nu} + \frac{p_\mu p_\nu}{p^2}$$
$$H_{\mu\nu} = (q_\mu - \frac{p\cdot q}{p^2}\ p_\mu)(q_\nu - \frac{p\cdot q}{p^2}\ p_\nu) \qquad (5.2)$$

Expression (5.1) can be considered as the "Feynman rule" needed for calculations involving the scalar particle. For our purpose this is sufficient, and in particular it is not necessary to introduce a coupling in a rigorous way via the lagrangian. When more rigor is needed - which will be the case if one considers higher orders - one can use gravitons instead of the scalar particle. Then the coupling can be introduced at the lagrangian level, but the fact that the graviton is a spin two particle leads to some technical complications which are absent if a scalar is used. For a discussion of gravitons, used as a probe for the gluon distributions see [Fis 79].

The calculations can be done in a way, completely analogous to deep-inelastic photon scattering. First of all we introduce a structure function. Because the probe is a scalar there is only one such function:

$$W_S^{\alpha} = \frac{1}{2\pi} \int d^4x \, e^{iqx} \, \langle P,\alpha | [J(x),J(0)] | P,\alpha \rangle_{av} \tag{5.3}$$

where J is the current to which the scalar couples. The subscript S means "scalar". The index α can denote either a physical hadron or quarks and gluons.

First of all we have to calculate the leading order contribution to W_S. This contribution is given by the diagram of fig. 5.1. Multiplying (5.1) with polarization vectors for the external gluon and averaging over the spin and color of this gluon we get

$$W_S^{g,T} = \frac{1}{2\pi} \frac{1}{2} \sum_{\lambda=1,2} \varepsilon_{\mu,a}^{T,\lambda} \varepsilon_{\nu,b}^{T,\lambda *} \frac{1}{N^2-1} T^{\mu\nu,ab}(p,q) \tag{5.4}$$

$$W_S^{g,L} = \frac{1}{2\pi} \varepsilon_{\mu,a}^{L} \varepsilon_{\nu,b}^{L*} \frac{1}{N^2-1} T^{\mu\nu,ab}(p,q) \tag{5.5}$$

for transversal and longitudinal gluons respectively.

To introduce the polarization vectors we choose the center of mass frame of the scalar and the gluon, and direct their momenta along the third axis. Then these vectors can be chosen as follows:

$$\begin{aligned} \varepsilon_{\mu}^{T,1} &= (0,1,0,0) \\ \varepsilon_{\mu}^{T,2} &= (0,0,1,0) \\ \varepsilon_{\mu}^{L} &= \left[\frac{(p\cdot q)^2}{p^2} - q^2 \right]^{-1/2} \left(q_{\mu} - \frac{p\cdot q}{p^2} p_{\mu} \right) \end{aligned} \tag{5.6}$$

These vectors are spacelike, orthogonal to each other and to p_{μ}, and normalized to -1. The first two are directed orthogonal to the third axis, and the third one is directed along that axis. In a Lorentz covariant notation the polarization sum for the transverse gluons is:

$$\sum_{\lambda=1,2} \epsilon^{T,\lambda}_{\mu,a}\, \epsilon^{T,\lambda *}_{\nu,b} = \{(-g^{\mu\nu} + \frac{p^\mu p^\nu}{p^2}) - \frac{1}{\frac{(p\cdot q)^2}{p^2} - q^2} (q^\mu - \frac{p\cdot q}{p^2} p^\mu)$$

$$\times (q^\nu - \frac{p\cdot q}{p^2} p^\nu)\} \delta_{ab} \qquad (5.7)$$

Using this result we obtain:

$$W_S^{g,T}(x) = \frac{1}{4} A^T \delta(1-x) \qquad (5.8)$$

$$W_S^{g,L}(x) = \frac{1}{4} A^L \delta(1-x) \qquad (5.9)$$

This explains why we have chosen expression (5.1) that way: the tensors multiplying A^T and A^L project out the longitudinal and transversal components of the gluon.

The hadronic structure function can be obtained by comparing hadron and parton cross sections in a way analogous to section II.1. The parton model leads to the following relation:

$$W_S^H(x) = \int_0^1 \sum_i \frac{f_i(\xi)}{\xi} W^i(\frac{x}{\xi})\, d\xi \qquad (5.10)$$

The summation is over quarks and longitudinal and transverse gluons. From (5.10), (5.8) and (5.9) we derive:

$$W_S^H(x) = \frac{1}{4} [f_g^L(x)\, A^L + f_g^T(x)\, A^T] \qquad (5.11)$$

This result can be used as the definition of the gluon distribution in exactly the same way as the structure function F_2 was used to define the quark distributions. Higher orders are subtracted in such a way that (5.11) is not modified, except by scaling deviations in the distribution functions. This defines the quark-gluon transition function for both the on-shell and the off-shell regularization method.

To calculate that transition function we need the contribution to

W_S^H from the imaginary part of the diagram of fig. 5.2.

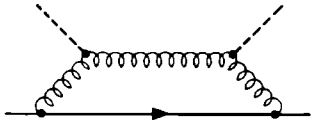

fig. 5.2: scalar-quark scattering amplitude.

According to (5.1) the imaginary part of this diagram equals:

$$W_S^q(x) = \frac{1}{2\pi}\frac{1}{2}\frac{1}{N} g^2 \, \mathrm{Tr}\,(T^a T^b) \int \frac{d^4p_3}{(2\pi)^4} 2\pi\delta(p_3^2-m^2) A^{\mu\nu}(p_1,p_3) T_{\mu\nu,ab}(p_1-p_3,q) \tag{5.12}$$

The tensor $A^{\mu\nu}$ is defined in section 3. The incoming quark has momentum p_1, the outgoing one - the cut quark line in fig. 5.2 - has momentum p_3; m is the mass of the quark. A straightforward calculation yields

$$\begin{aligned} W_S^q(x) = \frac{N^2-1}{4N}\frac{\alpha_s}{4\pi} \{ & A^T[-\frac{3}{2x} + (1-x)\ \frac{-2m^2+\lambda^2-2\lambda^2/x}{m^2x+\lambda^2(1-x)} \\ & + x(-1-\frac{2}{x^2}+\frac{2}{x})\ \ln\left(\frac{m^2x^3}{Q^2(1-x)} + \frac{\lambda^2x^2}{Q^2}\right)] \\ & + A^L[-2+\frac{2}{x}-\frac{1}{4}\frac{\lambda^4}{x}\frac{(1-x)^2}{(m^2x+\lambda^2(1-x))^2} + \lambda^2\frac{(\frac{2}{x}-\frac{3}{2})(1-x)}{m^2x+\lambda^2(1-x)} \\ & + (\frac{2}{x}-2)\ \ln\left(\frac{m^2x^3}{Q^2(1-x)} + \frac{\lambda^2x^2}{Q^2}\right)]\} \end{aligned} \tag{5.13}$$

where $\lambda^2 = m^2 - p_1^2$.

This result has to be convoluted with the quark distribution function and added to (5.11). The resulting expression is then re-interpreted as an expression similar to (5.11), but with f_g^L and f_g^T replaced by scale dependent distributions. The factors multiplying A^T and A^L are the "renormalized" distribution functions. The longitudinal gluon distributions are however not very relevant, because we have shown in section 2 that longitudinal gluons decouple from the physical

cross section. The renormalized transversal gluon distribution is:

$$f_g^T(x,Q^2) = f_g^T(x) + \frac{N^2-1}{N}\,\frac{\alpha_s}{4\pi}\int_x^1 d\xi\,\frac{f_q(\xi)}{\xi}\left\{-\frac{(1-\eta)^2+1}{\eta}\ln\frac{-p_1^2\eta^2}{Q^2} + 1 - \frac{7}{2\eta}\right\} \tag{5.14}$$

where $\eta = \frac{x}{\xi}$.

This is the result for the off-shell regularization method. The corresponding on-shell result is:

$$f_g^T(x,Q^2) = f_g'^T(x) + \frac{N^2-1}{N}\,\frac{\alpha_s}{4\pi}\int_x^1 d\xi\,\frac{f_q'(\xi)}{\xi}\left\{-\frac{(1-\eta)^2+1}{\eta}\ln\frac{m^2\eta^3}{Q^2(1-\eta)} + 2 - \frac{7}{2\eta}\right\} \tag{5.15}$$

The primes indicate that the "unrenormalized" distributions depend upon the regularization method in such a way that the renormalized ones are identical to a given order in perturbation theory.

The difference between (5.14) and (5.15) is one of the results we wanted to obtain in this section. The definition of the gluon distribution is given by (5.14) or (5.15), but because we used an unphysical scalar particle to obtain this result, this definition is arbitrary. Another definition, used in second order deep-inelastic scattering calculations, is the minimal subtraction scheme. This definition is physically just as arbitrary. To combine our results with these deep inelastic scattering results it is necessary to know the relation between the two definitions. We will postpone the calculation, necessary to obtain that relation, until chapter IV. There it will also be shown that the definition given above does not satisfy the momentum sum rule. Because it is very convenient to use distributions which satisfy this rule, it is better to modify (5.14) and (5.15) by the same finite terms, without changing their difference. Therefore we will use the following definition:

$$f_g(x,Q^2) = f_g(x) + \frac{N^2-1}{N}\frac{\alpha_s}{4\pi}\int_x^1 d\xi\,\frac{f_q(\xi)}{\xi}\left\{-\frac{(1-\eta)^2+1}{\eta}\ln\frac{-p_1^2\eta^2}{Q^2} - \frac{7}{2\eta} + 2\right\} \tag{5.16}$$

$$f_g(x,Q^2) = f_g(x) + \frac{N^2-1}{N}\frac{\alpha_s}{4\pi}\int_x^1 d\xi\,\frac{f_q(\xi)}{\xi}\left\{-\frac{(1-\eta)^2+1}{\eta}\ln\frac{m^2\eta^3}{Q^2(1-\eta)} - \frac{7}{2\eta} + 3\right\} \tag{5.17}$$

for off-shell and on-shell regularization respectively. The superscript 'T' has been left out here. We will show in chapter IV that this definition satisfies the momentum sum rule.

6. Subtraction of the mass singularities

In this section we combine the results of sections 3, 4 and 5 to obtain the final (and finite) result. First of all the relevant transition functions have to be determined. The general expression for a renormalized parton distribution is:

$$f_i(x,Q^2) = \int_x^1 \Gamma_{ij}\left(\frac{x}{\xi}, \mu^2\right) f_j(\xi)\,\frac{d\xi}{\xi} \tag{6.1}$$

where μ^2 is m^2/Q^2 or $-p^2/Q^2$.

Expanding (6.1) in α_s and considering the antiquark distribution only, we obtain:

$$f_{\bar{q}_i}(x,Q^2) = f_{\bar{q}_i}(x) + \frac{\alpha_s}{4\pi}\int_x^1 \frac{d\xi}{\xi}\left[\Gamma^{(1)}_{\bar{q}_i g} f_g(\xi) + \Gamma^{(1)}_{\bar{q}_i\bar{q}_i} f_{\bar{q}_i}(\xi)\right] + \left(\frac{\alpha_s}{4\pi}\right)^2 \int_x^1 \frac{d\xi}{\xi}\left[\sum_j \Gamma^{(2)}_{\bar{q}_i q_j} f_{q_j}(\xi) + \ldots\right] \tag{6.2}$$

The two terms of order α_s are only needed for processes with an incoming gluon or antiquark, and are irrelevant for the quark-quark process which we are considering. The second order term $\Gamma^{(2)}_{\bar{q}_i q_j}$ is the transition function we need (other second order terms have been left out). This transition function can be obtained explicitly by absorbing

the entire function νW_2 calculated in section 4 into the quark and antiquark distribution. It is natural to distribute the finite terms equally over the quarks and the antiquarks, so that the transition function becomes:

$$\Gamma^{(2)}_{\bar{q}_i q_j}(x,\mu^2) = \Gamma^{(2)}_{q_i q_j}(x,\mu^2) = \frac{N^2-1}{N}\,\tilde{\Omega}(x,\mu^2) \tag{6.3}$$

where $\tilde{\Omega}$ is defined in section 4.

The second transition function we need is the one calculated in section 5, which involves the gluon distribution. The expansion of (6.1) for this distribution is:

$$f_g(x,Q^2) = f_g(x) + \frac{\alpha_s}{4\pi}\int_x^1 \frac{d\xi}{\xi}\left[\sum_i \left(\Gamma^{(1)}_{gq_i} f_{q_i}(x) + \Gamma^{(1)}_{g\bar{q}_i} f_{\bar{q}_i}(x)\right) + \Gamma^{(1)}_{gg} f_g(x)\right] \tag{6.4}$$

The last two terms are irrelevant for our purpose, and Γ_{gq} can be read off from (5.16) and (5.17).

The factorization procedure for the non-identical quark cross section is given by the following relations:

$$\begin{aligned}\tilde{\sigma}^{q_1 q_2}(\mu_1^2,\mu_2^2) &= e_1^2\,\tilde{\sigma}^{qq}(\mu_2^2) + e_2^2\,\tilde{\sigma}^{qq}(\mu_1^2) + 2e_1e_2\,\sigma_I^{qq} \\ &= e_1^2\,\sigma^{q\bar{q}}\,\Gamma_{\bar{q}q}(\mu_2^2) + e_2^2\,\sigma^{q\bar{q}}\,\Gamma_{\bar{q}q}(\mu_1^2) \\ &+ e_1^2\,\sigma^{qg}\,\Gamma_{gq}(\mu_2^2) + e_2^2\,\sigma^{qg}\,\Gamma_{gq}(\mu_1^2) \\ &+ e_1^2\,\sigma^{qq} + e_2^2\,\sigma^{qq} + 2e_1e_2\,\sigma_I^{qq}\end{aligned} \tag{6.5}$$

where $\sim$ indicates the presence of a mass singularity, and σ denotes $\frac{d\sigma}{dQ^2}$. The functions $\tilde{\sigma}^{qq}$ and σ_I^{qq} are defined by (3.18), and are related by trivial factors to $\tilde{\Sigma}^{qq}$ and Σ_I^{qq}; the function σ^{qg} is related in an analogous way to Σ^{qg}, defined by (2.6); $\sigma^{q\bar{q}}$ finally is the leading Drell-Yan term:

$$\sigma^{q\bar{q}}(\tau) = \frac{4\pi\alpha^2}{3Q^4} \frac{1}{N} \delta(1-\tau) \tag{6.6}$$

The terms in (6.5) containing Γ-factors vanish when the distribution functions are redefined. The remaining terms are σ^{qq} and σ_I^{qq}. The latter could already be given in section 3, because it is finite. The other term is, according to (6.5):

$$\sigma^{qq} = \frac{4\pi\alpha^2}{3Q^4} \left(\frac{\alpha_s}{4\pi}\right)^2 \frac{N^2-1}{N^2} \tau \Sigma^{qq}(\tau) \tag{6.7}$$

where

$$\frac{N^2-1}{N^2} \Sigma^{qq}(\tau) = \frac{N^2-1}{N^2} \tilde{\Sigma}^{qq}(\tau,\mu^2) - \frac{1}{N} \Gamma_{qq}^{(2)}(\tau,\mu^2) - \int_\tau^1 \frac{d\xi}{\xi} \frac{1}{N} \Sigma^{qg}\left(\frac{\tau}{\xi}\right) \Gamma_{gq}^{(1)}(\xi,\mu^2) \tag{6.8}$$

Notice that in the left hand side of (6.8) $\tilde{\Sigma}^{qq}$, $\Gamma_{qq}^{(2)}$ and $\Gamma_{gq}^{(1)}$ are all different for on-shell and off-shell regularization. This regularization dependence cancels completely and the following expression is obtained:

$$\begin{aligned}
\Sigma^{qq}(\tau) = {} & (1+\tau)\,[8\mathrm{Li}_3(1-\tau) + 10\mathrm{Li}_3(1-1/\tau) - 6\mathrm{Li}_2(1-\tau)\ln\tau \\
& + 2\mathrm{Li}_2(1-\tau)\ln(1-\tau) + \ln\tau\ln^2(1-\tau) - \ln(1-\tau)\ln^2\tau - \ln^3\tau] \\
& + \mathrm{Li}_2(1-\tau)\,[9-2\tau+4\tau^{-1}] + \ln^2(1-\tau)\,[\tfrac{1}{2} - \tfrac{1}{2}\tau - \tfrac{2}{3}\tau^2 + \tfrac{2}{3}\tau^{-1}] \\
& + \tfrac{4}{3}\tau^{-1}(1+\tau)^3\,[\ln(1+\tau)\ln\tau - \mathrm{Li}_2(\tfrac{1}{\tau})] \\
& + \ln(1-\tau)\ln\tau\,[4 + 3\tau + \tfrac{8}{3}\tau^2 + \tfrac{4}{3}\tau^{-1}] \\
& + \ln^2\tau\,[-\tfrac{3}{2} - 9\tau - \tfrac{4}{3}\tau^2 - \tfrac{2}{3}\tau^{-1}] \\
& + \ln(1-\tau)\,[-\tfrac{37}{6} + \tfrac{19}{6}\tau - \tfrac{17}{9}\tau^2 + \tfrac{44}{9}\tau^{-1}] \\
& + \ln\tau\,[\tfrac{19}{2} - \tfrac{11}{3}\tau + \tfrac{28}{9}\tau^2 - \tfrac{4}{9}\tau^{-1}] \\
& + \tfrac{229}{18} - \tfrac{119}{9}\tau + \tfrac{110}{27}\tau^2 - \tfrac{193}{54}\tau^{-1} - \tfrac{2\pi^2}{3}(1 + \tfrac{1}{3}\tau^2)
\end{aligned} \tag{6.9}$$

The terms proportional to $\ln^2(1-\tau)$ in this expression have the same coefficient as the leading mass singularity.

7. The identical quark contribution

The results presented in sections 3 and 6 form the complete cross section for the quark-quark subprocess as long as the quarks are not identical. When two identical quarks scatter there is an additional contribution due to diagrams with crossed quark lines. The squares of the crossed diagrams, added to the squares of the non-crossed diagrams yield the results of the previous sections. (There are twice as many terms in this case, but all results have to be multiplied by a factor $\frac{1}{2}$ to correct for double-counting of the identical quark final state.) The new contribution comes from the interference between crossed and non-crossed diagrams. These diagrams will be the subject of this section.

The effect of the additional diagrams will turn out to be much smaller than the terms which we have already calculated. A few reasons for the fact that the new terms are small can be given a priori.

First of all the diagrams under consideration are all non-planar, and such diagrams are known to be suppressed in the large N limit compared to planar diagrams, like the ones discussed in section 3. This suppression factor is $\frac{1}{N}$ for an SU(N) gauge theory, which even for N = 3 is a considerable effect.

A second reason is the fact that the new diagrams, as we will show later in this section, have only a single logarithmic mass singularity as opposed to the double singularity of the diagrams of section 3. As was shown in the previous sections these mass singularities are linked to $\ln(1-\tau)$-terms which remain after factorization and dominate the finite terms in the limit $\tau \to 1$. This property, which is shared by all Drell-Yan corrections calculated up to now, reveals itself also in the results of this section. This implies that the finite correction terms

will behave as a single $\ln(1-\tau)$ for $\tau \to 1$, whereas the results of section 6 had a $\ln^2(1-\tau)$ behavior, and hence the new terms are suppressed in that limit.

The most important reason for the smallness of the identical quark contribution is however the power of the factors $(1-\tau)$ multiplying the logarithms mentioned above. It turns out that this factor is $(1-\tau)^5$ and this power is much larger than could be expected.

The diagrams can be subdivided into two classes, drawn in fig. 7.1 and fig. 7.2. In addition to these diagrams there are equivalent ones with p_1 and p_2 interchanged. If the external lines are on-shell the diagrams of fig. 7.1 and 7.2 form two gauge-invariant sets of diagrams.

To investigate the singularity of each set one can consider the double propagator diagrams as explained in section II.2. Each set contains one diagram of that type, namely the first one of fig. 7.1 and the fourth one of fig. 7.2. The double denominator of the first set has a singularity in the integration region, but the one of the second set is finite. From this fact one may conclude that only the first set will contribute to the mass singularity. As usual this identification of the singular terms applies only to the axial gauge. In other gauges the singularities are distributed over the diagrams within one set, and then the argument is only valid for the sum of all diagrams in that set.

As in section 3 we have to make a choice for the regularization method. Having shown explicitly that the results are independent of that choice, we will now restrict ourselves to the off-shell method. To cut off the mass singularity it turns out to be sufficient to take only p_1 off-shell.

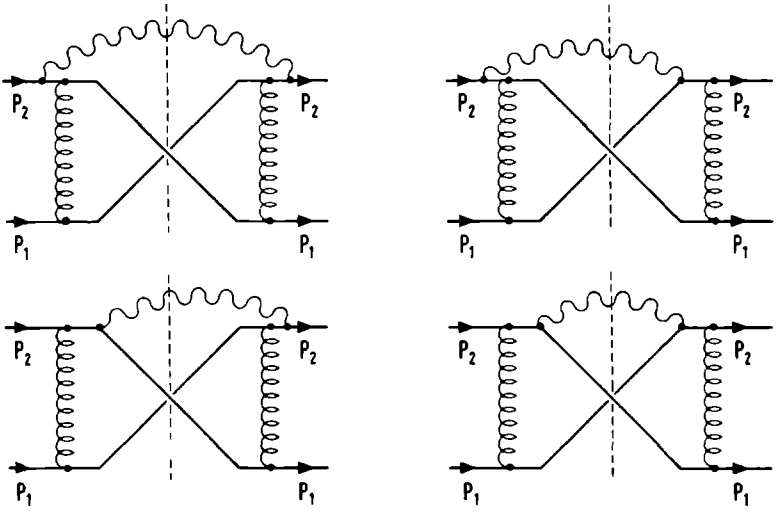

fig. 7.1: Class of diagrams contributing to the mass singularity.

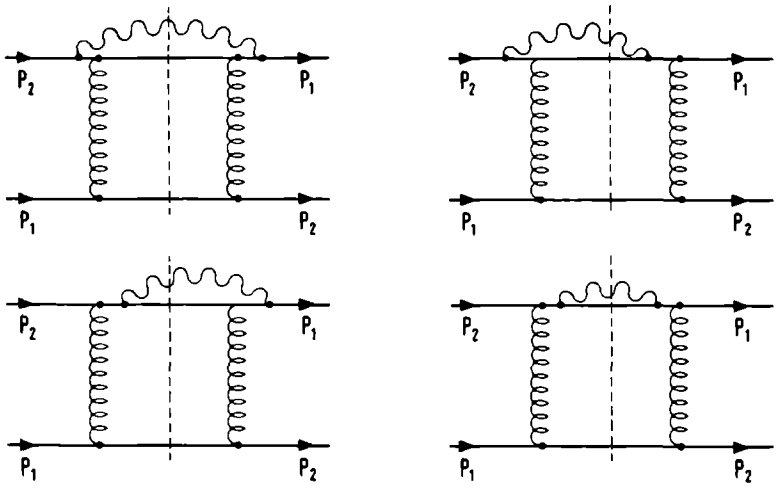

fig. 7.2: Class of non-singular diagrams. (Notice that the incoming momenta are interchanged in the right half of the diagram.)

The complete expression to be evaluated consists of several factors appearing as follows:

$$\frac{d\sigma^{qq}_{cr}}{dQ^2} = \frac{1}{4}\frac{1}{N^2} F_c(N)\; e_q^2 e^2 g^2\; \frac{e^2}{6\pi Q^2} [(-1)(1/2)(2)]$$

$$\times \frac{1}{2s} \int \frac{d^3p_3}{2E_3(2\pi)^3} \frac{d^3p_4}{2E_4(2\pi)^3} \frac{d^4q}{(2\pi)^3} \delta(q^2-Q^2)\; 2\pi^4\delta^4(p_1+p_2-p_3-p_4-q)$$

$$\times [-g^{\mu\nu} M^1_{\mu\nu}(p_1) - g^{\mu\nu} M^1_{\mu\nu}(p_2) - 2\, g^{\mu\nu} M^2_{\mu\nu}] \qquad (7.1)$$

These factors are respectively:

- a spin averaging factor $\frac{1}{4}$.
- a color averaging factor $1/N^2$.
- a color factor $F_c(N)$, which is the result of the following trace:

  $$F_c(N) = \sum_{a,b} Tr\; (T^a T^b T^a T^b) = -\frac{N^2-1}{4N} \quad .$$

  The 1/N suppression mentioned above can be seen by comparing this with (3.19).
- the squares of the quark charge, the electromagnetic and strong coupling constant.
- a factor coming from the lepton pair phase-space integral.
- a factor -1 because of the crossed fermion lines.
- a factor 1/2 to correct for double-counting in the identical quark phase space integral.
- a factor 2 because each interference term appears twice in the squared amplitude.
- a flux factor 1/2s.

In the integrand M^1 denotes the sum of the traces of the diagrams of fig. 7.1 and M^2 the equivalent result for fig. 7.2.

To calculate the integrals we use the second method of the two

discussed in section 3. The phase space integral is exactly the same, but a few extra terms appear in the integrand. These are due to two new propagators:

$$N_7 = (p_1 - p_4)^2$$
$$N_8 = (p_2 - p_3)^2 \qquad (7.2)$$

In most cases the symmetry of the phase space integral with respect to p_3 and p_4 can be used to transform these denominators into the ones already taken into account. This is however not possible when due to exchange of p_3 and p_4 one of the denominators $N_1..N_6$ multiplying N_7^{-1} or N_8^{-1} would transform into such a new denominator itself. Therefore we can conclude that the only new combinations are

1. N_1, N_8 and N_2, N_7
2. N_2, N_8 and N_1, N_7 .

For the first set we can use the relations:

$$N_1 + N_8 = p_1^2 + p_2^2 - \sqrt{s}\, E_3$$
$$N_2 + N_7 = p_1^2 + p_2^2 - \sqrt{s}\, E_4 \qquad (7.3)$$

to make a fractional decomposition with respect to the angular variables. One of the combinations in the second set, namely $N_2^{-1}N_8^{-1}$ does not occur in the diagrams considered here, but only in the ones with p_1 and p_2 interchanged. So only one new combination, $N_1^{-1}N_7^{-1}$, remains.

The integral over the angular variables can be performed by means of the formulae of appendix A. The result is a new type of double integral. The last integral can be calculated by means of the algorithms discussed in section 3 and appendix C, and therefore only the first integral remains to be calculated.

The new integrals are:

$$\int_0^{\rho_m} d\rho \, \frac{1}{\sqrt{X}} \ln Q \qquad \int_0^{\rho_m} d\rho \, \frac{\rho}{\sqrt{X}} \ln Q$$

$$\int_0^{\rho_m} d\rho \, \frac{\mu^2}{[\rho+\mu^2 \frac{\lambda-\tau}{\lambda}]\sqrt{X}} \ln Q \qquad \int_0^{\rho_m} d\rho \, \frac{\mu^2}{(\rho+\mu^2)\sqrt{X}} \ln Q \tag{7.4}$$

where

$$\rho = s_1/s \; ; \quad \lambda = s_3/s \; ; \quad \kappa = s_4/s \qquad \mu^2 = -p_1^2/s$$

$$\rho_m = 1 + \tau - \lambda - \tau/\lambda$$

$$X = \rho^2 + 2a\rho + b \qquad Q = \frac{4\mu^4\kappa\lambda(1-\kappa)(1-\lambda)}{[\rho+a+\sqrt{X}]^2}$$

$$a = \mu^2(1+\tau) - 2\mu^2\lambda(1+\tau-\lambda)$$

$$b = [\mu^2(1+\tau-2\lambda)]^2$$

Beside these four integrals there are a few simpler ones. The integrals can be simplified by means of the substitution

$$\rho = \frac{u^2 - ua + \frac{1}{4}(a^2-b^2)}{u}$$

where u is the new integration variable.

This reduces the calculation to straightforward but tedious algebra, which we do not need to discuss any further.

The diagrams of fig. 7.1 yield the following result:

$$\frac{d\sigma^1_{cr}(p_1)}{dQ^2} = \frac{4\pi\alpha^2}{3Q^4}\left(\frac{\alpha_s}{4\pi}\right)^2 \frac{N^2-1}{N^3} e_q^2 \, \tau \left\{ \Sigma^{(1)}_{cr}(\tau) \ln\left(\frac{-p_1^2}{Q^2}\frac{\tau^2}{1-\tau}\right) + \Sigma^{(2)}_{cr}(\tau) \right\} \tag{7.5}$$

The function $\Sigma^{(2)}_{cr}$ (where 'cr' means 'crossed') is given explicitly in appendix D; the function $\Sigma^{(1)}_{cr}$ equals:

$$\Sigma^{(1)}_{cr}(\tau) = \frac{1+\tau^2}{1+\tau}\left[\ln^2\tau - 4\ln\tau\ln(1+\tau) - 4Li_2(-\tau) - \frac{\pi^2}{3}\right]$$

$$+ 2(1+\tau)\ln\tau + 4(1-\tau) \tag{7.6}$$

This factor is related to part of the second order anomalous dimension of the quark operator, and is discussed in that respect by [Ros 79, Cur 80b] who obtain the same result. (Apart from a factor 4 in the result of the first authors; see [Sch 80b], footnote 10.)

For the diagrams of fig. 2 we find:

$$\frac{d\sigma^2_{cr}}{dQ^2} = \frac{4\pi\alpha^2}{3Q^4}\left(\frac{\alpha_s}{4\pi}\right)^2 \frac{N^2-1}{N^3} e_q^2 \, \tau \, \Sigma^{(3)}_{cr}(\tau) \tag{7.7}$$

This expression is surprisingly simple:

$$\Sigma^{(3)}_{cr}(\tau) = (1-\tau)^2 \left[2Li_3(1-1/\tau) - 3Li_2(1-1/\tau)\right] + \left(\frac{7}{2} - 3\tau\right)\ln\tau + \frac{1}{2}(1-\tau) + \frac{13}{4}(1-\tau)^2 \tag{7.8}$$

All functions are analytic in the neighborhood of $\tau = 1$; all factors $\ln(1-\tau)$ which would disturb this analyticity are explicitly factorized in (7.5). The leading terms in an expansion in $(1-\tau)$ are:

$$\begin{aligned}
\Sigma^{(1)}_{cr}(\tau) &= \frac{1}{10}(1-\tau)^5 + O((1-\tau)^6) \\
\Sigma^{(2)}_{cr}(\tau) &= \left(\frac{\pi^2}{6} - 1\right)(1-\tau)^2 + O((1-\tau)^3) \\
\Sigma^{(3)}_{cr}(\tau) &= -\frac{2}{3}(1-\tau)^3 + O((1-\tau)^4)
\end{aligned} \tag{7.9}$$

According to (7.1) the complete, unsubtracted result is:

$$\frac{d\tilde{\sigma}^{qq}_{cr}}{dQ^2} = \frac{d\tilde{\sigma}^1_{cr}(p_1)}{dQ^2} + \frac{d\tilde{\sigma}^1_{cr}(p_2)}{dQ^2} + 2\frac{d\sigma^2_{cr}}{dQ^2} \tag{7.10}$$

Now we have to subtract the mass singularities, and for that subtraction we will use the same convention as in section 6. Therefore the deep-inelastic scattering diagrams related to the diagrams of fig. 7.1 have to be calculated. These diagrams are drawn in fig. 7.3. For the calculation the algorithms described in section 4 can be used, provided that some additions are made, which are necessary to include the

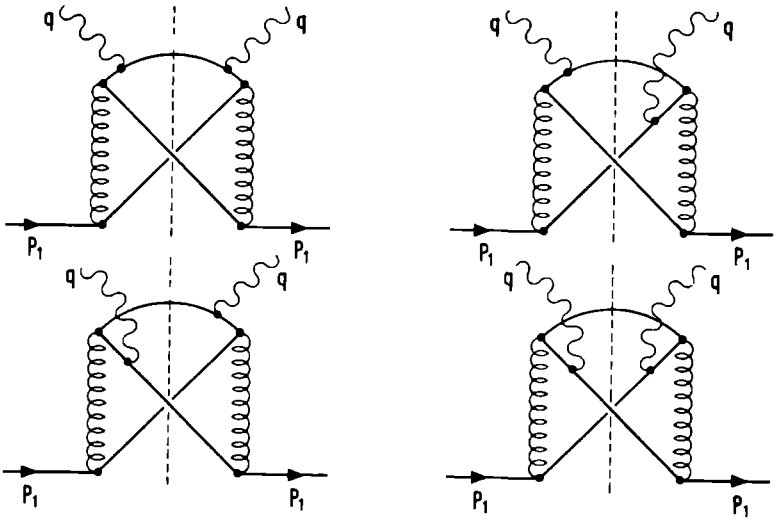

fig. 7.3: Deep-inelastic scattering diagrams corresponding to fig. 7.1.

following new combinations of propagators:

$$\frac{1}{(p_2-q)^2(p_1-p_4)^2} \quad \text{and} \quad \frac{1}{(p_2-q)^2(p_3-q)^2} \ .$$

(Combinations related to these by exchange of final state quarks have been left out.) The first combination contributes to the mass singularity, the second gives a finite result. The calculation of all integrals originating from the first combination can be carried out along the lines of section 4. The calculation of the integrals coming from the other combination is more complicated. Therefore we will restrict ourselves to a brief outline of the calculation of this integral. This type includes some of the integrals needed in section 4.

After angular integration, according to appendix A, we obtain the following integrals:

$$\int ds_3\, ds_4\, \frac{y^n}{\sqrt{X}} \ln Q \qquad \int ds_3\, ds_4\, \frac{s_4^2 y^n}{\sqrt{X}} \ln Q$$

$$\int ds_3\, ds_4\, \frac{y^n}{s_4 - s - Q^2}\, \frac{1}{\sqrt{X}} \ln Q$$

$$\int ds_3\, ds_4\, \frac{1}{s_4 - s - Q^2}\, \frac{1}{s_2 - s - Q^2}\, \frac{1}{\sqrt{X}} \ln Q$$

where

$$y = \frac{s_3 + Q^2}{Q^2} \quad ; \quad \tau = \frac{Q^2}{s + Q^2} \quad ;$$

$$X = \frac{1}{64\tau^2 (1-\tau)^2} \left[-y + 4x^2\tau^2 y + y^2(1+\tau^2) - y^3\tau^2 \right]$$

$$Q = \frac{\frac{1}{2} + \frac{1}{2} y^2\tau^2 - 2x^2\tau^2 - y + \sqrt{4x^2\tau^2 y + y^2(1+\tau^2) - y^3\tau - y}}{\frac{1}{2} + \frac{1}{2} y^2\tau^2 - 2x^2\tau^2 - y - \sqrt{4x^2\tau^2 y + y^2(1+\tau^2) - y^3\tau - y}}$$

$$x = \frac{1}{Q^2} \left(-s_4 + \frac{1}{2} (s - s_3) \right)$$

This integral can be transformed into a much simpler one by making the following substitutions:

$$x = \frac{q^2 + (y-1)(\tau^2 y - 1)}{4q\tau} \quad ; \qquad y = z^2 \quad .$$

Then, for example, the first integral becomes:

$$8(1-\tau) \int_1^{1/\sqrt{\tau}} dz \int_{(z-1)(1+z\tau)}^{(z+1)(1-z\tau)} \frac{dq}{q}\, z^{2n}$$

$$\times \ln \frac{[q-(1+z)(1-z\tau)][q-(z-1)(1+z\tau)][q-(1+z)(1+z\tau)][q-(z-1)(1-z\tau)]}{[q+(1+z)(1-z\tau)][q+(z-1)(1+z\tau)][q+(1+z)(1+z\tau)][q+(z-1)(1-z\tau)]}$$

This clearly solves the problem as far as the q-integration is concerned. The other integrals give similar expressions, which are also integrable in principle.

When the q-integral is performed the result can be adapted to be acceptable input for the program which does the final integration,

described in section 3 and appendix C. This is achieved by means of the substitution $z = \sqrt{\lambda/\tau}$. A few new monomials of λ appear in the integrand, which made an extension of the program necessary. These monomials are $\lambda - 1/\tau$ and $\lambda + 1$. This does not change the algorithms on which the program was based, but requires additions to the set of built-in integrals. The non-trivial additions are given in appendix C.

After this procedure we arrive at the following result:

$$\nu W_2^{cr}(x,Q^2) = \frac{N^2-1}{N^2}\left(\frac{\alpha_s}{4\pi}\right)^2 e_q^2 \times [\Omega_{cr}^{(1)}(x) \ln \frac{-p_1^2 x^2}{Q^2} + \Omega_{cr}^{(2)}(x)] \qquad (7.11)$$

The function $\Omega_{cr}^{(2)}(x)$ is given in appendix D; $\Omega_{cr}^{(1)}$ is equal to $\Sigma_{cr}^{(1)}$. Near $x = 1$ $\Omega_{cr}^{(2)}$ is analytic and behaves as follows:

$$\Omega_{cr}^{(2)}(x) = (2 - \frac{\pi^2}{6})(1-x) + ()((1-x)^2) \qquad (7.12)$$

Concerning the subtraction of the mass singularity an important difference with the previous sections should be mentioned. In section 6 the deep-inelastic scattering mass singularity was distributed equally over a $q_i\bar{q}_j$ and a $q_i q_j$ transition. One may be tempted to conclude that the same is true in this case, because the photon couples both to the quark and the antiquark in fig. 7.3. However in this case the diagrams are clearly not symmetrical with respect to the outgoing quark, created by the gluon, and the outgoing antiquark, and therefore the argument is wrong. The correct way of factorizing the singularity is to attribute it completely to the quark-antiquark transition function. This can be seen in two ways.

The first argument is that only the cut diagrams with the photon line attached to the outgoing antiquark have double divergent propagators. In the axial gauge only these diagrams contribute to the mass singularity, which indicates that this singularity should be

factorized into the $q\bar{q}$ transition function.

The second argument uses the universality of mass singularities. Suppose we change the external electromagnetic current by a flavor changing one. To be able to construct a diagram with crossed lines we need a situation where the two final quarks are identical to the initial one. There is no restriction on the flavor of the outgoing antiquark. From the electromagnetic process we learn that a process as in fig. 7.3 can only contribute to a transition function from a quark to its own antiquark or to itself. Therefore universality restricts the flavor of that part of the upper quark line which couples to the gluon to be identical to the flavor of the incoming quark. On the other hand, the topology of the diagram restricts the flavor of all outgoing quarks to be identical to that of the incoming quark. Therefore, as far as the mass singularity is concerned, there can be no contribution from a diagram with a flavor changing vertex in the outgoing quark line.

These arguments force us to absorb the mass singularity entirely into the antiquark distribution, but in principle we are free to absorb the finite terms in a different way. The most natural procedure is, however, to absorb these terms in the antiquark distributions as well, by means of the following definition:

$$f_{\bar{q}}(x,Q^2) = f_{\bar{q}}(x) + \left(\frac{\alpha_s}{4\pi}\right)^2 \frac{N^2-1}{N^2} \int_x^1 d\xi \, \frac{f_q(\xi)}{\xi} \left[\Omega_{cr}^{(1)}\left(\frac{x}{\xi}\right) \ln \frac{-p_1^2 x^2}{Q^2 \xi^2} + \Omega_{cr}^{(2)}\left(\frac{x}{\xi}\right) \right] \tag{7.13}$$

This defines the non-singlet part of the $q\bar{q}$ transition function. Using (7.13) we obtain the following final result:

$$\frac{d\sigma_{cr}^{qq}}{dQ^2} = \frac{4\pi\alpha^2}{3Q^4} \left(\frac{\alpha_s}{4\pi}\right)^2 \frac{N^2-1}{N^3} e_q^2 \, 2\tau \, \Sigma_{cr}^{qq}(\tau) \tag{7.14}$$

where

$$\Sigma_{cr}^{qq}(\tau) = \Sigma_{cr}^{(2)}(\tau) + \Sigma_{cr}^{(3)}(\tau) - \Sigma_{cr}^{(1)}(\tau) \ln(1-\tau) - \Omega_{cr}^{(2)}(\tau) \quad . \quad (7.15)$$

An explicit expression can be constructed out of the results of appendix D.

Appendix A

In this appendix results are given for the following type of integrals:

$$I(n,m) = \int d\cos\theta\, d\xi\, \{[a+b\cos\theta]^{-n}\,[A+B\cos\theta + C\cos\theta\cos\xi]^{-m}\}$$

The symbol X used below is defined as follows:

$$X = (aA - bB)^2 - (A^2 - B^2 - C^2)(a^2 - b^2) \quad .$$

The results are:

$$I(1,0) = \frac{2\pi}{b} \ln\frac{a+b}{a-b}$$

$$I(0,1) = \frac{2\pi}{\sqrt{B^2+C^2}} \ln\frac{A+\sqrt{B^2+C^2}}{A-\sqrt{B^2+C^2}}$$

$$I(1,1) = \frac{2\pi}{\sqrt{X}} \ln\frac{aA-bB+\sqrt{X}}{aA-bB-\sqrt{X}}$$

$$I(1,-1) = \frac{4\pi B}{b} + \frac{2\pi(Ab-aB)}{b^2} \ln\frac{a+b}{a-b}$$

$$I(-1,1) = \frac{4\pi Bb}{B^2+C^2} + \frac{2\pi(a(B^2+C^2)-ABb)}{(\sqrt{B^2+C^2})^3} \ln\frac{A+\sqrt{B^2+C^2}}{A-\sqrt{B^2+C^2}}$$

$$I(2,0) = \frac{4\pi}{a^2-b^2}$$

$$I(0,2) = \frac{4\pi}{A^2-B^2-C^2}$$

$$I(2,1) = \frac{4\pi b}{X(a^2-b^2)}(Ab-aB) + \frac{2\pi(a(B^2+C^2)-ABb)}{(\sqrt{X})^3} \ln\frac{aA-bB+\sqrt{X}}{aA-bB-\sqrt{X}}$$

$$I(1,2) = \frac{4\pi(a(B^2+C^2)-bAB)}{X(A^2-B^2-C^2)} + \frac{2\pi b(bA-aB)}{(\sqrt{X})^3} \ln\frac{aA-bB+\sqrt{X}}{aA-bB-\sqrt{X}}$$

$$I(2,2) = \frac{4\pi b^2}{X(a^2-b^2)} + \frac{4\pi(B^2+C^2)}{X(A^2-B^2-C^2)} - \frac{12\pi b^2C^2}{X^2} + \left(\frac{2\pi Bb}{(\sqrt{X})^3} + \frac{6\pi b(bA-aB)(a(B^2+C^2)-bAB)}{(\sqrt{X})^5}\right) \ln\frac{aA-bB+\sqrt{X}}{aA-bB-\sqrt{X}}$$

$$I(2,-1) = \frac{2\pi B}{b^2} \ln\frac{a+b}{a-b} + \frac{4\pi}{b}\frac{Ab-aB}{a^2-b^2}$$

$$I(-1,2) = \frac{2\pi Bb}{(\sqrt{B^2+C^2})^3} \ln \frac{A+\sqrt{B^2+C^2}}{A-\sqrt{B^2+C^2}} + \frac{4\tau(a(B^2+C^2)-ABb)}{(B^2+C^2)(A^2-B^2-C^2)}$$

These results are valid for $|a| > |b|$ and $A^2 > (B^2 + C^2)$.

Appendix B

In this appendix the integration of the results of the previous appendix will be discussed. We use the following variables:

$$\lambda = s_3/s \qquad \kappa = s_4/s$$

$$\rho = s_1/s \qquad \tau = Q^2/s$$

$$\mu_1^2 = -p_1^2/s \quad (\text{or } m_1^2/s) \qquad \mu_2^2 = -p_2^2/s \quad (\text{or } m_2^2/s) \quad .$$

The integrals can be subdivided into several classes, depending upon the combination of angle-dependent factors from which they originate. In each case we will give the necessary substitutions and other relevant steps, and the most difficult integrals.

a. Integrals originating from single denominators N_3 or N_5 (defined by (3.13)). We define the following variables:

$$Q = \frac{\rho-1+\tau+\sqrt{\lambda(1,\rho,\tau)}}{\rho-1+\tau-\sqrt{\lambda(1,\rho,\tau)}} \qquad X = \lambda(1,\rho,\tau)$$

$$A_1 = \left|\frac{\sqrt{\tau}-\lambda}{\sqrt{\tau}-\tau}\right| \qquad A_2 = \frac{\sqrt{\tau}+\lambda}{\sqrt{\tau}+\tau}$$

$$\gamma = \rho - 1 - \tau$$

(The function λ is defined by $\lambda(a,b,c) = a^2+b^2+c^2-2ab-2ac-2bc$.) The integration variable ρ is bounded as given by (3.12). We will omit these boundaries in the following. The integrals can be calculated by means of the substitution:

$$z = \rho - 1 - \tau + \sqrt{\lambda(1,\rho,\tau)} \quad .$$

The results are:

$$\int \frac{1}{\sqrt{X}} \ln Q \, d\rho = \ln^2 \lambda - \ln \lambda \ln \tau + Li_2(\tau/\lambda) + Li_2(\lambda) - Li_2(\tau) - \frac{\pi^2}{6}$$

$$\int \frac{Y}{\sqrt{X}} \ln Q \, d\rho = -(\lambda-\tau/\lambda) \ln \frac{\lambda(\lambda-\tau)}{\tau(1-\lambda)} + (1-\tau) \ln\left(\frac{\lambda(1-\tau)^2}{\tau(1-\lambda)(\lambda-\tau)}\right) - 1 - \tau + \tau/\lambda + \lambda$$

$$\int \frac{1}{X} \, d\rho = \frac{1}{2\sqrt{\tau}} [\ln (A_2) - \ln (A_1)]$$

$$\int \frac{Y}{X} \, d\rho = \ln (A_1) + \ln (A_2) + \ln (\tau/\lambda)$$

$$\int \frac{1}{(\sqrt{X})^3} \ln Q \, d\rho = -\frac{1}{2} \frac{1}{\lambda^2-\tau} \ln \frac{\lambda(\lambda-\tau)}{\tau(1-\lambda)} + \frac{1}{2\tau} \ln (\tau/\lambda) + \frac{1}{2(1-\tau)} \ln \frac{1-\tau}{1-\lambda}$$

$$+ \frac{1}{2} \frac{1}{\tau(1+\sqrt{\tau})} \ln (A_2) + \frac{1}{2} \frac{1}{\tau(1-\sqrt{\tau})} \ln (A_1) - \frac{1}{2} \frac{1}{\tau(1-\tau)} \ln \frac{\lambda-\tau}{1-\tau}$$

$$\int \frac{Y}{(\sqrt{X})^3} \ln Q \, d\rho = \frac{\lambda}{\lambda^2-\tau} \ln \frac{\lambda(\lambda-\tau)}{\tau(1-\lambda)} - \frac{1}{1-\tau} \ln \frac{(1-\tau)^2}{(\lambda-\tau)(1-\lambda)}$$

$$+ \frac{1}{\tau-\sqrt{\tau}} \ln (A_1) + \frac{1}{\tau+\sqrt{\tau}} \ln (A_2) \quad .$$

When all integrals of this type are added one finds that all terms containing $\ln A_1$, $\ln A_2$, $\sqrt{\tau}$ or $\lambda^2-\tau$ cancel.

b. Integrals originating from combinations of the denominators N_1 and N_2.

1. Off-shell.

The following variables are used*:

$$X = \frac{1}{\lambda^2} \{[\sigma + \mu_1^2(\sigma+\lambda-\tau) + \mu_2^2(\frac{\sigma+\tau}{\lambda} + \sigma - \tau)]^2 - 4\mu_1^2\mu_2^2\lambda\kappa(1-\lambda)(1-\kappa)\}$$

$$Q = \frac{[\sigma + \mu_1^2(\lambda-\tau) + \mu_2^2 \frac{\tau}{\lambda}(1-\lambda) + \sqrt{X}]^2}{4\mu_1^2\mu_2^2(\sigma+\tau)(1-\lambda)\frac{1}{\lambda}(\lambda-\tau-\sigma)}$$

where $\sigma = \kappa\lambda - \tau$.

A convenient substitution is:

---

*This variable X differs by a factor $\frac{64}{s^4}$ from the one defined in appendix A. Moreover some allowed approximations are made. The same remark applies to the on-shell result.

$$2z = \sigma + \mu_1^2(\lambda-\tau) + \mu_2^2 \frac{\tau}{\lambda}(1-\lambda) + \sqrt{X} \quad .$$

Then the integral becomes:

$$\int \frac{1}{\sqrt{X}} \ln Q \, d\kappa = \int_{z_{min}}^{z_{max}} \frac{dz}{z} \ln \frac{z^2}{\mu_1^2\mu_2^2(z+\tau)\frac{1}{\lambda}(1-\lambda)(\lambda-\tau-z)}$$

In this step some approximations are made, which are allowed for μ_1^2 and $\mu_2^2 << 1$. The upper boundary for z is $(\lambda-\tau)(1-\lambda)$; the lower boundary is either $\mu_1^2(\lambda-\tau)$ or $\mu_2^2 \frac{\tau}{\lambda}(1-\lambda)$, depending upon the relative magnitude of these expressions. The result, however, turns out to be the same for both possibilities:

$$\int \frac{1}{\sqrt{X}} \ln Q \, d\kappa = \ln \frac{\mu_2^2\tau}{\lambda(\lambda-\tau)} \ln \frac{\mu_1^2}{1-\lambda} + Li_2\left(-\frac{(\lambda-\tau)(1-\lambda)}{\tau}\right) + Li_3(1-\lambda) \quad .$$

This integrand can also occur in combination with a factor $\frac{1}{\kappa}$, κ or $\frac{1}{\kappa-\tau}$. In those cases one can use an approximate fractional decomposition, e.g.:

$$\frac{1}{\kappa}\frac{1}{\sqrt{X}} = \left(\frac{1}{\sqrt{X}} - \frac{1}{\kappa}\right)\frac{\lambda}{\tau} + O(\mu^2) \quad .$$

The last term is negligible.

By means of this procedure one obtains additional integrands $\ln Q$, $\frac{1}{\kappa}\ln Q$ and $\frac{1}{\kappa-\tau}\ln Q$. None of these has a singularity at one of the boundaries, and therefore the following approximation is allowed:

$$Q \sim \frac{\sigma^2}{\mu_1^2\mu_2^2(\sigma+\tau)\frac{1}{\lambda}(1-\lambda)(\lambda-\tau-\sigma)} \quad .$$

The integrals are then straightforward.

ii. On-shell.

In this case we have:

$$X = \frac{1}{\lambda^2}\{[\sigma + (\mu_1^2+\mu_2^2)(\tau-\sigma)]^2 - 4\mu_1^2\mu_2^2(\sigma+\tau)^2\}$$

$$Q = \frac{[\sigma + (\mu_1^2+\mu_2^2)(\tau-\sigma) + \sqrt{X}]^2}{4\mu_1^2\mu_2^2(\sigma+\tau)^2}$$

The calculation can be done in the same way as for the off-shell case, and we will only give the result:

$$\int \frac{1}{\sqrt{X}} \ln Q \, d\kappa = \ln\left(\mu_1^2 \frac{\lambda}{(1-\lambda)^2}\right) \ln\left(\mu_2^2 \frac{\tau^2}{\lambda(\lambda-\tau)}\right) + 2 \, Li_2 \left(-\frac{(\lambda-\tau)(1-\lambda)}{\tau}\right)$$

c. Integrals originating from combinations of N_1 and N_3 (or N_2 and N_5).

1. Off-shell.

In this case we define:

$$\sqrt{X} = \rho + \mu_1^2 \left(\frac{\lambda-\tau}{\lambda}\right) \quad *$$

$$Q = \frac{\mu_1^2 \frac{\tau}{\lambda}(1-\lambda)}{\rho+\mu_1^2(1-\tau)}$$

$$V = \rho + \mu_1^2(1-\tau)$$

Combinations of ρ, V and $\sqrt{X}$ can be separated by means of fractional decompositions. The following integrals can be simplified by an integration by parts:

$$\int \frac{d\rho}{(\sqrt{X})^n} \ln Q = \frac{-1}{n-1} \int d\rho \, \frac{1}{(\sqrt{X})^{n-1}} \frac{1}{V} + \frac{1}{n-1} \left[\frac{\lambda}{\mu_1^2(\lambda-\tau)}\right]^{n-1} \ln \frac{\tau(1-\lambda)}{\lambda(1-\tau)}$$

Notice the power-singularity in μ_1^2 which appears in this intermediate step. Singularities like this will always cancel in the final result. The integral which remains to be calculated can be simplified further by fractional decomposition. Then a number of trivial integrals is obtained. This procedure does not work for n = 1, but in that case the result can be obtained directly by means of the definition of the

---

*The definition of appendix A for X yields:

$$X = \frac{\lambda^2 s^4}{64} (\rho + \mu_1^2(\frac{\lambda-\tau}{\lambda}))^2 (1 + 2\mu_1^2 + 2\mu_2^2(1 + \frac{1}{\lambda})) + ()(\mu^4)$$

The first factors have been omitted here. The last factor has to be expanded in μ_1^2 and μ_2^2 when X appears with a negative power.

dilog (3.16):

$$\int \frac{d\rho}{\sqrt{X}} \ln Q = -\frac{1}{2}\ln^2 \frac{\lambda-\tau}{\mu_1^2\tau} + Li_2 \frac{\lambda-\tau}{\lambda(1-\tau)} + \frac{1}{2}\ln^2 \frac{\lambda(1-\tau)}{\tau(1-\lambda)} - \frac{\pi^2}{6} \quad .$$

Beside these integrands there are factors $\frac{1}{\kappa}$ or $\frac{1}{\kappa-\tau}$ which can be separated from the others by fractional decompositions, as described under b. None of these integrals leads to serious complications.

ii. On-shell.

In this case the relevant variables are:

$$X = \rho^2 - 4\mu_1^2\mu_2^2 \qquad *$$

$$Q = \frac{\rho + 2\mu_1^2\tau - \sqrt{\rho^2-4\mu_1^2\mu_2^2}}{\rho + 2\mu_1^2\tau + \sqrt{\rho^2-4\mu_1^2\mu_2^2}}$$

$$V = \rho + \mu_1^2\tau + \mu_2^2\frac{1}{\tau}$$

Integrals with factors $(\sqrt{X})^{-n}$ $n \neq 1$ can be simplified by integration by parts, as described above. For n = 1 we use the substitution:

$$z = \rho + \sqrt{\rho^2 - 4\mu_1^2\mu_2^2}$$

Then we obtain the following result:

$$\int \frac{d\rho}{\sqrt{X}} \ln Q = -\frac{1}{2}\ln^2 \frac{\mu_1^2\tau\lambda}{(\lambda-\tau)(1-\lambda)} + \frac{1}{2}\ln^2\left(1 + \frac{\mu_2^2}{\mu_1^2}\frac{(1-\lambda)}{\tau(\lambda-\tau)}\right) + \frac{1}{2}\ln^2\frac{\lambda(1-\tau)}{\tau(1-\lambda)}$$

$$+ Li_2 \frac{\mu_2^2(1-\lambda)}{\mu_1^2\tau(\lambda-\tau) + \mu_2^2(1-\lambda)} + Li_2 \frac{\lambda-\tau}{\lambda(1-\tau)} - \frac{\pi^2}{6}$$

Notice the appearance of mass-ratio's in this expression. The other integrals of this type are simple, although more complicated than in

---

*The definition of appendix A yields in this case:

$$X = \frac{\lambda^2 s^4}{64}(\rho^2 - 4\mu_1^2\mu_2^2)(1 - 2\mu_1^2 - 2\mu_2^2)$$

The factor $\frac{1}{64}\lambda^2 s^4$ has been omitted here and the last factor can be expanded in μ_1^2 and μ_2^2.

the off-shell case.

d. Integrals originating from combinations of N_1 and N_5 (or N_2 and N_3).

i. Off-snell.

Omitting a factor $\frac{s^2}{8}$ for $\sqrt{X}$ compared to the definition of appendix A we get:

$$\sqrt{X} = \kappa + \lambda\tau - 2\tau$$

$$Q = \frac{(\kappa+\lambda\tau-2\tau)^2}{\mu_1^2\lambda\tau(1+\tau-\lambda-\kappa)(1-\lambda)}$$

All integrals can now be calculated by means of fractional decompositions and the definition of the dilog function.

ii. On-shell.

The only difference with the off-shell case is the argument of tne logarithm:

$$Q = \frac{(\kappa+\lambda\tau-2\tau)^2}{\mu_1^2\lambda^2\tau(1+\tau-\lambda-\kappa)}$$

Since the only source of divergences is the explicit μ_1-dependence of Q one can neglect the μ-dependence of the boundaries. Then all results are calculable in the same way as the off-shell ones.

e. Some other integrals.

We have omitted integrals which come from single denominators N_1 or N_2. These integrals turn out to depend upon only one of the integration variables of the double integral, and can be treated as constants in this stage. A second omission is a factor $[1-\tau-\rho]^{-1}$ which multiplies some integrands. Such a factor can appear in integrals of types a, c and d, and gives rise to a complicated expression. Instead of calculating these integrals directly we use an integration by parts of the final integral. For example:

$$\int_\tau^1 d\lambda \int_0^{1+\tau-\lambda-\tau/\lambda} \frac{d\rho}{1-\tau-\rho} \frac{1}{\sqrt{\lambda(1,\rho,\tau)}} \ln \frac{\rho-1+\tau-\sqrt{\lambda(1,\rho,\tau)}}{\rho-1+\tau+\sqrt{\lambda(1,\rho,\tau)}}$$

$$= \int_\tau^1 \frac{d\lambda}{\lambda + \frac{\tau}{\lambda} - 2\tau} \ln \frac{\tau(1-\lambda)}{\lambda(\lambda-\tau)}$$

Now the complications occur in the final integral, because the denominator is not a monomial in λ like all other ones. We will consider this case separately in appendix C.

Appendix C

In this appendix we give some results for integrals with a single denominator and a double logarithm. Combinations which are not discussed here can be obtained by substitutions (either $\lambda \to \frac{\tau}{\lambda}$ or $\lambda \to 1+\tau-\lambda$) or by integration by parts.

$$\int_\tau^1 \frac{1}{\lambda} \ln(1-\lambda)\ln(\lambda-\tau) = Li_3(\tau) + 2\,Li_3(1-\tau) - Li_3(1) - \ln\tau \ln^2(1-\tau) - 2\ln(1-\tau)\,Li_2(1-\tau) \tag{C1}$$

$$\int_\tau^1 \frac{1}{\lambda-1} \ln(\lambda)\ln(\lambda-\tau) = Li_3(\tau) - Li_3(1-\tau) - Li_3(1) - \frac{1}{2}\ln^2\tau \ln(1-\tau) + \ln(1-\tau)\,Li_2(1-\tau) - \ln\tau\,Li_2(\tau) \tag{C2}$$

$$\begin{aligned}\int_\tau^1 \frac{1}{\lambda} \ln(1-\lambda)\ln(1+\tau-\lambda) &= Li_3(-\tau) - Li_3(1-\tau^2) - Li_3(1) + 2\,Li_3(1-\tau) \\ &+ 2\,Li_3\frac{1}{1+\tau} - 2\ln(1-\tau)\,Li_2(-\tau) - \ln\tau\,Li_2(-\tau) \\ &- \frac{\pi^2}{6}\ln(1-\tau) + \frac{\pi^2}{6}\ln(1+\tau) - \frac{1}{2}\ln^2\tau\ln(1+\tau) \\ &- 2\ln\tau\ln(1-\tau)\ln(1+\tau) - \frac{1}{3}\ln^3(1+\tau)\end{aligned} \tag{C3}$$

$$\int_\tau^1 \frac{1}{\lambda-1} \ln\lambda \ln(1+\tau-\lambda) = -2\,Li_3(\tau) - 4\,Li_3(-\tau) - Li_3(1) + \ln\tau\,Li_2(\tau) + 2\ln\tau\,Li_2(-\tau) \tag{C4}$$

$$\int_\tau^1 \frac{1}{\lambda - \frac{1}{\tau}} \ln\lambda \ln(1-\lambda) = 2\,\mathrm{Li}_3(\tau) + 4\,\mathrm{Li}_3(-\tau) + \mathrm{Li}_3(1) - \mathrm{Li}_3(1-\tau)$$
$$- \ln\tau\,\mathrm{Li}_2(-\tau) - \ln(1-\tau)\,\mathrm{Li}_2(\tau) - \ln\tau\,\mathrm{Li}_2(\tau)$$
$$- 2\ln(1-\tau)\,\mathrm{Li}_2(-\tau) - \ln\tau\ln^2(1-\tau)$$
$$- \ln\tau\ln(1-\tau)\ln(1+\tau) \qquad (C5)$$

$$\int_\tau^1 \frac{1}{\lambda-\tau} \ln\lambda \ln(1+\lambda) + \int_\tau^1 \frac{1}{\lambda - \frac{1}{\tau}} \ln(1+\lambda)\ln(1-\lambda) - \int_\tau^1 \frac{1}{\lambda-\tau} \ln(1+\lambda)\ln(1-\lambda)$$
$$= -\mathrm{Li}_3\frac{1}{1+\tau} + \frac{7}{8}\mathrm{Li}_3(1) + \mathrm{Li}_2(-\tau)\ln\frac{\tau}{1-\tau^2} - \ln(1+\tau)\mathrm{Li}_2(\tau)$$
$$- \ln(1-\tau)\ln^2(1+\tau) - \ln(1+\tau)\ln^2(1-\tau) + \frac{1}{2}\ln(1+\tau)\ln^2\tau$$
$$+ \frac{1}{6}\ln^3(1+\tau) + \frac{\pi^2}{4}\ln(1+\tau) - \frac{\pi^2}{12}\ln(1-\tau)$$
$$+ \ln\delta\ln(1+\tau)\ln\frac{1-\tau}{\tau} \qquad (C6)$$

In (C6) we have replaced the lower boundary of the integral by $\tau+\delta$ to regularize the logarithmic singularity. The resulting $\ln\delta$ is cancelled in the final result by other integrals. Integrals (C5) and (C6) are not needed in section 3, but have been added because they occur in the calculation of the crossed diagrams. The three integrals in (C6) appear only in this combination. Separately these integrals yield Spence functions which cannot be expressed in trilogs.

This list is incomplete, because integrals with identical arguments for the two logarithms, or integrals related to these by integration by parts are not given. For these one can use the indefinite integral:

$$\int \frac{\ln x \ln(ax+b)}{x}\,dx = \frac{1}{2}\ln b \ln^2 x - \ln x\,\mathrm{Li}_2\left(\frac{-ax}{b}\right) + \mathrm{Li}_3\left(\frac{-ax}{b}\right) \qquad (C7)$$

This does not work for (C1...C6), but by differentiating the left hand sides with respect to τ one obtains expressions which can be integrated by means of (C7).

Finally, we give the results for the integrals mentioned at the end of appendix B:

$$\int_{\tau}^{1} \frac{1}{\lambda + \frac{\tau}{\lambda} - 2\tau} \ln \frac{\tau(1-\lambda)}{\lambda(\lambda-\tau)} = \frac{1}{2} \mathrm{Li}_2\left(1 - \frac{1}{\tau}\right) \tag{C8}$$

$$\int_{\tau}^{1} \frac{1-\tau/\lambda^2}{\lambda + \frac{\tau}{\lambda} - 2\tau} \ln \left[\frac{\tau}{\lambda} \frac{1-\lambda}{\lambda-\tau}\right] \ln (\lambda-\tau) = -\frac{3}{2} \mathrm{Li}_3\left(1 - \frac{1}{\tau}\right) + \ln (1-\tau)\, \mathrm{Li}_2\left(1 - \frac{1}{\tau}\right) \tag{C9}$$

Appendix D

In this appendix we give the complete expressions for the functions introduced in section 7.

These functions are:

$$\begin{aligned}
\Sigma_{cr}^{(2)}(\tau) = \frac{1+\tau^2}{1+\tau} \{ & \frac{\pi^2}{2} \ln \tau - \pi^2 \ln (1+\tau) - \frac{11}{6} \ln^3 \tau + 3 \ln (1+\tau) \ln^2 \tau \\
& + 2 \ln^3(1+\tau) - 2 \ln \tau\, \mathrm{Li}_2 (1-1/\tau) - 10\, \mathrm{Li}_3 (1-\tau) - 6\, \mathrm{Li}_3 (1-1/\tau) \\
& + 2\, \mathrm{Li}_3 (1-\tau^2) + 2\, \mathrm{Li}_3 (-\tau) - 12\, \mathrm{Li}_3 \frac{1}{1+\tau} + 12\, \mathrm{Li}_3 (1) \\
& + 2 \ln \tau\, \mathrm{Li}_2 (-\tau)\} + \tau \{10 \ln \tau - 3 \ln^2 \tau + \frac{2}{3} \pi^2 \ln (1+\tau) \\
& + 2 \ln (1+\tau) \ln^2 \tau - \frac{4}{3} \ln^3 (1+\tau) + 4\, \mathrm{Li}_3 (-\tau) + 8\, \mathrm{Li}_3 \frac{1}{1+\tau} \\
& - 4\, \mathrm{Li}_3 (1)\} + (1-\tau) \{14 - \frac{\pi^2}{6} \ln \tau + \frac{1}{6} \ln^3 \tau\} - 2(1+1/\tau) \\
& \times \{\ln \tau \ln (1+\tau) + \mathrm{Li}_2(-\tau)\} + 4\, \mathrm{Li}_2 (1-1/\tau) + \frac{\pi^2}{6} (2\tau-4)
\end{aligned}$$

and

$$\Omega_{cr}^{(2)}(\tau) = \frac{1+\tau^2}{1+\tau}\ \{-2\ \ln\tau - \frac{\pi^2}{3}\ \ln\tau + \frac{\pi^2}{3}\ \ln(1+\tau) - 3\ \ln(1+\tau)\ \ln^2\tau$$

$$- \frac{2}{3}\ \ln^3(1+\tau) + 2\ \mathrm{Li}_2(-\tau)\ \ln\tau + 2\ \mathrm{Li}_3(-\tau) + 4\ \mathrm{Li}_3\frac{1}{1+\tau}$$

$$- 2\ \mathrm{Li}_3(1)\} + \tau\{4\ \ln^2\tau\ \ln(1+\tau) + \frac{4}{3}\ \pi^2\ \ln(1+\tau) - \frac{8}{3}\ \ln^3(1+\tau)$$

$$+ 8\ \mathrm{Li}_3(-\tau) + 16\ \mathrm{Li}_3\frac{1}{1+\tau} - 8\ \mathrm{Li}_3(1)\} + \{8 + 6\tau + 12\tau^2 + 2\tau^{-1}$$

$$- \frac{18}{5}\ \tau^3 + \frac{2}{5}\ \tau^{-2}\}\{\mathrm{Li}_2(-\tau) + \ln(1+\tau)\ \ln\tau\} + \ln\tau\{-\frac{24}{5} - \frac{54}{5}\ \tau$$

$$+ \frac{18}{5}\ \tau^2 - \frac{2}{5}\ \tau^{-1}\} + \ln^2\tau\{-2 - 2\tau - 6\tau^2 + \frac{9}{5}\ \tau^3 + \frac{\pi^2}{6}\{2 + 2\tau$$

$$+ 12\tau^2 - \frac{18}{5}\ \tau^3\} + \frac{2}{5}\ \tau^{-1} + \frac{18}{5}\ \tau^2 + \frac{48}{5}\ \tau - \frac{68}{5} \qquad .$$

CHAPTER IV: THE RELATION BETWEEN DEEP-INELASTIC SCATTERING AND LEPTON PAIR PRODUCTION

1. The connection with the minimal subtraction scheme

The results we have presented in the previous chapter depend on the renormalization scheme we have used, as discussed in chapter II. This scheme differs from the one which is used in the calculations of second order corrections to deep-inelastic scattering processes, and in particular the second order anomalous dimension matrix. This matrix was calculated [Flo 77, Flo 79] in the minimal subtraction scheme. The Wilson coefficients for the structure function F_2, obtained in this scheme, have nonvanishing corrections of order α_s, and therefore they do not agree with our convention to absorb all perturbative corrections into the distribution functions. Nevertheless we would like to be able to extract information about the structure of hadrons out of deep-inelastic scattering data and transfer that information in a consistent way to lepton pair production. For that purpose we need the finite renormalization which connects the lepton pair production and deep-inelastic scattering results calculated up to now.

Beside this consistency argument there are two other reasons why we want to know this relation. First of all we can use the non-leading mass singularities appearing in (III.4.10) or (III.4.11) to calculate one of the elements of the second order anomalous dimension matrix and use the finite renormalization matrix to convert this result to the minimal subtraction scheme, to compare it with the corresponding one of [Flo 79].

The other reason was already mentioned in section III.5: our

convention, and especially the one for the quark-gluon transition does not automatically satisfy the momentum sum rule. This means that in an arbitrary convention the total momentum fraction of quarks and gluons,

$$\int_0^1 dx\, x \left[\sum_i \left(f_{q_i}(x) + f_{\bar{q}_i}(x) \right) + f_g(x) \right]$$

is not conserved. In the parton model this integral is expected to be one, i.e. the quarks and gluons carry all the momentum of the hadron. Although the magnitude of this integral can not be derived within QCD, it can at least be shown that first order QCD corrections do not violate the momentum sum rule. This means that the leading scaling deviations vanish for this combination of moments. In the operator product expansion the corresponding operator has the same quantum numbers as the energy momentum tensor, and then the statements made above correspond to the fact that a conserved operator is not renormalized. Beyond the leading order this remains true if one chooses the correct subtraction scheme. For conserved operators this scheme is fixed by the requirement that the Ward-identities are respected. Although nothing forces us to use such a scheme for the anomalous dimensions - the relevant operator has the quantum numbers of the energy momentum tensor, but it plays a somewhat different role in the problem; moreover parton distributions are not physical quantities - it is very convenient phenomenologically to use distributions which satisfy the momentum sum rule. This implies a relation between the second moments of the quark gluon and the quark-quark transition function.

The anomalous dimension which can be calculated from the results of the previous chapter is the difference between the singlet and the non-singlet quark-quark anomalous dimension. Consider the expansion of the transition function:

$$\Gamma(x,Q^2/Q_0^2) = \mathbb{1}\cdot\delta(1-x) + [A_{11}(x)v + A_{10}(x)]\,\frac{\alpha_s(Q^2)}{4\pi}$$
$$+ [A_{22}(x)v^2 + A_{21}(x)v + A_{20}(x)]\left(\frac{\alpha_s(Q^2)}{4\pi}\right)^2 + \ldots \qquad (1.1)$$

where $v = \frac{1}{2}\ln(Q^2/Q_0^2)$. Each coefficient A_{ab} is a matrix which works in a space, spanned by the distribution functions. The transition function operates on these functions in the following way:

$$f_i(x,Q^2) = \int_x^1 \Gamma_{ij}\left(\frac{x}{\xi}, \frac{Q^2}{Q_0^2}\right)\,\frac{f_j(\xi,Q_0^2)}{\xi}\,d\xi \qquad (1.2)$$

Comparing (1.2) with several relations in chapter II and III one can find explicit expressions for some of the coefficients in (1.1), both for on-shell and off-shell regularization.

To determine the anomalous dimension we can not directly use (II.3.11) because that definition was obtained for transition functions satisfying (II.3.9), from which one derives:

$$\Gamma_{ki}(x,0) = \delta_{ki} \qquad (1.3)$$

This requirement is clearly not met by (1.1). The reason is that (1.1) is related to the transition function defined according (II.3.9) by a finite renormalization which is only applied at the left hand side, not at both sides as in (II.6.9). This must first be adjusted by applying simultaneously a finite renormalization to the input distributions in (1.2), as is shown in (II.6.10). This finite renormalization matrix is completely fixed by the requirement that the resulting transition function - obtained by multiplying (1.1) with this matrix from the right - should satisfy (1.3). After multiplication with this matrix we can use (II.3.11), and we find the following result:

$$\gamma_1^{q_i q_j} = -A_{21}^{q_i q_j} + A_{11}^{q_i g} \otimes A_{10}^{g q_j} \qquad (1.4)$$

The symbol $\otimes$ denotes multiplication if one is considering moments, and a convolution if x-dependent expressions are considered. This is the anomalous dimension of Γ^S_{qq}, which is defined by (II.4.1). Diagonalizing the transition function as explained in section II.4 we get:

$$(\gamma_1^S - \gamma_1^{NS})^{QQ} = 2\, N_f\, \gamma_1^{q_1 q_J} \tag{1.5}$$

The left hand side is the difference of second coefficients of the anomalous dimensions of the singlet and non-singlet quark-quark transition functions, defined as follows:

$$\begin{aligned} \Gamma^S_{QQ} &= \Gamma^{NS}_{qq} + \Gamma^{NS}_{q\bar{q}} + 2\, N_f\, \Gamma^S_{qq} \\ \Gamma^{NS}_{QQ} &= \Gamma^{NS}_{qq} + \Gamma^{NS}_{q\bar{q}} \end{aligned} \tag{1.6}$$

These are the combinations which appear in (II.4.6). Combining (1.4) and (1.5) we get the following second order coefficient:

$$[\gamma_1^S(x) - \gamma_1^{NS}(x)]^{QQ} = 2\, N_f \left[-\, A_{21}^{q_1 q_J}(x) + \int_x^1 A_{11}^{q_1 g}\left(\frac{x}{\xi}\right) A_{10}^{g q_J}(\xi)\, \frac{d\xi}{\xi} \right] \tag{1.7}$$

In this expression both $A_{21}(x)$ and $A_{10}(x)$ depend upon the regularization method; A_{21} is given by (III.4.13) and (III.4.14):

$$A_{21}^{qq}(x) = -\, 2\, \frac{N^2-1}{N}\, \Omega^{(2)}_{OFF}(x) \quad \text{or} \quad A_{21}^{qq}(x) = -\, 2\, \frac{N^2-1}{N}\, \Omega^{(2)}_{ON}(x) \tag{1.8}$$

for off-shell and on-shell regularization respectively; $A_{10}^{gq}(x)$ is implicitly defined by (5.16) and (5.17). The other coefficient is related to the leading order gluon-quark anomalous dimension, and is regularization independent:

$$A_{11}^{qg}(x) = 2\, [(1-x)^2 + x^2] \tag{1.9}$$

Since we have renormalized both the on-shell and the off-shell results in such a way that the same perturbative corrections to all processes

are obtained, we expect the anomalous dimension to be regularization independent. That turns out to be correct, and for both regularization methods we find:

$$[\gamma_1^S(x) - \gamma_1^{NS}(x)]^{QQ} = 4N_f \frac{N^2-1}{N} \left\{ (1+x)\ln^2 x + (-1 + 3x - \frac{8}{3}x^2 - \frac{4}{3}x^{-1})\ln x + \frac{21}{2} - \frac{11}{2}x + \frac{1}{3}x^2 - \frac{16}{3}x^{-1} \right\} \quad (1.10)$$

Taking moments we get:

$$[\gamma_1^{n,S} - \gamma_1^{n,NS}]^{QQ} = 4N_f \frac{N^2-1}{N} \left[\frac{4}{3} \frac{1}{(n-1)^2} - \frac{16}{3} \frac{1}{n-1} + \frac{2}{n^3} + \frac{1}{n^2} + \frac{21}{2n} + \frac{2}{(n+1)^3} - \frac{3}{(n+1)^2} - \frac{11}{2(n+1)} + \frac{8}{3} \frac{1}{(n+2)^2} + \frac{1}{3} \frac{1}{n+2} \right] \quad (1.11)$$

The finite renormalization matrix which converts this result to a corresponding one in the minimal subtraction scheme can be determined by comparing the Wilson coefficients in both schemes. In the minimal subtraction scheme the coefficients for F_2 are [Flo 79]:

$$\tilde{C}_{Q,2}^n = 1 + \frac{\alpha_s}{4\pi} \frac{N^2-1}{2N} [-2S_1^2(n) - 2S_2(n) + 6S_1(n) + \frac{3}{n} + \frac{4}{n+1} + \frac{2}{n^2} - 9] + \frac{1}{2} \frac{\alpha_s}{4\pi} \gamma_0^{n,qq} (\ln 4\pi - \gamma + S_1(n)) \quad (1.12)$$

$$\tilde{C}_{G,2}^n = \frac{\alpha_s}{4\pi} 2 N_f \left[\frac{1}{n^2} - \frac{1}{n} + \frac{6}{n+1} - \frac{6}{n+2} \right] + \frac{1}{2} \frac{\alpha_s}{4\pi} \gamma_0^{n,qg} (\ln 4\pi - \gamma + S_1(n)) \quad (1.13)$$

where

$$S_\ell(n) = \sum_{k=1}^{n} \frac{1}{k^\ell}$$

γ is Eulers constant ($\gamma = .5772156649...$)

γ_0^n is the first order coefficient matrix of the anomalous dimension of the singlet operators.

Here and in the following a $\sim$ is used to indicate results, obtained in

the minimal subtraction scheme. The corresponding results in our scheme are:

$$C^n_{Q,2} = 1 \tag{1.14}$$

$$C^n_{G,2} = 0 \tag{1.15}$$

The relation between (1.12-1.13) and (1.14-1.15) determines the non-singlet finite renormalization factor and two out of four elements of the singlet anomalous dimension matrix. To determine the other two we need an addition process, which is sensitive to the gluon distribution. For that purpose we can use the fictitious scalar particle introduced in section III.5.

The relevant formulae for deep-inelastic scattering of this scalar can be derived in complete analogy to the corresponding ones for electromagnetic probes (see e.g. [Pol 74]). In section III.6 a structure function W^α_S was introduced. This structure function is related to the imaginary part of a forward Compton amplitude:

$$T^\alpha_S = i \int d^4x\, e^{iqx} \langle P,\alpha | T\, J(x)\, J(0) | P,\alpha \rangle_{av} \tag{1.16}$$

$$W^\alpha_S = \frac{1}{\pi} \mathrm{Im}\, T^\alpha_S \tag{1.17}$$

To establish the link with the minimal subtraction scheme used in combination with the operator product expansion, we postulate the following O.P.E. for the product of currents appearing in (1.16):

$$i \int d^4x\, e^{iqx}\, T\, J(x)\, J(0) = 2 \sum_{n,k} \left(\frac{2}{Q^2}\right)^n q_{\mu_1} \ldots q_{\mu_n}\, C^n_{k,S}\, O_k^{\mu_1 \ldots \mu_n} \tag{1.18}$$

where $O_k^{\mu_1 \ldots \mu_n}$ are the electroproduction operators, (I.5.8-10). The matrix elements of these operators are:

$$\langle P,\alpha | O_k^{\mu_1 \ldots \mu_n} | P,\alpha \rangle_{av} = A^n_{k,\alpha}\, P^{\mu_1} \ldots P^{\mu_n} + \text{trace terms} \tag{1.19}$$

where α indicates a quark, gluon or hadron. The moments of the structure function can be expressed in terms of the coefficient functions and the operator matrix elements:

$$\int_0^1 x^{n-1} W_S^{\alpha}(x,Q^2) = \sum_k A^n_{k,\alpha} C^n_{k,S} \tag{1.20}$$

The coupling of the scalar to the gluon has to be chosen in such a way that the absorptive part of the first diagram of fig. 1.1 is equal to (III.5.1) (so that (1.17) is satisfied in tree approximation).

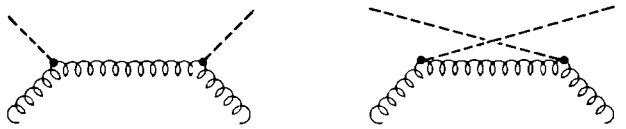

fig. 1.1: leading order contribution to the scalar/gluon forward Compton amplitude.

Therefore we have to choose:

$$T_{\mu\nu,ab} = \frac{1}{(p+q)^2 + i\varepsilon} \delta_{ab} \left[A^T \left(\frac{q^2 p^2 - (q\cdot p)^2}{q^2} \right) G_{\mu\nu} + \frac{p^2}{q^2} H_{\mu\nu} \right] \tag{1.21}$$

with indices and momenta as in (III.5.1). Since it was shown in section III.2 that longitudinally polarized gluons can be ignored we will only consider the transversal part here. Taking matrix elements as in (III.5.4) we obtain the following result for the diagrams of fig. 1.1:

$$T_S^g = \frac{1}{2} A^T \sum_{k=1}^{\infty} \left(\frac{1}{x^2} \right)^k \tag{1.22}$$

where $x = \dfrac{Q^2}{2p\cdot q}$.

The quark-gluon transition function is now determined by the diagrams of fig. 1.2. Substituting (1.21) we find that the following integral has to be evaluated:

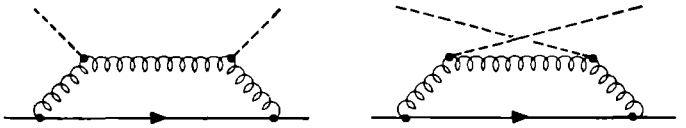

fig. 1.2: scalar/quark Compton amplitude.

$$T_S^q = -\frac{N^2-1}{4N}\, ig^2 \int \frac{d^4k}{(2\pi)^4}\, \mathrm{Tr}\,[\not p \gamma^\rho \not k \gamma^\sigma]\, A^T\, \frac{1}{k^2 (q+p-k)^2 (p-k)^4}$$

$$\times \left\{ \frac{q^2 (p-k)^2 - (q\cdot(p-k))^2}{q^2} \left[- g_{\rho\sigma} + \frac{(p-k)_\rho\, (p-k)_\sigma}{(p-k)^2} \right] \right.$$

$$\left. + \frac{(p-k)^2}{q^2} \left(q_\rho - \frac{(q\cdot(p-k))^2}{(p-k)^2} (p-k)_\rho\right) \left(q_\sigma - \frac{(q\cdot(p-k))^2}{(p-k)^2} (p-k)_\sigma\right) \right\}$$

$$+ (q \to -q) \qquad (1.23)$$

The result of the calculation is:

$$T_S^q = \frac{\alpha_s}{4\pi} \frac{N^2-1}{4N} A^T \left[\ln (p^2/q^2) \left[1 - \frac{3}{2x} + (x + \frac{2}{x} - 2) \ln (1 - \frac{1}{x}) \right] \right.$$

$$\left. - 2 + \frac{1}{x} + (\frac{7}{2x} - 1) \ln (1 - \frac{1}{x}) + 2(x + \frac{2}{x} - 2) \mathrm{Li}_2 (\frac{1}{x}) \right]$$

$$+ (x \to -x) \qquad (1.24)$$

Expanding this result in powers of $\frac{1}{x}$ we get:

$$T_S^q = \sum_{\substack{n=2 \\ n \text{ even}}}^{\infty} \frac{1}{x^n} \frac{\alpha_s}{4\pi} \frac{N^2-1}{4N} A^T \left[\ln (p^2/q^2) \left[\frac{4}{n} - \frac{2}{n+1} - \frac{4}{n-1} \right] \right.$$

$$\left. + \frac{2}{n} - \frac{7}{n-1} + \frac{4}{(n+1)^2} + \frac{8}{(n-1)^2} - \frac{8}{n^2} \right] \qquad (1.25)$$

These are the matrix elements of the left hand side of (1.18). To determine the coefficients we have to calculate the same matrix elements for the right hand side. The leading order operator matrix elements are:

$$A^n_{Q,q} = 1 \qquad ; \qquad A^n_{G,g} = 1 \tag{1.26}$$

This defines the normalization we have chosen for the operators. The quark matrix element of the gluon operator is given by the diagram of fig. 1.3. Performing the loop integral and neglecting terms proportional to p^2 we find:

$$\langle p,q|O_G^{\mu_1..\mu_n}|p,q\rangle_{av} = -\frac{N^2-1}{N}\frac{\alpha_s}{4\pi}\left\{\left(\frac{1}{n+1}+\frac{2}{n-1}-\frac{2}{n}\right)(\ln(-p^2) - S_1(n))\right.$$
$$\left. - \frac{3}{n} + \frac{4}{n-1} + \frac{1}{n+1} - \frac{2}{(n+1)^2} - \frac{2}{(n-1)^2} + \frac{2}{n^2} - \frac{\pi^{-\varepsilon/2}}{(2\pi)^{-\varepsilon}}\,\Gamma\left(\frac{\varepsilon}{2}\right)\right.$$
$$\left.\times\left[\frac{1}{n+1}+\frac{2}{n-1}-\frac{2}{n}\right]\right\}\mu^{-\varepsilon}\,p^{\mu_1}..p^{\mu_n} \tag{1.27}$$

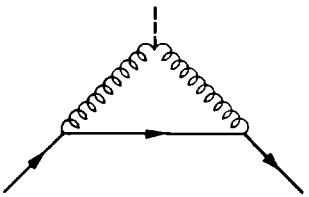

fig. 1.3: quark matrix element of the gluon operator.

The last term contains the ultraviolet pole:

$$\frac{\pi^{-\varepsilon/2}}{(2\pi)^{-\varepsilon}}\,\Gamma\left(\frac{\varepsilon}{2}\right) = \frac{2}{\varepsilon} + \ln 4\pi - \gamma + O(\varepsilon) \tag{1.28}$$

In the minimal subtraction scheme a counter term is introduced to subtract this pole. Only the term $\frac{2}{\varepsilon}$ is subtracted. The renormalized operator matrix element $A^n_{G,q}$ is obtained by adding this counter term to (1.27), and is defined by:

$$\langle p,q|O_G^{\mu_1..\mu_n}|p,q\rangle_{av,ren} = A^n_{G,q}\,p^{\mu_1}..p^{\mu_n} \tag{1.29}$$

Substituting (1.19) into (1.18) we get

$$T^S_q = \sum_n \frac{2}{x^n}\left[A^n_{Q,q}\,\tilde{C}^n_{Q,S} + A^n_{G,q}\,\tilde{C}^n_{G,S}\right] \tag{1.30}$$

$$T_g^S = \sum_n \frac{2}{x^n} \left[A_{Q,g}^n \tilde{C}_{Q,S}^n + A_{G,g}^n \tilde{C}_{G,S}^n \right] \tag{1.31}$$

The first term in the right hand side of (1.31) is of order α_s^2 and can be ignored (by construction the scalar does not have a direct coupling to the quarks, and hence $\tilde{C}_{Q,S}^n$ is of order α_s). Then this equation can be used to calculate the coefficient function of the gluon operator:

$$\tilde{C}_{G,S}^n = \frac{1}{4} A^T \tag{1.32}$$

Now the first equation determines the other coefficient function:

$$\tilde{C}_{Q,S}^n = \frac{\alpha_s}{4\pi} \frac{1}{4} A^T \frac{N^2-1}{N} \left[\left(\frac{2}{n} - \frac{1}{n+1} - \frac{2}{n-1} \right) \left(\ln (\mu^2/Q^2) + \ln 4\pi - \gamma \right.\right.$$

$$\left.\left. + S_1(n) \right) - \frac{2}{n} + \frac{1}{2} \frac{1}{n-1} + \frac{1}{n+1} + \frac{2}{(n-1)^2} - \frac{2}{n^2} \right] \tag{1.33}$$

To determine the finite renormalization matrix we need the corresponding result in our convention. Subtracting the mass singularity in (III.5.13) at a point μ^2 in the way defined by (III.5.16) or (III. 5.17) we find:

$$W_S(x) = \frac{1}{4} A^T f_g(x,\mu^2) + \frac{1}{4} A^T \frac{\alpha_s}{4\pi} \frac{N^2-1}{N} \int_x^1 \frac{d\xi}{\xi} \sum_i \left(f_{q_i}(\xi) + f_{\bar{q}_i}(\xi) \right)$$

$$\times \left[- \frac{(1-\eta)^2+1}{\eta} \ln (\mu^2/Q^2) - 1 \right] \tag{1.34}$$

where $\eta = \frac{x}{\xi}$. A Mellin inversion yields now:

$$W_S^n = \frac{1}{4} A^T \left\{ f_g^n(\mu^2) + \frac{\alpha_s}{4\pi} \frac{N^2-1}{N} \sum_i \left(f_{q_i}^n + f_{\bar{q}_i}^n \right) \left[\left(\frac{2}{n} - \frac{1}{n+1} - \frac{2}{n-1} \right) \right.\right.$$

$$\left.\left. \times \ln (\mu^2/Q^2) - \frac{1}{n} \right] \right\} \tag{1.35}$$

To translate this into an O.P.E. result we make the following identification:

$$f_g^n(\mu^2) = A_{G,H}^n(\mu^2) \tag{1.36}$$

$$\sum_i (f_{q_i}(\mu^2) + f_{\bar{q}_i}(\mu^2)) = A^n_{Q,H}(\mu^2) \tag{1.37}$$

These identifications can be obtained by comparing the leading order results of the O.P.E. and the parton model. The normalization (1.26) is crucial for these relations. The Mellin-inverted form of (1.26) implies that in leading order the probability for finding a parton with momentum fraction x inside itself is $\delta(1-x)$. Substituting (1.36-37) into (1.35) we get:

$$C^n_{G,S} = \frac{1}{4} A^T \tag{1.38}$$

$$C^n_{Q,S} = \frac{\alpha_s}{4\pi} \frac{1}{4} A^T \frac{N^2-1}{N} \left[\left(\frac{2}{n} - \frac{1}{n+1} - \frac{2}{n-1} \right) \ln (\mu^2/Q^2) - \frac{1}{n} \right] \tag{1.39}$$

The finite renormalization matrix which relates the two schemes is defined by the following requirements

$$C^n_{j,S} = \sum_i \tilde{C}^n_{i,S} X^n_{ij} \tag{1.40}$$

$$C^n_{j,2} = \sum_i \tilde{C}^n_{i,2} X^n_{ij} \tag{1.41}$$

We parametrize this matrix in the following way:

$$X^n = 1 + \frac{\alpha_s}{4\pi} Y^n - \frac{1}{2} \frac{\alpha_s}{4\pi} \gamma^n_0 [\ln 4\pi - \gamma + S_1(n)] \tag{1.42}$$

The explicit expression for Y^n is:

$$\begin{aligned} Y^n_{QQ} &= - \frac{N^2-1}{2N} \left[- 2S_1^2(n) - 2S_2(n) + 6S_1(n) + \frac{3}{n} + \frac{4}{n+1} + \frac{2}{n^2} - 9 \right] \\ Y^n_{QG} &= - 2N_f \left[\frac{1}{n^2} - \frac{1}{n} + \frac{6}{n+1} - \frac{6}{n+2} \right] \\ Y^n_{GQ} &= - \frac{N^2-1}{2N} \left[- \frac{2}{n} + \frac{1}{n-1} + \frac{2}{n+1} + \frac{4}{(n-1)^2} - \frac{4}{n^2} \right] \end{aligned} \tag{1.43}$$

The gluon-gluon matrix element is irrelevant, because none of the results we will use depends on it. There is also a finite renormalization like (1.42) for the non-singlet case. Then X^n, γ^n_0 and Y^n are single constants instead of matrices. In one-loop order the constant Y^n equals the matrix element Y^n_{QQ}; the same is true for γ^n_0 and hence for

X^n.

It can now be shown easily that the results presented in the previous chapter are in agreement with the anomalous dimensions calculated in the minimal subtraction scheme. The transformation of the anomalous dimension matrix is according to (II.6.12) and (II.3.28):

$$\tilde{\gamma}(\lambda) = X(\lambda)\ \gamma(\lambda)\ X^{-1}(\lambda) + 2\ X(\lambda)\ \beta(\lambda)\ \frac{\partial}{\partial\lambda} X^{-1}(\lambda) \tag{1.44}$$

where $\lambda = \frac{\alpha_s}{4\pi}$. For the combination of anomalous dimensions which we are considering (1.44) is explicitly:

$$\begin{aligned}[\tilde{\gamma}_1^{n,S} - \tilde{\gamma}_1^{n,NS}]^{QQ} &= [\gamma_1^{n,S} - \gamma_1^{n,NS}]^{QQ} - [\gamma_0^n, \gamma^n]^{QQ} \\ &= -4\ \frac{N^2-1}{N}\ N_f\ \frac{5n^5+32n^4+49n^3+38n^2+28n+8}{n^3(n+1)^3(n-1)(n+2)^2}\end{aligned} \tag{1.45}$$

The anomalous dimension matrix calculated by [Flo 79] is presented in an analytical form by [Gon 80]. Our result (1.45), which is calculated in a completely different way, agrees with theirs. This is an important check of the consistency of the entire procedure.

The explicit expression for the finite renormalization matrix allows us to check if the momentum sum rule is satisfied. For that purpose we consider relations (II.4.6), which we write in the following way:

$$\begin{aligned}G^{(n)} &= \Gamma_{GQ}^{n,S}\ Q_0^{(n)} + \Gamma_{GG}^{n,S}\ G_0^{(n)} \\ Q^{(n)} &= \Gamma_{QQ}^{n,S}\ Q_0^{(n)} + \Gamma_{QG}^{n,S}\ G_0^{(n)}\end{aligned} \tag{1.46}$$

The momentum sum rule is satisfied if the following relation holds:

$$G^{(2)} + Q^{(2)} = 1 \qquad \text{(for all } Q^2\text{)} \tag{1.47}$$

This is true if

$$G_0^{(2)} + Q_0^{(2)} = 1 \qquad \text{and}$$

$$\Gamma^{2,S}_{GQ} + \Gamma^{2,S}_{QQ} = 1 \qquad ; \qquad \Gamma^{2,S}_{GG} + \Gamma^{2,S}_{QG} = 1 \tag{1.48}$$

The first criterium ensures that the momentum sum rule is satisfied at the definition point Q^2_0. The second relation leads to the following requirements for the anomalous dimension matrix:

$$\gamma^{2,S}_{GQ} = - \gamma^{2,S}_{QQ} \qquad ; \qquad \gamma^{2,S}_{GG} = - \gamma^{2,S}_{QG} \tag{1.49}$$

As discussed in the beginning of this section these relations correspond to the fact that the energy momentum tensor is a conserved operator, which is not renormalized. Therefore they hold automatically in the minimal subtraction scheme, which respects all Ward-identities. To check that they hold also for our conventions, we only have to consider the finite renormalization matrix. The requirement is:

$$Y^2_{QQ} = - Y^2_{GQ} \tag{1.50}$$

This relation holds for (1.43), as one can check easily.

Part of the freedom in the definition of the gluon distribution is fixed by (1.50). When a different definition is chosen both the quark quark cross section and the finite renormalization matrix are modified:

$$\Sigma^{qq}(\tau) \to \Sigma^{qq}(\tau) - \int_{\tau_1}^{1} \frac{d\xi}{\xi} \Sigma^{qg}\left(\frac{\tau}{\xi}\right) \Delta(\xi) \tag{1.51}$$

$$Y^n_{GQ} \to Y^n_{GQ} - \frac{N^2-1}{N} \int_0^{\tau_1} x^{n-1} \Delta(x)\, dx \tag{1.52}$$

The arbitrary function $\Delta(x)$ respects the momentum sum rule if

$$\int_0^1 x\, \Delta(x)\, dx = 0 \quad . \tag{1.53}$$

Relations (1.51) to (1.53) can be used to make sure that changes in the definition of the quark-gluon transition function are taken into account in a consistent way.

2. Determination of the parton distribution functions

The best source of information about the distribution functions and their Q^2-dependence is deep-inelastic scattering. Most analyses of the data have concentrated on tests of QCD by means of scaling deviations. A determination of all parton distributions is not necessary for that purpose, because, depending on the structure function one is considering, only certain combinations of the distributions appear. Only a gluon distribution, a non-singlet and a singlet quark distribution are needed. If one wants to compare different processes however, more information is needed. Since we want to calculate the Drell-Yan continuum we have to determine all distributions. As we have emphasized in the previous sections, this determination has to be done in a way, consistent with the conventions we have chosen. This is why we cannot use any of the results published up to now.

The best available deep-inelastic scattering data are the SLAC electron data and the muon data from FNAL (see [Gor 79] for references). Both hydrogen and deuterium targets are used. The SLAC and FNAL data supplement each other in such a way that an accurate calculation of the moments of the structure function F_2 can be made for $1\ \text{GeV}^2 \leq Q^2 \leq 22\ \text{GeV}^2$. (The other structure function, F_1, is related to F_2 by the Callan-Gross relation and the way this relation is violated. The violation of the Callan-Gross relation is however not measured very accurately and is an important source of uncertainty in the determination of F_2.) Since QCD predictions are simplest in terms of moments we will use these moments instead of the structure function itself.

Two moment analyses of combined SLAC and FNAL data have been published, one by Duke and Roberts [Duk 79], and one by the FNAL

experimental group [Gor 79]. In the remainder of this section we will refer to these analyses as 'I' and 'II'.

The moments, computed by the two groups, do not completely agree with each other, and in some cases this can have a rather large effect on the fitted parameters. The differences are larger for the deuterium than for the proton data, but in both cases the moments at Q^2 = 22.5 GeV^2 show a large disagreement. For the proton data all other moments agree. Of course the Λ-parameter will be very sensitive to a discrepancy of this sort. There are several causes of these discrepancies. The most obvious one is the fact that different sets of values of Q^2 are used (3.5, 4.5, 5.5, 6.5, 7.5, 9.0, 12.5 and 22.5 GeV^2 for I and 3.25, 3.75, 4.5, 5.5, 7.0, 9.0, 12.5, 22.5 and 40 GeV^2 for II. The moments at Q^2 = 40 GeV^2 are however not supported by many datapoints and have large errors). For these Q^2-values the moments are calculated for $2 \leq n \leq 10$, but, according to I, the second moment may not be completely reliable.

Several corrections have been applied to deal with effects which are known to cause deviations from leading twist QCD and the parton model. There is, however, no theoretical agreement about the details of these corrections, and in some cases the two groups have used a different approach. This probably explains the major part of the discrepancy. We will briefly summarize these corrections.

First of all one can correct for the fact that the target has a non-vanishing mass M, causing an M^2/Q^2-dependence which is not predicted by QCD. Both groups use Nachtmann-moments [Nac 73] to take this into account. Recently it was shown, however, [Fra 80] that this does not remove all dependence on the target mass.

A second important correction is the elastic contribution. In the region near $x = 1$ resonances are present in the SLAC-data, which cannot be explained by the incoherent scattering picture of the parton model. Moreover the structure function has a peak at $x = 1$ due to elastic scattering, which is also not produced by single parton processes. It has been suggested however [Blo 70, DeR 77a] that by integrating over the resonance region and adding an elastic contribution - which can be calculated from the known proton and neutron form factors - an average is obtained which should correspond to the parton model results. Since the parton model does not reproduce the fluctuations around this average it is clear that this is only approximately true. Corrections are present due to deviations from the incoherent scattering approximation upon which the parton model is based. These deviations can be attributed to processes involving more than one parton from the target hadron. Such processes, which yield corrections proportional to inverse powers of Q^2, are theoretically not fully understood, and are usually neglected. Nevertheless such effects will be present in the data. Both analyses include the elastic contribution, but in different ways.

Finally, one must make corrections for nuclear effects if the target is deuterium. This includes all effects which cause deviations from the assumption that the structure function of deuterium is the sum of those of the proton and the neutron. The most important effect is the smearing of the nucleon structure functions by nuclear Fermi motion. The two groups correct for this effect in different ways. This probably explains the differences in the deuterium data.

Also the errors are estimated in different ways. The errors published by I include statistical errors and an estimated uncertainty

of the elastic contribution. The errors given by the second group include in addition to this an estimate of the extrapolation error and the error in the overall normalization of the inelastic data. Since it is in principle incorrect to handle a systematic error in this way we have subtracted the latter and considered the normalization separately.

The theoretical parametrization to be compared with these data consists of a set of moments of input distributions at some point Q_0^2 and the renormalization group equations governing the Q^2 evolution of these moments. Assuming that only four flavors are relevant - which is allowed for $Q^2 < 40\ GeV^2$ - we get 9 parameters for each moment, plus the QCD Λ-parameter which determines the Q^2-dependence.

To reduce the number of parameters we make some assumptions. For protons and neutrons it is clearly correct to take $s(x) = \bar{s}(x)$ and $c(x) = \bar{c}(x)$ (we denote the distribution of a quark q_i by $q_i(x)$). Further we will assume $\bar{u}(x) = \bar{d}(x)$, although this relation is broken by isospin-violating effects and, even with exact isospin symmetry, by identical quark effects as discussed in section III.7 (see also [Fey 77, Ros 79]). We will also assume $\bar{u}(x) = \bar{s}(x)$, although the y-distributions in deep-inelastic neutrino scattering do not seem to favor this relation [DeG 79]. The effect of these assumptions is however small. This reduces the number of input distributions to five, the up-quark and down-quark valence distributions, the non-charmed sea, the charm- and the gluon-distribution. To reduce this number even further we relate different moments by assuming a certain shape of the distributions. Following [Bur 78] we choose the following parametrization:

$$u_v(x) = \frac{2}{B(\alpha_1+1,\beta_1+1)}\ x^{\alpha_1}\ (1-x)^{\beta_1}$$

$$d_v(x) = \frac{1}{B(\alpha_2+1,\beta_2+1)}\, x^{\alpha_2}\,(1-x)^{\beta_2}$$

$$S(x) = F_1^2\, R\, \frac{1}{B(\alpha_3+2,\beta_3+1)}\, x^{\alpha_3}\,(1-x)^{\beta_3} \qquad (2.1)$$

$$C(x) = F_2^2\, R\, \frac{1}{B(\alpha_3+2,\beta_3+1)}\, x^{\alpha_3}\,(1-x)^{\beta_3}$$

$$G(x) = R\, \frac{1}{B(\alpha_4+2,\beta_4+1)}\, x^{\alpha_4}\,(1-x)^{\beta_4}$$

where

$$R = \left[1 - 2\,\frac{\alpha_1+1}{\alpha_1+\beta_1+2} - \frac{\alpha_2+1}{\alpha_2+\beta_2+2}\right][1 + F_1^2 + F_2^2]^{-1}$$

$$B(\alpha,\beta) = \frac{\Gamma(\alpha)\,\Gamma(\beta)}{\Gamma(\alpha+\beta)}$$

These distributions are defined as follows:

$$u_v(x) = u(x) - \bar{u}(x)$$

$$d_v(x) = d(x) - \bar{d}(x)$$

$$S(x) = 6\, s(x) \qquad (s = \bar{s} = \bar{u} = \bar{d})$$

$$C(x) = 2\, c(x)$$

This parametrization is in agreement with the momentum sum rule and the number of valence quarks inside the proton (the neutron is obtained by exchanging u and d distributions).

The moments of these distributions are calculated and used as input values at a point Q_0^2. To calculate the moments at another point Q^2 we use (II.4.6). The moments of the transition functions Γ_{ij} are obtained by solving the renormalization group equation (II.3.16) numerically, with a boundary condition $\Gamma_{ij}\big|_{Q^2=Q_0^2} = \delta_{ij}$. It turns out to be very simple to obtain an accurate solution of this equation. Moreover, when we fit the shape of the distributions we have to calculate

the transition functions only once, since the only parameter on which they depend is Λ. For this reason equation (II.3.16) is preferable to (II.3.23).

The second order anomalous dimension matrix which we need is presented in a manageable form by [Gon 80]. These results are based on the calculation by [Flo 79], who use the minimal subtraction scheme. We have to adapt this result to our convention. There is also a convention to be fixed concerning the off-diagonal terms of the matrix. Since only the product $\gamma^n_{GQ} \cdot \gamma^n_{QG}$ is relevant there is some freedom in the choice of these terms. When operator matrix elements are associated with parton distributions one is lead to a natural choice, which is most conveniently defined by the momentum sum rule relations (1.49). For completeness we give the first order anomalous dimension matrix:

$$\begin{aligned}
\gamma^n_{0,QQ} &= \frac{N^2-1}{N} \left[4S_1(n) - \frac{2}{n(n+1)} - 3\right] \\
\gamma^n_{0,QG} &= -4 N_f \frac{n^2+n+2}{n(n+1)(n+2)} \\
\gamma^n_{0,GQ} &= -2 \frac{N^2-1}{N} \frac{n^2+n+2}{n(n^2-1)} \\
\gamma^n_{0,GG} &= 2N \left(4S_1(n) - \frac{4}{n(n-1)} - \frac{4}{(n+1)(n+2)} - \frac{11}{3}\right) + \frac{4}{3} N_f
\end{aligned} \tag{2.2}$$

where N_f is the number of flavors. With the exception of the gluon-gluon matrix element these anomalous dimensions can all be derived from the transition function given by (II.5.1), (II.5.3) and (III.5.16). To obtain the second order terms we take the results of [Gon 80], make sure that the off-diagonal terms satisfy our convention and use the finite renormalization (1.42) in the following way

$$\gamma^n_1 = \tilde{\gamma}^n_1 - [\gamma^n, \gamma^n_0] - 2\beta_0 \gamma^n + \beta_0 \gamma^n_0 \left[\ln(4\pi) - \gamma + S_1(n)\right] \tag{2.3}$$

where $\tilde{\gamma}^n_1$ is the minimal subtraction result, and β_0 is defined by

(II.3.26). For the non-singlet transition function (2.3) can be used without the commutator term. To be able to use (2.3) we have to specify γ^n_{GG}, which was not yet defined. The momentum sum rule requires $\gamma^2_{GG} = \frac{1}{2} N_f$, and we use this as the definition for all moments.

The $\ln (4\pi) - \gamma$ term appearing in (2.3) is a remnant of dimensional regularization; it does not cancel because $\tilde{\gamma}^n_1$ does not contain such terms. Since the anomalous dimensions we use are not minimally subtracted these terms can only be attributed to coupling constant renormalization, and hence they can be transformed away by making a finite renormalization of the coupling constant. According to section II.6 this is equivalent to a change in the definition of Λ. We use the following expression for the second order running coupling constant:

$$\lambda(Q^2/\Lambda^2) = \frac{1}{\beta_0} \frac{1}{\ln (Q^2/\Lambda^2)} - \frac{\beta_1}{\beta_0^3} \frac{\ln (\ln (Q^2/\Lambda^2))}{\ln^2 (Q^2/\Lambda^2)} \tag{2.4}$$

according to (II.6.28):

$$\lambda(Q^2/\Lambda^2) = \lambda(Q^2/\Lambda^2_\delta) - 2\beta_0\lambda^2(Q^2/\Lambda^2_\delta) \ln \delta + O(\lambda^3) \tag{2.5}$$

assuming both Λ and $\Lambda_\delta = \delta\Lambda$ are much smaller than Q^2. When (2.5) is substituted into the expansion of the anomalous dimension (II.3.29), the second coefficient is modified as follows:

$$\gamma^n_1 \to \gamma^n_{1,\delta} = \gamma^n_1 - 2\beta_0\gamma^n_0 \ln \delta \tag{2.6}$$

By choosing $\delta = \exp \frac{1}{2} (\ln (4\pi) - \gamma)$ the $(\ln (4\pi) - \gamma)$ terms vanish. We will take this as our standard definition of Λ. This is what is usually called the $\overline{\text{MS}}$-scheme [Bar 78]. The choice $\delta = 1$ corresponds to the MS-scheme.

We neglect the masses of the u, d and s quarks, but for the charmed quark that may not be a good approximation. When masses are taken into

account in the calculation of the photon-gluon process, which in lowest order acquires a contribution from the diagrams of fig. II.5.2, one finds that charm production is only possible for $x < [1 + (4m_c^2/Q^2)]^{-1}$, where m_c is the mass of the charmed quark. In addition to this there are other terms proportional to m_c^2/Q^2 (the complete result can be found in [Wit 76]). The large Q^2 limit is correctly described by the transition functions we use, but near $Q^2 = 4m_c^2$, which is in the middle of the considered Q^2-region, corrections are needed. We have modified the gluon-charm transition function so that the correct high Q^2 limit is maintained, but that in the threshold region the mass-dependence of the lowest order contribution to the photon-gluon process is reproduced. In this region normal perturbation theory works, since the effective expansion parameter is $\alpha_s \ln (m_c^2/Q^2)$, which is small. The effect of the correction is to suppress the growth of the charmed distribution at low Q^2. It is reasonable to assume that the input charm distribution is small. We take the parameter F_2^2 in (2.1) somewhat arbitrarily equal to $\frac{1}{15} F_1^2$ at $Q_0^2 = 3\ \text{GeV}^2$, which implies that the charmed distribution is 20% of the distributions of the light quarks. This percentage increases very slowly with Q^2 due to the fact that the threshold suppression factors become less important. In the Q^2-region we will consider, the effect of charm on the structure functions is small, and therefore the assumptions we made do not have important consequences for the results. Only when charm production data are considered one may get more detailed information about charm distributions.

Beside the charm distributions there are also indirect manifestations of charm through factors N_f, the number of flavors, appearing in β and γ. We have used $N_f = 4$, but since we are in the charm threshold

region that is not completely correct. An approximation of the threshold effects due to $N_f - 3$ heavy quarks with masses m_i is [DeR 76, Pog 76]:

$$N_f(Q^2) = 3 + \sum_{i=4}^{N_f} \frac{1}{1 + 5(m_i^2/Q^2)} \qquad (2.7)$$

This has only a small effect on the χ^2 of the fits, but can have an effect of about 20% on the value of Λ.

The parameters can now be determined by choosing different values for Λ and different input distributions and comparing the moments and their Q^2-evolution with the data. By this procedure we use information from all values of Q^2 to obtain the distributions at Q_0^2. The results are sensitive to the gluon distribution even though the gluon has no coupling to the photon. This is because the gluon distribution affects the Q^2-evolution of the sea, which does couple to the photon. Nevertheless we find that the sensitivity to the gluon and sea distributions is small and that the shapes of these distributions can not be determined very well. Therefore we fix these parameters in the following way:

$$\alpha_3 = \alpha_4 = -1$$

$$\beta_3 = 8 \quad ; \quad \beta_4 = 5 \quad .$$

There are both theoretical arguments [Bro 73, Far 74] and phenomenological indications (e.g. [Ito 80]) for values of β_3 and β_4 in this neighborhood.

This leaves 6 fitparameters, F_1, Λ and the shape parameters of the valence distributions. To make sure that these distributions remain normalizable during the fit procedure, we introduce four new parameters η_1, η_2, ρ_1 and ρ_2:

$$\alpha_i = \eta_i^2 - 1 \quad ; \quad \beta_i = \rho_i^2 - 1$$

The results of the fit are summarized in table I for two values of the input point Q_0^2.

	I; 144 points		II; 162 points	
	$Q_0^2 = 3$ GeV^2	$Q_0^2 = 10$ GeV^2	$Q_0^2 = 3$ GeV^2	$Q_0^2 = 10$ GeV^2
χ^2	1285.	1273.	423.	421.
η_1	.810±.003	.772±.003	.836±.005	.797±.005
η_2	.88 ±.02	.81 ±.02	1.02 ±.03	.94 ±.03
ρ_1	1.803±.003	1.935±.003	1.838±.005	1.959±.005
ρ_2	2.13 ±.02	2.24 ±.02	2.34 ±.04	2.43 ±.04
F_1	.55 ±.01	.57 ±.01	.47 ±.02	.52 ±.02
Λ(MeV)	579±3.	582±3.	548±10	552±10

table I: best fit to moments of F_2^p and F_2^{p+n}.

There is a clear discrepancy between I and II, which must be attributed to the differences mentioned at the beginning of this section. The larger χ^2 and smaller errors of I are due to the fact that the errors on the moments given by I are smaller than those of II. With respect to the effect of a change of Q^2 the following can be expected. The parameters which determine the shape of the distributions will change, because the input distributions are Q_0^2-dependent. If Q_0^2 becomes larger the valence distributions are expected to shrink to smaller values of x, which corresponds to a decrease of η_1 and η_2 and an increase of ρ_1 and ρ_2. The sea distributions are expected to increase. The values of χ^2 and Λ should, however, be independent of the input point. All this agrees reasonable well with the results of the fits. In the following we will restrict ourselves to $Q_0^2 = 3$ GeV^2, which is just below the

lowest Q^2-value we will consider.

The errors in the parameters which we have given in table I and will give later in this section are all calculated as if the errors on the moments were purely statistical and the moments completely uncorrelated. In reality, however, some systematic effects are included in the errors, and moments at the same Q^2 are correlated, because they are determined by integrating the same experimental data with a different weighting factor. The information given in I and II is insufficient to disentangle these effects, but in any case a correct treatment will give larger errors.

To see whether there is a normalization discrepancy between the hydrogen and deuterium data we have done the fits with the normalizations as additional parameters. The estimated error in these normalization is 2.5% [Gor 79]. For I we find no significant decrease of χ^2, and a shift of all parameters within the errors. The fitted normalizations are .999 and .994 for hydrogen and deuterium respectively. For II we find a decrease of χ^2 to 412, and a shift of η_1, η_2 and ρ_1 which is larger than the error in these parameters. The fitted normalizations are .967 and 1.03. In both cases Λ turns out to be surprisingly stable.

We have checked whether the parametrizations we use correctly represent the data. This can be done by introducing a normalization for each moment of u_v and d_v, and fitting these parameters to the data, starting from the shape which gave the best fit. The results are given in table II. (These normalizations are multiplication factors for the theoretical predictions. All other normalizations we will discuss are multiplying the data.) We conclude that there is no evidence for a deviation from the simple parametrization we have chosen, except for

	I		II	
n	u_v	d_v	u_v	d_v
2	.985±.012	1.13+.06	1.006±.01	1.03±.04
3	.991±.007	1.01±.03	.988±.007	.98±.03
4	.997±.006	1.00±.03	.985±.01	1.04±.05
5	1.001±.005	1.01±.03	.995±.008	1.08±.05
6	1.003±.005	1.02±.03	1.001±.009	1.10±.06
7	1.004±.005	1.06±.04	1.006±.008	1.06±.07
8	1.001±.005	1.08±.05	1.009±.008	.94±.08
9	.999±.006	.99±.06	1.017±.01	.65±.11
10	1.001±.006	.89±.06	1.021±.01	.25±.15
χ^2	1256.		327.	

table II: normalizations of valence quark moments.

the high-n moments of d_v for II (this might be related to the Fermi-motion corrections to the deuterium data, which will affect d_v more than u_v, and which are largest for high n). We have also considered the effect of fitting Λ and F_1 in addition to these normalizations. We find that Λ does not change at all, but F_1 turns out to be strongly correlated to the n = 2 and 3 moments of the valence quarks. This results in a best fit with F_1 = 0.±.2, an increase of the second and third moment of the valence distributions by 10% to 50% and only a relatively small decrease in χ^2. This correlation is due to the fact we have only two structure functions to determine the moments of three distributions. Then the relative magnitude can only be determined from the Q^2-dependence, which is apparently described slightly better by the evolution

of valence distributions. Since there is probably an important Q^2-dependence due to higher twist this is a dangerous procedure.

When the valence quark moments are related by a parametrization like (2.1), the n = 2 and 3 moments are determined by the higher ones, and then a much more accurate value of F_1 can be obtained, as is shown in table I. The fact that this value depends on the shape of the valence distribution, is however an important source of uncertainty. We will show later in this section that the correlations disappear by adding neutrino data.

It is questionable whether these data can be expected to show scaling deviations which are entirely due to leading twist QCD corrections. The fact that resonances are seen in the data, and that the elastic contribution is rather large in the small Q^2-large n region casts some doubt upon that hypothesis. It has been shown [Abb 80.a,b, Mah 80] that the scaling deviations can be fitted equally well by purely higher twist effects. These effects are theoretically expected and certainly not in disagreement with QCD, but unfortunately not much is known about the relative magnitude of leading and non-leading twist effects. Adding $1/Q^2$-terms to the theoretical prediction for $F_2(x)$ is known to have an enormous inpact on the Λ parameter [Abb 80.a,b].

We have investigated whether the data can be fitted in a consistent way by leading twist QCD alone by rejecting those datapoints for which higher twist effects may be large. As a criterium to locate the higher twist region we use the relative contribution of the elastic peak. Since elastic scattering is a typical coherent effect, which cannot be described by the parton picture of a single parton which interacts with the photon we expect that this is a reasonable criterium. The fact that

the elastic form factor vanishes as $1/Q^4$ supports this idea. This does not imply that the elastic contribution should be omitted; it is simply impossible to disentangle leading and higher twist effects experimentally and therefore the only correct approach is to calculate the moments, including resonances and elastic scattering, and compare them with QCD predictions which include higher twist terms. Apart from convergence problems which may appear, the operator product expansion offers, at least in principle, a complete description of all scaling deviations. It is however a serious shortcoming of most analyses that elastic scattering is included in the experimental data, but that higher twist effects are ignored in the theoretical formulation.

In order to investigate the effect of this approximation we cut the data by keeping only those moments for which the relative elastic contribution is less than C × 100%, for various values of C. For each C we consider both the data with and the data without elastic contribution. Then we fit the six parameters to each of the four sets of data which we obtain this way, and plot their values versus C. With decreasing C the number of datapoints decreases and consequently the errors on the parameters will increase. For a consistent fit the values of the parameters should agree within the errors, for all C. When such a consistency is not found, that indicates that the theory does not completely describe the data. The plots, shown in fig. 2.1 suggest quite clearly that a leading twist QCD fit lacks consistency. This is most obvious for the Λ-parameter, which decreases significantly with decreasing C for the data which include the elastic contribution. For the other parameters there are similar inconsistencies, but these are much smaller. These plots also show that there are large discrepancies

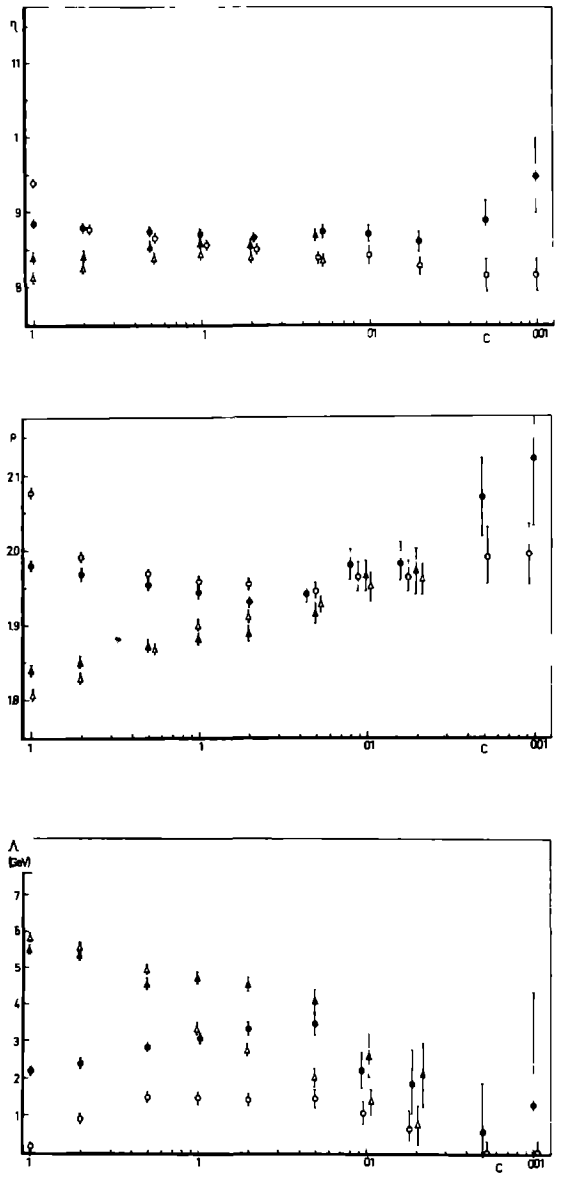

symbols:

Δ I, el. incl.

o I, el. not incl.

▲ II, el. incl.

● II, el. not incl.

fig. 2.1: approach of the parameters η_1, ρ_1 and Λ to their asymptotic values (continued on next page).

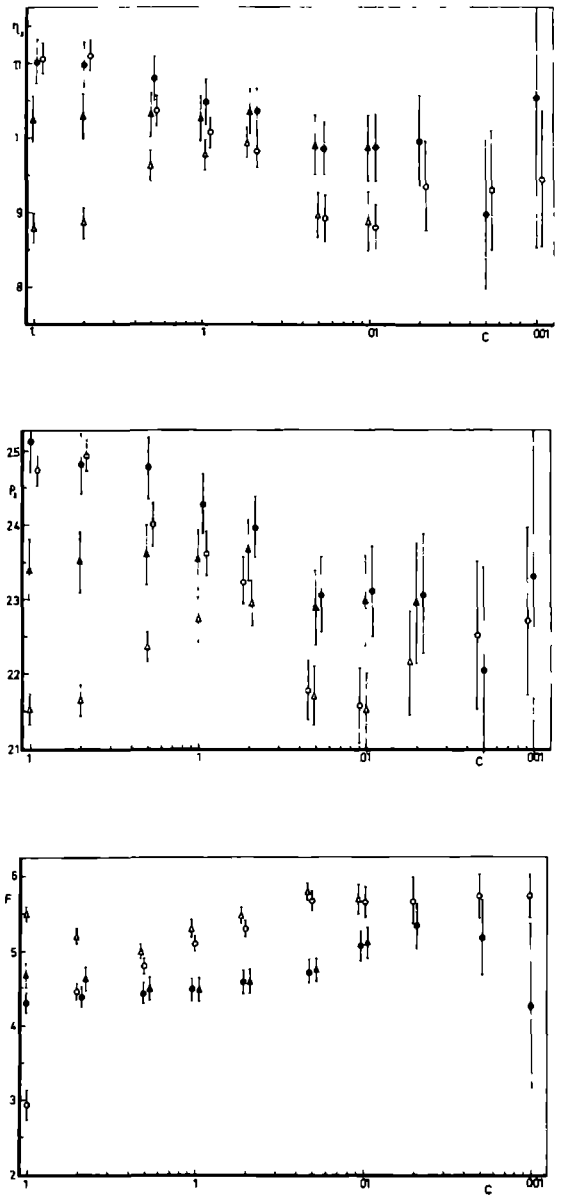

fig. 2.1: (continued) the same for η_2, ρ_2 and F_1.

between the moments from I and those from II. Nevertheless both show the same trend.

These plots can be used to determine the asymptotic values of the parameters. These are defined as those values of Λ and the input parameters at $Q_0^2 = 3\ GeV^2$ which give a correct description of the data at large Q^2, if only leading twist QCD is correct for their evolution. The distributions at Q_0^2, which are determined in this way, will of course not describe the structure function at that point very well, because at low Q^2 there are additional higher twist terms. But when we want to transfer the distributions to another process, e.g. the Drell-Yan process, we must try to get rid of the higher twist terms, which may not have the universality property of the parton distributions, or a different kind of universality. Of course there are higher twist contributions to lepton pair production as well, but with this method one may expect to obtain the correct result at large Q^2, where higher twist can be ignored.

The asymptotic values of the parameters are the ones which are approached for $C \to 0$. Since the rightmost points are based on only a small number of moments ($\sim$ 25 for 6 parameters) these values may not be reliable. It is clear that for a decreasing number of points the value of χ^2/degree of freedom will go to zero, and then one is fitting the statistical fluctuations instead of their average. If the errors were completely statistical and uncorrelated a value of χ^2/d.o.f. which is less than 1 would indicate over-parametrization. The published errors on the moments include however systematic effects, and there is also a correlation between different moments at the same Q^2. Therefore the range of reliability of the results is probably somewhat beyond the

point where χ^2/d.o.f. = 1, which is at C = .02 for the data from I and between C = .02 and C = .01 for those of II. We cannot be sure whether or not the parameters have reached their asymptotic value at these points.

On the basis of fig. 2.1 we can conclude that safe estimates for the parameters are:

$$\eta_1 = .85 \pm .03 \qquad \rho_1 = 1.95 \pm .05$$
$$\eta_2 = .95 \pm .1 \qquad \rho_2 = 2.25 \pm .15 \qquad (2.8)$$
$$F_1 = .52 \pm .06 \qquad \Lambda < 400 \text{ MeV}$$

These values are based on the fits for C = .05, .02 and .01. For still smaller C none of the parameters, except Λ, shows a significant tendency to deviate from these values. The results for Λ suggest that the asymptotic value of this parameter may be much smaller than the upper limit given above. This would agree with the preliminary results for the EMC-data [Gab 80] which indicate $\Lambda \sim 100$ MeV. The consequence of this is a much smaller value of α_s, and better convergence of the perturbation expansion. For example at $Q^2 = 900$ GeV^2 $\Lambda = 100$ MeV gives $\alpha_s = .11$ (in the $\overline{\text{MS}}$-scheme).

Since there are correlations between the parameters not any arbitrary choice within the limits given above results in a good fit to the data. Therefore we choose the set of parameters which fits the data of I, without elastic contribution, when only those points are kept for which the elastic contribution is smaller then the errors. For these data we get the following results:

$$\eta_1 = .844 \qquad \rho_1 = 1.967$$
$$\eta_2 = .884 \qquad \rho_2 = 2.165 \qquad (2.9)$$

$F_1 = .573$ $\quad\quad$ $\Lambda = 100.5$ MeV

$\chi^2 = 39.1$ $\quad\quad$ Hydrogen: $\chi^2 = 23.1$; 25 points

$\quad\quad\quad\quad\quad\quad$ Deuterium: $\chi^2 = 16.0$; 27 points

The fit is shown in fig. 2.2. For comparison we show the same lines together with the moments which include elastic scattering. The results suggest that, if Λ is indeed small, in the region 5 GeV^2 < Q^2 < 20 GeV^2 no improvement is obtained by adding the elastic contribution. Towards still lower Q^2 however purely inelastic moments decrease and the elastic contribution is needed to compensate for that decrease. But this seems to cause a slight over-compensation in the intermediate Q^2-region.

We have used this choice out of the data for the rest of the analyses. The part of data which has been rejected corresponds to a value of C between .01 and .02 in fig. 1, and therefore we expect that the results are not very sensitive to higher twist effects. The differences between the parameters obtained with data from I and II give an indication of the uncertainties in (2.9). This is probably more meaningful than the statistical errors, which we have therefore omitted.

To investigate the effect of the definition of Λ we have varied the parameter δ introduced in (2.5). This parameter changes Λ in a multiplicative way, but χ^2 should be insensitive to it. To check this we have done the fit for different values of δ and compared the fitted value of Λ with the predicted value. Since we use the $\overline{\text{MS}}$-scheme as a starting point the predicted value is:

$$\Lambda_{\text{pred}} = \delta \exp\left[-\frac{1}{2}(\ln(4\pi) - \gamma)\right] \times 100.5 \text{ MeV} \qquad (2.10)$$

In fig. 2.3 we have plotted χ^2 and $\ln \Lambda$ versus $\ln \delta$. The insensitivity of χ^2 is impressive, considering the extended scale we use for χ^2 and

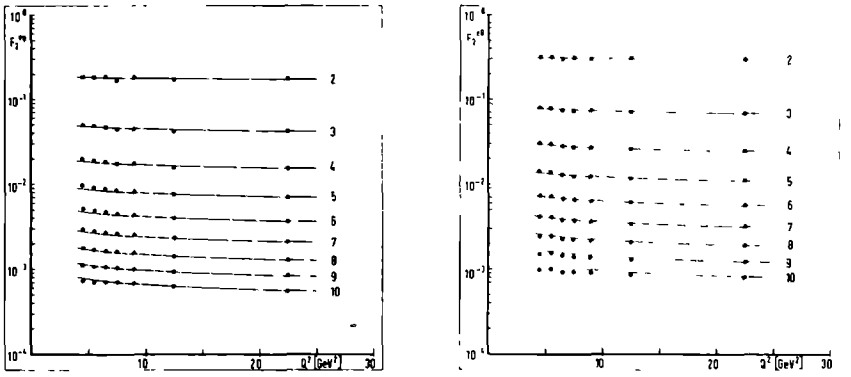

fig. 2.2.a: theoretical values for the moments of the proton and deuterium (proton + neutron) structure functions compared to the data from I, without elastic contribution. The parameters are obtained by fitting only to the points indicated by squares.

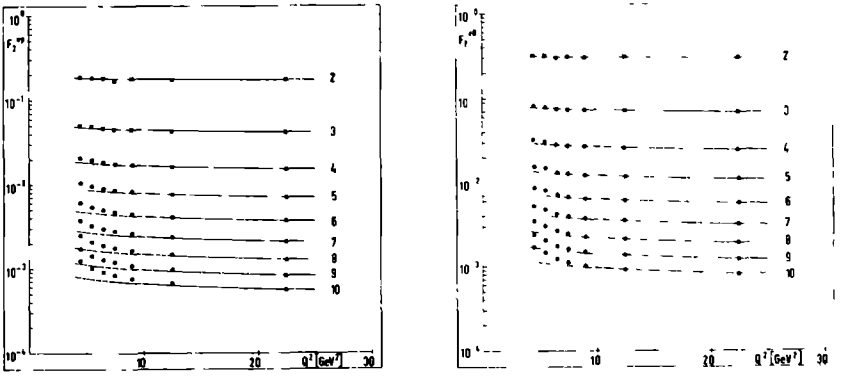

fig. 2.2.b: the lines are the same as in a, but the elastic contribution is included in the datapoints.

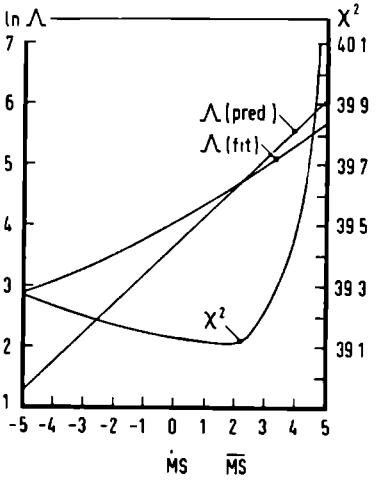

fig. 2.3: effect of the definition of Λ. χ^2, ln Λ (fitted) and ln Λ (predicted) are plotted versus ln δ.

the fact that δ changes by many orders of magnitude. The fact that the $\overline{\text{MS}}$-scheme is very close to the minimum of χ^2 can only be considered as a coincidence, but it shows that this is a reasonable choice. The values of Λ which different definitions allow, range from $\Lambda \sim 300$ MeV to practically zero. The deviation of the fitted values from the predicted ones can be attributed to uncalculated higher order corrections (which for example cause the differences between the curves in fig. II.6.1, which demonstrates the same effect) or higher twist effects in the data.

To get additional information about the distributions we have supplemented the electron and muon data by neutrino data from CDHS [DeG 79]. We have calculated the Nachtmann-moments of the structure functions $xF_3(x,Q^2)$ and $F_2(x,Q^2)$ and combined them with the electromagnetic scattering data.

To calculate the Nachtmann moments the following integrals have to be evaluated [Nac 73]:

$$M_3^n(Q^2) = \int_0^1 dx \frac{\xi^{n+1}}{x^3} \left[\frac{1+(n+1)R}{n+2}\right] x F_3(x,Q^2) \qquad (2.11)$$

$$M_2^n(Q^2) = \int_0^1 dx \frac{\xi^{n+1}}{x^3} \left[\frac{3+3(n+1)R+n(n+2)R^2}{(n+2)(n+3)}\right] F_2(x,Q^2) \qquad (2.12)$$

where

$$\xi = \frac{2x}{1+R} \quad ; \quad R = \sqrt{1 + \frac{4M^2x^2}{Q^2}}$$

and M is the nucleon mass. Experimental data on $x F_3$ and F_2 are available for $x < .65$, but for small Q^2 there are no data in the large x region, whereas for large Q^2 the small x region is missing. When reasonable Q^2-bins are chosen only a small number of datapoints per bin is available. This implies that extrapolation and interpolation is needed both in x and in Q^2. For that purpose we use a global fit to the data for all x and Q^2. The following parametrization turned out to be very suitable:

$$f(x,Q^2) = A(Q^2)\ x^{\alpha(Q^2)}\ (1-x)^{\beta(Q^2)} \qquad (2.13)$$

For the Q^2-dependence of the parameters we have considered a QCD-like behavior, $a_0 + a_1 \ln[(\ln(Q^2/\Lambda^2))/(\ln(Q_0^2/\Lambda^2))]$, and a higher twist-like behavior, $a_0 + a_1/Q^2$. Further we have investigated the effect of modifying the x-dependence of (2.13) by factors $[\ln(1/x)]^\gamma$ and $[-\ln(1-x)]^\delta$. In all cases the data could be fitted very well, and we obtained values of χ^2/d.o.f. which were less than 1. This indicates that the statistical errors of the data have been overestimated.

The fitted functions are only used as interpolation formulae. To determine the distribution function F at x,Q^2 we take the experimental datapoint which is closest to it and use the fit $f(x,Q^2)$ in the

following way:

$$F(x,Q^2) = \frac{f(x,Q^2)}{f(x_0,Q_0^2)} \; F(x_0,Q_0^2) \tag{2.14}$$

where x_0, Q_0 is the position of an experimental point. As a criterium for the distance of two data points in the x-Q^2 plane we used $\sqrt{(x-x_0)^2 + \lambda \ln^2 (Q^2/Q_0^2)}$, where λ is a parameter which determines the size of a Q^2-bin. In practice $\lambda = 1$ turned out to give reasonable values of Q_0^2 for a given Q^2. This method gives a natural extrapolation of the data into the region $x > .65$. Since the structure functions vanish at $x = 1$ the contribution of this region is small except for high n. Therefore we will restrict the calculation to $2 \leq n \leq 6$. The extrapolation towards $x = 0$ is less certain, and therefore we do not consider values of Q^2 greater than 55 GeV^2, for which there is no direct information about the small x region.

By means of a numerical integration procedure we can express every moment as a weighted sum of experimental data, which we use to determine the moment and its statistical error. To estimate the effect of different parametrizations we have considered several other fits to the data. These include all functions obtained by shifting each of the parameters in (2.13) by one standard deviation, functions with a different Q^2-dependence, and functions with a different x-dependence. We have calculated the Nachtmann moments of all these functions and compared the maximal difference between them with the statistical errors. The maximum of these two quantities, which were usually of the same order of magnitude, is used as error on the moments. The differences, introduced by using each of the alternative fits as interpolation formula instead of the best fit are much smaller than these errors.

n \ Q^2		5.5	7.5	9.	12.5	17.5	22.5	30	40	55
2	$F_2^{\nu N}$	.557 ±.022	.512 ±.022	.522 ±.023	.471 ±.023	.490 ±.028	.441 ±.029	.471 ±.030	.463 ±.030	.491 ±.029
3		.140 +.007	.124 ±.008	.120 ±.006	.110 ±.007	.108 ±.007	.0953 ±.0064	.102 +.005	.0985 ±.0038	.100 ±.003
4		.0545 ±.0035	.0471 ±.0042	.0446 ±.0037	.0403 ±.0041	.0392 ±.0036	.0337 ±.0030	.0356 ±.0022	.0342 ±.0017	.0335 ±.0014
5		.0259 ±.0019	.0221 ±.0023	.0208 ±.0023	.0186 ±.0024	.0180 ±.0021	.0151 ±.0017	.0158 ±.0012	.0151 ±.0009	.0144 ±.0007
6		.0139 ±.0011	.0117 +.0014	.0110 +.0015	.0098 +.0016	.0095 ±.0013	.0079 ±.0011	.0081 ±.0008	.0077 ±.0005	.0071 ±.0004
2	$F_3^{\nu N}$	.346 ±.085	.384 ±.048	.336 ±.051	.352 ±.035	.367 ±.023	.294 +.023	.325 ±.021	.304 ±.016	.290 ±.016
3		.104 ±.039	.108 ±.022	.101 ±.017	.101 ±.012	.106 ±.010	.0740 +.0070	.0887 ±.0072	.0811 +.0053	.0775 ±.0044
4		.042 ±.020	.042 ±.011	.0400 ±.0077	.0390 ±.0057	.0420 ±.0055	.0268 ±.0030	.0334 ±.0037	.0300 ±.0025	.0283 ±.0020
5		-	.0192 ±.0062	.0185 ±.0042	.0180 ±.0029	.0198 ±.0032	.0122 +.0015	.0152 ±.0022	.0134 ±.0013	.0124 ±.0011
6		-	.0099 ±.0036	.0096 ±.0025	.0094 +.0015	.0104 ±.0019	.0064 ±.0009	.0078 ±.0013	.0068 ±.0008	.0062 ±.0006

table III: neutrino Nachtmann moments.

This shows that the moments we obtain are determined by the data, and not by the theoretical bias which made us choose (2.13) and its Q^2-dependence. The results are shown in table III.

We have not included an elastic contribution, since we will restrict ourselves to the region in n and Q^2 where it can be neglected. We have also omitted corrections for nuclear effects, because they are probably not yet fully understood, considering the disagreement about such corrections for deuterium. According to [Gor 79] these corrections are less than 5% for the deuterium moments with $n \leq 6$, but since the CDHS experiment uses an iron target we are not sure whether this estimate will hold. In any case the corrections are expected to have very little Q^2-dependence [Atw 73].

The theoretical prediction for the neutrino moments is:

$$M_2^n(Q^2) = u_v^n(Q^2) + d_v^n(Q^2) + s^n(Q^2) + c^n(Q^2) \qquad (2.15)$$

$$M_3^n(Q^2) = [u_v^n(Q^2) + d_v^n(Q^2)][1 + \frac{\alpha_s(Q^2)}{4\pi} \frac{4}{3} (- \frac{2}{n} - \frac{2}{n+1})] \qquad (2.16)$$

The term proportional to α_s is the difference between the coefficient functions for F_3 and F_2. These expressions are valid for the average of the proton and neutron structure functions. Moreover (2.16) is only correct for the average of the ν and $\bar{\nu}$ structure functions. The difference between the two is however proportional to s-c, and therefore almost negligible.

The set of data which we have used consists of the data from I which are indicated by the black squares in fig. 2.2, and neutrino data, with the same cuts in Q^2 and n. This means that the region which is most sensitive to higher twist effects is not considered, so that one may hope that the observed Q^2-dependence is mainly caused by QCD. The

neutrino moments at Q^2 = 30, 40 and 50 GeV^2 give additional information about the higher Q^2 region.

We could not get a reasonable fit unless we allowed for a change in the normalization of the neutrino data. The experimental errors on the normalizations are 6% for F_2 and 8% for xF_3. We found however a difference which is two to three times as large. The results of the combined fit are shown in table IV.

parameters:	η_1 = .849	ρ_1 = 1.946
	η_2 = .801	ρ_2 = 2.146
	F_1 = .569	Λ = 171 MeV
χ^2 :	118.0 (normalizations included)	

structure function	normalization	number of points	χ^2
F_2^{ep}	1.010 ± .021	25	21.0
F_2^{eD}	.967 ± .021	27	22.9
$F_2^{\nu N}$	1.12 ± .020	38	28.9
$F_3^{\nu N}$	1.21 ± .022	38	35.7

table IV: results for combined charge-lepton/neutrino data.

The increase of Λ compared to (2.6) is not incompatible with the results of fig. 2.1, and is due to the fact that the neutrino data prefer Λ = 480 MeV. All neutrino data of table III can however be fitted very well (χ^2/d.o.f. = .6) when we keep Λ fixed at a value of 100 MeV. Even when we extend these data with moments at higher Q^2 values and with higher n such an excellent fit can be obtained. When we keep only the neutrino data with $Q^2 \geq 22.5$ GeV^2 we obtain a value

of 90 MeV for Λ, in a fit to the neutrino data alone. The only other parameter which changes considerably is η_2. The parameter F_1 (which measures the amount of sea-quarks and is therefore very important for the normalization of the Drell-Yan cross section, to be calculated in the next section), is however surprisingly stable.

Apart from the normalization the agreement between charged lepton and neutrino data is good. We can show that this normalization problem is not due to the assumptions we made about the distributions. Using the parton model formula for the structure functions one can derive the following equality:

$$\frac{9}{5} F_2^{eD} + \frac{6}{5} (s-c) = F_2^{\nu N} \qquad (2.17)$$

The difference of the strange and charmed quark distribution is small, but in any case positive, so that $F_2^{\nu N}$ should be larger than $\frac{9}{5} F_2^{eD}$. Comparing table III with the results of [Gor 79] or [Duk 79] one finds that the neutrino moments lie systematically below the lower limits, for all n. This makes an explanation of this difference by Fermi motion corrections unlikely, since these corrections give an increase of the low-n moments and a decrease of the high-n moments. When this difference would be significant it would be a serious problem for the parton model, but considering the large uncertainty in the absolute normalization of the experimental data such a conclusion is certainly premature.

The two additional structure functions enable us to obtain more detailed information about the sea-quarks. We have fitted the shape-parameter α_3, defined in (2.1) together with the other six parameters and the normalizations, and found a value of 10 ± 3, which agrees with the value 8 which we have chosen a priori. The correlations between the

low-n valence quark moments and the parameter F_1 which was present in the fits to the electromagnetic structure functions is removed by the neutrino data, as table V shows quite clearly. The results in this table are obtained by fitting the normalizations of all valence quark moments together with Λ and F_1, keeping all other parameters fixed at the values given above. We find that the results are very stable, which gives some confidence both in the correctness of the shape of the valence distributions and in the normalization of the sea.

n	u_v	d_v
2	1.004±.015	1.03±.07
3	.999±.014	1.04±.06
4	1.010±.015	.96±.07
5	1.008±.022	.99+.08
6	1.025±.031	.94±.13
7	1.025±.031	.90±.12
8	1.007±.035	.97±.18
9	1.009±.031	1.17±.15
10	1.011±.032	1.07±.16
Λ	180. ± 30 MeV	
F_1	.56 ± .04	
χ^2	110.8	

table V.

In fig. 2.4 we show the neutrino data together with the prediction, based on the parameters (2.9), the combined fit (including normalizations) given by table IV and a fit to the neutrino data alone. For this fit we have only used the moments of table III, without the low Q^2-high n ones, as explained before. In fig. 2.4 we show all moments of table III and additional ones at higher and lower Q^2 values and higher n, which we have not considered before because they may not be reliable. Even if we would have kept them the best fit to the neutrino data would have been indistinguishable from the one shown in fig. 2.4.

Since the neutrino data extend to high Q^2-values they should offer a good test of QCD. We have considered two simple criteria to determine

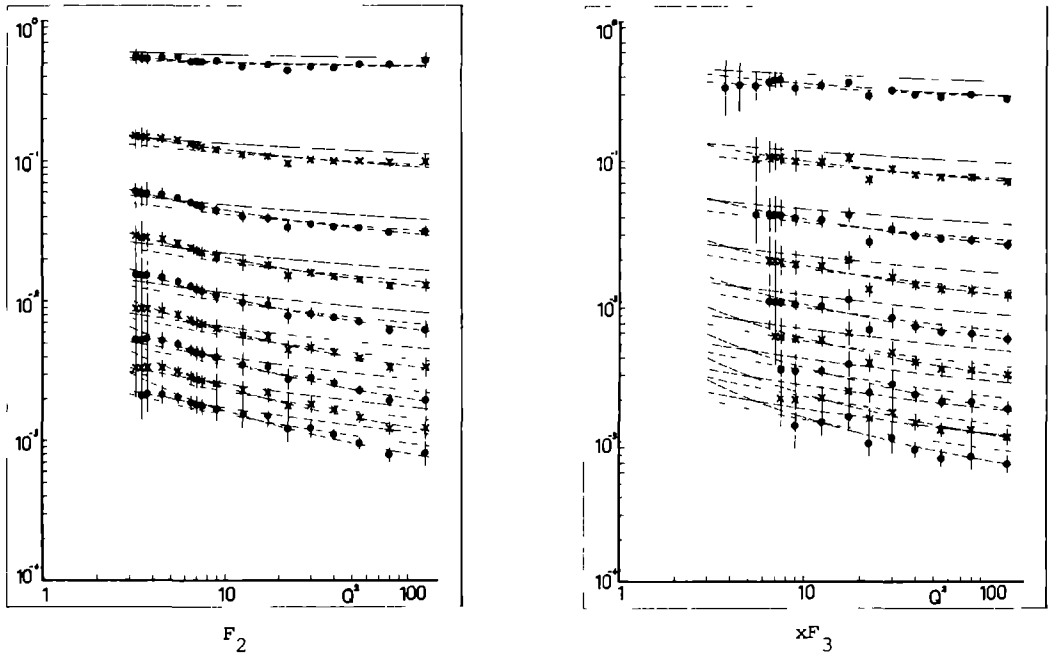

fig. 2.4: neutrino moments compared with prediction from SLAC-FNAL data (solid lines), combined fit (short dashed lines) and fit to neutrino data alone (long dashed lines). Moments with n = 2 - 10 are shown; ● indicates even moments, x odd moments.

whether the Q^2-dependence corresponds to QCD or not. The first one is to compare first order with second order QCD; we find that there is no significant difference. The second one is to determine the optimal value of N, the number of colors. Since all group theoretical factors are analytical in N we can simply use N as a fit parameter. We find a minimal χ^2 for $N \sim 3$, with $N = 2$ and $N \geq 5$ excluded by more than one standard deviation. Because of the arguments given earlier in this section the statistical significance of these results is however questionable. The new CDHS-data, which will be available shortly and have much better statistics, combined with an improved error analysis which takes correlations among the moments into account, will certainly give more reliable results. The same tests should be applied to the new high-Q^2 charged lepton data. The SLAC-FNAL data which we have used failed to satisfy these criteria, and moreover the results were very different for I and II. This failure can of course in principle be attributed to higher twist effects.

To obtain distribution at Q^2-values other than Q_0^2 we have to perform a moment inversion. We use a method similar to that of Buras and Gaemers [Bur 77, 78, Bia 80]. The procedure works as follows. Starting from the moments of the input distributions we calculate the moments at another Q^2-value by means of the transition functions. Because of the problems with the normalization of the neutrino data we will not use the results of table IV as input distributions, but those of (2.9). Next we try to find a parametrization of the shape of a distribution which reproduces these moments accurately over a large Q^2-range. The following parametrizations turned out to work satisfactory:

$$u_v(x) = \frac{2}{B(\alpha_1+1,\beta_1+1)}\, x^{\alpha_1}\,(1-x)^{\beta_1} \tag{2.18}$$

$$d_v(x) = \frac{1}{B(\alpha_2+1,\beta_2+1)}\, x^{\alpha_2}\,(1-x)^{\beta_2} \tag{2.19}$$

$$S(x) = A_3\, x^{\alpha_3}\,(1-x)^{\beta_3} + B_3\,(1-x)^{\gamma_3} \tag{2.20}$$

$$G(x) = A_4\, x^{\alpha_4}\,(1-x)^{\beta_4} + B_4\,(1-x)^{\gamma_4} \tag{2.21}$$

$$C(x) = A_5\, x^{\alpha_5}\,(1-x)^{\beta_5} \tag{2.22}$$

We determine the 17 parameters introduced in (2.18-22) at about 150 Q^2-values by fitting them to the moments for n = 2 to n = 20. The accuracy is better than 1% up to $Q^2 = 10^5$ GeV^2 for the valence distributions and up to 10^7 GeV^2 for the gluon and sea distributions and better than 5% up to $Q^2 = 10^5$ GeV^2 for the charm distributions. Since the accuracy for the sea and the gluons is much better than required we tried to reduce the number of parameters, but we did not succeed in finding an acceptable compromise.

To obtain explicit parametrizations for all x and Q^2 we need functions of Q^2 which represent the scale dependence of the parameters. The following kind of function turns out to be quite successful:

$$F(Q^2) = a_0 + a_1 s + a_2 c + a_3 s^2 + a_4 sc + a_5 c^2 \tag{2.23}$$

where

$$s = \ln \frac{\alpha_s(Q_0^2)}{\alpha_s(Q^2)} \qquad ; \qquad c = \alpha_s(Q_0^2) - \alpha_s(Q^2)$$

In each case only a subset of these parameters is used, chosen in such a way that the accuracy is sufficient for all Q^2. We will not give all these parameters, but only those which determine the valence distributions. According to [Bia 80] the second order Q^2-evolution of these

distributions can be fitted very well by choosing (2.18) and (2.19) with only the first two terms of (2.23). We have added one term to get even better agreement. The results are shown in table VI. The accuracy of these fits is at least .2%, and usually much better. The Q^2-dependence of the sea and gluon parameters was more difficult to fit, but with

parameter	a_0	a_1	a_2	a_3
α_1	-.287	-.206	-	.0127
β_1	2.87	.851	1.004	-
α_2	-.218	-.250	-	.0225
β_2	3.69	.883	1.027	-

table VI: valence-quark parameters

at most five parameters we could get sufficient accuracy. The Q^2-dependence of the parameters of the charm distribution is affected by the mass-effects which we have taken into account. When one does not require a too high accuracy one can still use (2.22) and (2.23) but to get further improvement it is probably necessary to modify these parametrizations. Because of the momentum sum rule there is a feedback of these mass effects to the gluon and sea distributions, but there the effect is small.

In total the distributions are determined by 69 parameters. The only way to handle such a large amount of parameters is to divide the procedure in steps; the first step is the determination of the input parameters, the second the determination of the Q^2-evolution of these parameters for each distribution separately, and the third step is to fit this Q^2-dependence for each parameter separately. In each step one is fitting at most six parameters. In the third step one may loose part

of the accuracy reached in the second one. A final check of the procedure is to compare the distributions directly to the QCD-predictions. The agreement turns out to be better than 1% for almost all valence, gluon and sea moments and better than 10% for the charmed quark moments, for the Q^2-ranges mentioned above. Although we have not used moments with $n > 20$ the agreement remains good for higher n. For example, at $Q^2 = 3000$ GeV^2 the accuracy is better than 10% for the first 50 sea and gluon moments and the first 500 valence quark moments.

The fact that high moments are represented very well implies that the distributions are reliable close to $x = 1$. The small x region is however less reliable, because it is mainly determined by a few low-n moments, which moreover are the least accurate ones for the valence distributions. It may be possible to improve the distributions in the small x region by using an analytical continuation in n for small n.

We show plots of the distributions in fig. 2.5, for Q^2 = 3, 30, 300 and 3000 GeV^2. The main difference of these results with those of [Bur 78] is the fact that a smaller value of Λ is used, and that the steepness of the sea and gluon distributions increases much more slowly with Q^2/Λ^2. To demonstrate the latter we give the sea and gluon parameters at these four Q^2-values in table VII. For comparison we also give the result at a very high Q^2 value. This table also shows the accuracy, averaged over the first 19 moments.

The distributions shown in fig. 2.5 are the main result of this section. The most important source of uncertainty in this result is the Λ-parameter, which unfortunately can not yet be determined with reasonable accuracy, because we cannot be sure how important higher twist effects are in the Q^2-region we have considered. Our results for

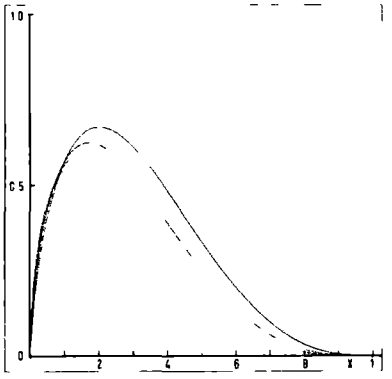

$x\, u_v(x,Q^2)$

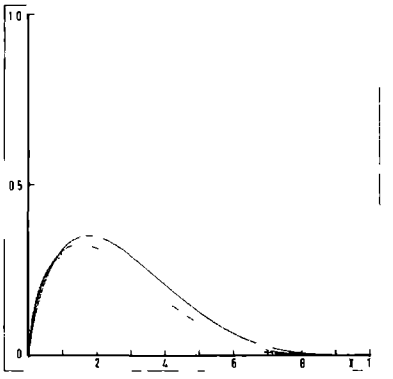

$x\, d_v(x,Q^2)$

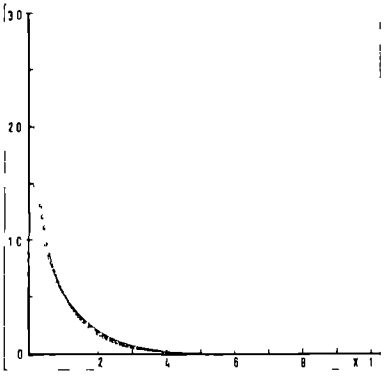

$x\, S(x,Q^2)$

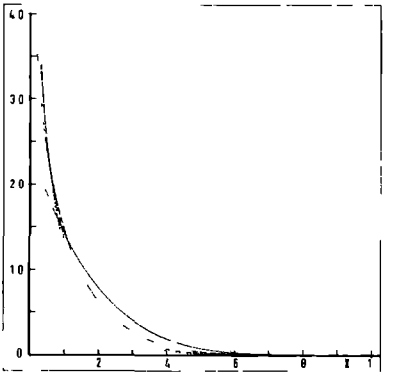

$x\, G(x,Q^2)$

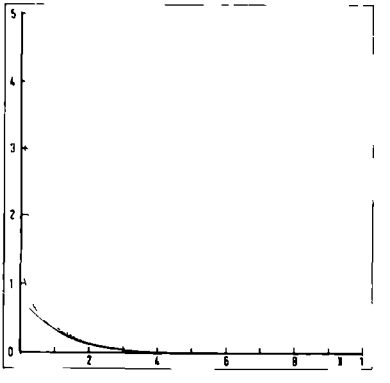

$x\, C(x,Q^2)$

fig. 2.5: distribution functions

solid line: $Q^2 = 3\ \text{GeV}^2$

dashed lines: $Q^2 = 30,\ 300,$

$3000\ \text{GeV}^2$ with decreasing

length of the dashes.

Q^2 (GeV^2)	A_3	α_3	β_3	B_3	γ_3	av. acc.	A_4	α_4	β_4	B_4	γ_4	av. acc.
3	1.31	-1.	8.	-	-	.0%	2.39	-1.	5.	-	-	.0%
30	.97	-1.11	8.35	.143	7.05	.03%	1.47	-1.25	5.71	.146	4.29	.03%
300	.81	-1.20	8.53	.125	7.03	.03%	1.09	-1.38	6.36	.280	4.77	.09%
3000	.70	-1.26	8.72	.117	7.08	.02%	.877	-1.45	6.87	.334	5.07	.15%
2×10^7	.47	-1.42	9.26	.114	7.41	.07%	.514	-1.61	8.08	.354	5.74	.38%

table VII: Q^2-dependence of sea and gluon parameters

the valence quark distributions are functions of (Q^2/Λ^2) instead of Q^2 and Λ^2 separately. Since the same is true for the transition functions which determine their Q^2-evolution the parameters in table VI are valid for any value of Λ. This is not exactly true for the sea, gluon and charm distributions, since their Q^2-evolution has a dependence on the charmed quark mass.

Since the gluon distribution moments, except for n = 2 can only be determined from the Q^2-dependence of the data higher twist effects will have a considerable effect on the shape of this distribution. Therefore, even if we would be able to determine this shape accurately, the result would not be very reliable. Even the normalization, which follows from the momentum sum rule, is rather uncertain. The charged lepton data give a value of 41-46% for the momentum fraction of the gluons, whereas the neutrino data give ~ 55%, unless one allows for a change in the normalization. (These momentum fractions are quoted from the papers of the FNAL-group and the CDHS-group ([Gor 79] and [DeG 79]) and agree with our results.) Fortunately the gluon distributions are not very important for the calculation of the Drell-Yan continuum,

irrespective of these uncertainties.

Fig. 2.1 gives a good impression of the uncertainties in the other parameters. For the results of section 3 F_1, which determines the amount of antiquarks in a proton, is the most important one. This parameter depends on the assumptions we made concerning the quark content of the sea. For example, assuming $\bar{s} = \frac{1}{2}\bar{u}$ instead of $\bar{s} = \bar{u}$ changes its value from .57 to .54 in a combined charged lepton/neutrino fit. Taking these uncertainties into account we expect that F_1 may change somewhat, but not by more than 20%.

3. Comparison of Drell-Yan corrections

The distributions, determined in the previous sections, and the Drell-Yan corrections presented in chapter III enable us to calculate the contribution of all processes to the hadron cross section in a consistent way. We will do that for proton-proton scattering. For proton-neutron scattering the relative magnitude of the corrections is not very different, whereas in valence-dominated processes ($p\bar{p}$ and most meson-baryon collisions) the quark-gluon and quark-quark contributions will be less important. The quark-antiquark radiative corrections are expected to give the same relative effect for all processes.

We will compare the contributions to the cross section $\frac{d\sigma}{dQ^2}$ for a fixed value of $\sqrt{s}$, for which we choose 27. GeV (corresponding to an incoming proton beam with a lab-energy of 400 GeV). As value for Λ we use 100 MeV. When the correct value of Λ turns out to be different, that implies simply that our results, which are a function of $\sqrt{s}/\Lambda$, will be valid at a different value of $\sqrt{s}$.

The results are plotted in fig. 3.2. We have included the following

contributions.

1. The leading Drell-Yan term, given by (III.1.6). Expressed in terms of the distributions u_v, d_v, S and C introduced in the previous section this term is

$$\frac{d\sigma_H^{DY}}{dQ^2} = \frac{4\pi\alpha^2}{3Q^4}\frac{1}{3}\int_\tau^1 dx\,\frac{\tau}{x}\left\{\frac{1}{6}S\left(\frac{\tau}{x}\right)\left[\frac{8}{9}u_v(x) + \frac{2}{9}d_v(x) + \frac{2}{9}S(x)\right] + \frac{2}{9}C\left(\frac{\tau}{x}\right)C(x)\right\} \tag{3.1}$$

2. The radiative correction to the $q\bar{q}$-process. The complete expression is given by (III.2.8), and the dependence on the distributions is as for (3.1). In the calculation of this term we have used values for the infrared cut off parameter ε in the order of 10^{-4} to 10^{-6}. As expected the result showed no dependence on ε. The effect of this contribution is about 50% of the leading Drell-Yan term for $\tau = .01$ and increases with τ. The two contributions are equally large at $\tau = .75$.

3. The quark-gluon contribution:

$$\frac{d\sigma_H^{qg}}{dQ^2}(\tau) = \frac{4\pi\alpha^2}{3Q^4}\frac{\alpha_s}{4\pi}\frac{1}{3}\int_0^1 dx_1\,dx_2\,G(x_1)\left[\frac{8}{9}u_v(x_2) + \frac{2}{9}d_v(x_2) + \frac{4}{9}S(x_2) + \frac{8}{9}C(x_2)\right]\frac{\tau}{x_1x_2}\Sigma^{qg}\left(\frac{\tau}{x_1x_2}\right)\theta(x_1x_2 - \tau) \tag{3.2}$$

This result can be derived from (III.2.5) and (III.2.6) by using the symmetry of the integrand with respect to exchange of x_1 and x_2.

4. The quark-quark contribution:

$$\frac{d\sigma_H^{qq}}{dQ^2}(\tau) = \frac{4\pi\alpha^2}{3Q^4}\left(\frac{\alpha_s}{4\pi}\right)^2 \frac{8}{9}\int_0^1 dx_1\, dx_2\, \frac{\tau}{x_1x_2}\,\theta(x_1x_2-\tau)$$

$$\times \Bigg\{ \Big[\frac{8}{9}u_v(x_1)u_v(x_2) + \frac{2}{9}d_v(x_1)d_v(x_2) + \frac{5}{9}(u_v(x_1)d_v(x_2)$$

$$+ u_v(x_2)d_v(x_1))\Big]\,\Sigma^{qq}\Big(\frac{\tau}{x_1x_2}\Big)$$

$$+ 2\left[\frac{2}{3}u_v(x_1) - \frac{1}{3}d_v(x_1)\right]\left[\frac{2}{3}u_v(x_2) - \frac{1}{3}d_v(x_2)\right]\Sigma_I^{qq}\Big(\frac{\tau}{x_1x_2}\Big)$$

$$+ \frac{1}{3}\Big(\frac{8}{9}u_v(x_1)u_v(x_2) + \frac{2}{9}d_v(x_1)d_v(x_2)\Big)\,\Sigma_{cr}^{qq}\Big(\frac{\tau}{x_1x_2}\Big)\Bigg\} \qquad (3.3)$$

The functions Σ^{qq}, Σ_I^{qq} and Σ_{cr}^{qq} are defined by (III.6.9), (III.3.27) and (III.7.15) respectively. We have plotted these functions, together with their colorfactors in fig. 3.1.

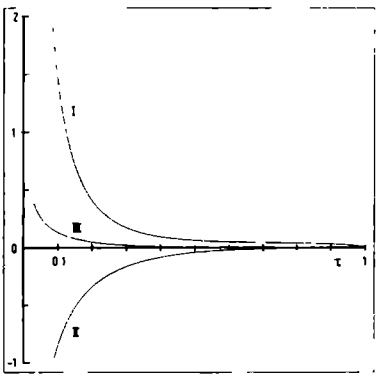

fig. 3.1: I: $\frac{N^2-1}{16N^2}\Sigma^{qq}(\tau)$; II: $\frac{N^2-1}{16N^2}\Sigma_I^{qq}(\tau)$; III: $\frac{N^2-1}{16N^3}\Sigma_{cr}^{qq}(\tau)$

It is clear that the identical particle contribution (curve III) is much smaller than the other terms. Due to the opposite signs of I and II there is however a partial cancellation which causes a suppression of the quark-quark contribution. Near $\tau = 1$ these two curves behave as

$$\Sigma^{qq}(\tau) = (1-\tau)\left[\frac{1}{2}\ln^2(1-\tau) - \frac{3}{2}\ln(1-\tau)\right]$$
$$\Sigma_I^{qq}(\tau) = -\frac{7}{8}(1-\tau)^2 \qquad (3.4)$$

This implies that Σ^{qq} is dominant in this limit. This can be attributed to the $\ln(1-\tau)$-terms discussed in chapter III. We have only considered valence distributions in (3.3) because the sea distributions are much smaller, and moreover we do not have the complete cross section for sea-valence scattering in order α_s^2.

5. The gluon-gluon contribution. Although we have not calculated the gluon-gluon scattering diagrams we can make a rough estimate of their effect on the basis of the mass singularities, which we can obtain without any calculation. For that purpose we consider the contribution of $q\bar{q}$-annihilation, qg scattering and gg scattering to the hadron cross section:

$$\frac{d\sigma_H^n}{dQ^2} = \frac{4\pi\alpha^2}{3Q^4}\sum_{flav}\frac{e_q^2}{N}\{(q_o^n\bar{q}_o^n + \bar{q}_o^n q_o^n)\,\Sigma_{q\bar{q}}^n + \lambda[(q_o^n + \bar{q}_o^n)g_o^n + g_o^n(q_o^n + \bar{q}_o^n)]\,\tilde{\Sigma}_{qg}^n + \lambda^2 g_o^n g_o^n\,\tilde{\Sigma}_{gg,q}^n\} \qquad (3.5)$$

where $\lambda = \frac{\alpha_s}{4\pi}$. To simplify the notation we have used moments here; for example:

$$\tilde{\Sigma}_{qg}^n = \int_0^1 \tau^{n-1}\,\tilde{\Sigma}_{qg}(\tau)\,d\tau \qquad (3.6)$$

where $\tilde{\Sigma}_{qg}(\tau)$ is the quark-gluon cross section before subtraction of the mass singularity (all quantities labelled by a $\sim$ have mass singularities). The last term of (3.5) is the cross section for the process $gg \to q\bar{q}\gamma^*$, for a $q\bar{q}$-pair with a given flavor, where γ^* is a virtual photon creating a lepton-pair. The sum is over all quark flavors. The distributions appearing in (3.5) are the unrenormalized ones; this is

indicated by the subscript 'o'. The renormalized distributions are, as far as gluon-quark transitions are concerned:

$$\begin{aligned} q &= q_o + \lambda\, \Gamma_{qg}\, g_o \\ \bar{q} &= \bar{q}_o + \lambda\, \Gamma_{qg}\, g_o \end{aligned} \tag{3.7}$$

We have omitted the moment indices. The transition function Γ_{qg} is given by (II.5.3). Substituting (3.7) into (3.5) we get:

$$\frac{d\sigma_H}{dQ^2} = \frac{4\pi\alpha^2}{3Q^4} \sum_{flav} \frac{e_q^2}{N} \{(q\bar{q}+\bar{q}q) + \lambda[(q+\bar{q})g_o + g_o(q+\bar{q})]\ (\tilde{\Sigma}_{qg} - \Gamma_{qg})$$

$$+ \lambda^2 g_o g_o\, [\tilde{\Sigma}_{gg,q} + 2\,\Gamma_{qg}\Gamma_{qg} - 4\,\Gamma_{qg}\tilde{\Sigma}_{qg}]\} \tag{3.8}$$

The second term is the finite part of the quark-gluon cross section:

$$\Sigma^n_{qg} = \tilde{\Sigma}^n_{qg} - \Gamma^n_{qg} \tag{3.9}$$

These are the moments of the function $\Sigma^{qg}(\tau)$ defined by (III.2.6). The terms multiplying the gluon distributions form the finite part of the gluon-gluon cross section. Therefore we know the mass singularities in $\tilde{\Sigma}_{gg,q}$, and conclude that this function can be written in the following way:

$$\tilde{\Sigma}^n_{gg,q} = 2(\tilde{\Sigma}^n_{qg}\tilde{\Sigma}^n_{qg} + \Delta^n_{gg,q}) \tag{3.10}$$

where $\Delta^n_{gg,q}$ is free of mass singularities. The mass singularities in the gluon-gluon cross section are correctly given by (3.10) because substitution into (3.8) yields a finite result:

$$\begin{aligned} \Sigma^n_{gg,q} &= \tilde{\Sigma}^n_{gg,q} + 2\,\Gamma^n_{qg}\Gamma^n_{qg} - 4\,\Gamma_{qg}\tilde{\Sigma}_{qg} \\ &= 2(\Sigma^n_{qg}\Sigma^n_{qg} + \Delta^n_{gg,q}) \end{aligned} \tag{3.11}$$

By means of an inverse Mellin transformation we obtain:

$$\Sigma_{gg,q} = 2 \int_\tau^1 \frac{d\xi}{\xi}\, \Sigma_{qg}\left(\frac{\tau}{\xi}\right)\, \Sigma_{qg}(\xi) + 2\,\Delta_{gg,q}(\tau) \tag{3.12}$$

Now we use the conjecture that all ln (1-τ) terms appear in combination with the mass singularities. The function $\tilde{\Sigma}_{qg}(\tau)$ - implicitly given by (III.2.3) - has that property. Moreover the property is preserved by convolution:

$$\int_\tau^1 F(\xi)\ \ln\left(\frac{p_1^2}{1-\frac{\tau}{\xi}}\right)\ \ln\left(\frac{p_2^2}{1-\xi}\right)\frac{d\xi}{\xi} = \int_\tau^1 F(\xi)\frac{d\xi}{\xi}\ln\left(\frac{p_1^2}{1-\tau}\right)\ln\left(\frac{p_2^2}{1-\tau}\right)$$
$$+ A_1(\tau)\ \ln\left(\frac{p_1^2}{1-\tau}\right) + A_2(\tau)\ \ln\left(\frac{p_2^2}{1-\tau}\right) + A_3(\tau) \qquad (3.13)$$

When $F(\xi)$ is analytic in $\xi = 1$ and $\xi = \tau$, then the functions $A_i(\tau)$ are analytic in $\tau = 1$. This implies that ln (1-τ) terms, which introduce a cut starting at $\tau = 1$, are absent in these coefficients and appear only together with a mass singularity. According to our conjecture these are the only ln (1-τ) terms in $\tilde{\Sigma}_{gg,q}(\tau)$ and therefore $\Delta_{gg,q}(\tau)$ must be an analytic function in $\tau = 1$, which is negligible compared to the first term of (3.12), at least near $\tau = 1$. Therefore we can approximate the gluon-gluon contribution as follows:

$$\frac{d\sigma_H^{gg}(\tau)}{dQ^2} = \frac{4\pi\alpha^2}{3Q^4}\left(\frac{\alpha_s}{4\pi}\right)^2\frac{1}{3}\sum_{flav} e_q^2 \int_0^1 dx_1\, dx_2\, \hat{\tau}\ \theta(x_1x_2 - \tau)\ G(x_1)G(x_2)$$
$$\times\ 2\int_{\hat{\tau}}^1 \frac{d\xi}{\xi}\,\Sigma_{qg}\left(\frac{\hat{\tau}}{\xi}\right)\,\Sigma_{qg}(\xi) \qquad (3.14)$$

where $\hat{\tau} = \frac{\tau}{x_1x_2}$. This is probably a crude approximation but it contains at least some of the basic features of the exact result: the α_s^2 suppression, the color suppression, the dependence on the gluon distributions and the correct limiting behavior for $\tau \to 1$. With this approximation the gg contribution turns out to be smaller than the $q\bar{q}$ contribution by three orders of magnitude, which means that it is very likely that it can be neglected, and that it is not worthwhile to calculate it exactly.

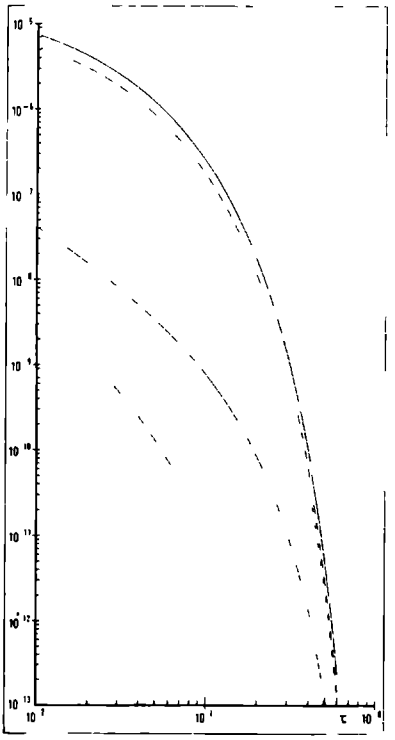

fig. 3.2: Plot of $Q^4 \frac{d\sigma}{dQ^2}$ (in mb GeV^2) vs τ for the lepton-pair production in proton-proton scattering. The lines represent, in decreasing order of magnitude, the sum of all contributions, the leading $q\bar{q}$ process, the radiative correction to the $q\bar{q}$-process, the qg process, the qq process and the gg process. The contribution of the qg process is actually negative.

This investigation, which includes all possible single parton processes, justifies the Drell-Yan formula (apart from the normalization) even for proton-proton scattering where this was not a priori correct. (We have not considered processes which involve more than one parton from each hadron; such processes may dominate in certain

kinematical regions [Duk 80].) The normalization of the Drell-Yan cross section with respect to deep-inelastic scattering is however modified considerably by the radiative corrections.

These corrections turn out to increase the magnitude of the Drell-Yan cross section. The origin of the large correction terms is explained in section III.2. There are several reasons which make an exact prediction of the increase however very uncertain. The ambiguities, described in section II.6 can have important consequences for the predictions. Since our approach is formally unambiguous up to first order in α_s, the effects of such ambiguities is of order α_s^2. But with a large first order correction the coefficients of the ambiguous terms may be large as well. In addition to that, the corrections of order α_s^2 may be large themselves.

Three kinds of ambiguities should be mentioned. The first one is the definition of the coupling constant. In second order this is equivalent to the definition of Λ. In deep-inelastic scattering this ambiguity does not play a very important role (see fig. 2.3), except of course for the value of Λ. Formally the same cancellation mechanism works for Drell-Yan corrections, but it remains to be shown that the effect on the final result is small. The effect of a redefinition of α_s is to make a replacement $\alpha_s \to \alpha_s(1 + c\alpha_s)$ for arbitrary c. This replacement carries the large coefficient of order α_s to order α_s^2. In order α_s^2 the effect will be cancelled by QCD vertex corrections, but the complete α_s^2 corrections are unfortunately not available. Therefore only the effect of this replacement on the second order anomalous dimensions is cancelled in the present analysis. For our method of analyzing deep-inelastic scattering results (i.e. when trivial

coefficient functions are chosen), this is the only necessary cancellation, but for Drell-Yan corrections that is no longer true.

Another problem is the continuation of the coupling constant to timelike q^2. It is not a priori clear how the quantity ln ($\frac{-q^2}{\Lambda^2}$) should be defined if $q^2 > 0$. We have used ln $\left|\frac{-q^2}{\Lambda^2}\right|$, but a study of the timelike process $e^+e^- \to$ hadrons indicates [Ros 80] that the choice $|\ln(-q^2/\Lambda^2)|$ leads to a better expansion parameter, since the other choice results in the occurrance of large π^2 coefficients in higher orders. The same may be true for the Drell-Yan process, but the numerical differences are not very large for the values of Q^2 we are considering.

The second ambiguity is the definition of the parton distributions. Formally one can transform the entire perturbative correction away by a change of the factorization of mass singularities. The consequence is however that the large terms will appear as corrections to deep-inelastic scattering processes. That may be an unreasonable procedure, but it is worth investigating whether a less rigorous finite renormalization of the parton distributions has dramatic consequences for the absolute predictions of the Drell-Yan cross sections which one would like to make. An incomplete investigation of this problem is given by [Har 80]. These authors present a complete and consistent calculation to order α_s, like we have done in this section. Their approach differs from ours because they use moments and because they adapt the perturbative corrections for the Drell-Yan process to the minimal subtraction scheme in which the anomalous dimensions have been calculated, whereas we have made the opposite choice. To solve the renormalization group equations they choose the scheme in which γ_1 vanishes, as explained in section II.6, and in this scheme they consider coupling constant redefinitions. A

change in the coupling constant introduces a contribution to γ_1, which can be transformed away by a finite renormalization of the anomalous dimensions. Via this mechanism the definition of the coupling constant influences the perturbative corrections of order α_s, and for a certain definition of the coupling constant (the "momentum subtraction scheme") the Drell-Yan corrections are reduced, without a large increase of the deep-inelastic scattering corrections. The fact that the relative magnitude of first and zeroth order terms is smaller does however not necessarily imply that the total Drell-Yan cross section has changed significantly, because the inevitable change in the parton distributions nor the change in Λ (which increases by a factor 2.16 relative to the $\overline{\text{MS}}$-scheme) has been taken into account. The only complete comparison of different definitions consists of repeating all the steps in sections 2 and 3, starting from a new fit, with new definitions, to the deep-inelastic scattering data, applying a moment inversion to obtain new distributions and calculating the convolution integrals presented in this section. Instead of the last two steps one may also use moments of the Drell-Yan cross section.

The third ambiguity is the choice of the Q^2-variable. This problem is, as explained in section II.6, completely unrelated to deep-inelastic scattering. Different choices instead of Q^2 lead to different perturbative corrections, but in present analyses only changes in the Q^2-variables of the parton distributions in the leading term (3.1) and the quark-gluon correction (3.2) are (partly) cancelled. In particular, a change in the Q^2-variable of the large perturbative corrections can have rather large effects on α_s, and hence on the normalization of the cross section, but the α_s^2-corrections which should control such changes

have not yet been calculated.

The most obvious problem associated with large corrections of order α_s is the possibility of a breakdown of perturbation theory. Perturbation theory may be cured either by exploiting the ambiguities in the perturbation expansion (by choosing a more suitable expansion parameter or a different factorization prescription), or by summing the large terms to all orders. The large terms are due to π^2-factors, originating from the analytical continuation of the elastic quark form factors from space-like to time-like q^2, and ln $(1-\tau)$ factors, which are related to the mass singularities. Part of the π^2-terms can probably be summed and exponentiated [Par 80]; the origin of the ln $(1-\tau)$terms suggests that a change of Q^2 into $Q^2(1-\tau)$ may remove the effect of such terms. It remains to be shown however that the α_s^2-terms are indeed small after the application of these procedures.

It is clear that a calculation of the radiative corrections of order α_s^2 may contribute to the solution of some of the problems mentioned above. In principle such corrections have to be combined with anomalous dimensions of order α_s^3 to get a cancellation of the subtraction ambiguities of order α_s^2. This objection applies also to the qq cross section calculated in chapter III. In practice this is however not really necessary, since we are not interested in normal second order corrections, but only in abnormally large π^2 and ln $(1-\tau)$-terms, which are determined by ambiguities of lower order. For example, the ln $(1-\tau)$ terms in the qq cross section are completely fixed by the quark-gluon transition function.

Keeping in mind all the reservations made above we do nevertheless expect that the main effect of QCD on the Drell-Yan cross section is

an increase in the normalization by a factor between 1.5 and 3. This effect is present in all recent lepton pair production data [Ito 80, Bad 79, Cor 80, Bar 79], although there seems to be some disagreement about the exact magnitude.

The enhancement factor can be determined in a simple way by comparing the sea distributions obtained from proton-proton Drell-Yan scattering to those obtained from deep-inelastic scattering data. We have done such a comparison for the sea distributions of [Ito 80] and those of section 2. The result obtained from lepton-pair production data is $2\,\bar{u}(x) + 2\,\bar{d}(x) + s(x) + \bar{s}(x) = 2.52\,x^{-1}\,(1-x)^{8.69}$ [Ito 80]. The ratio of this function with S(x), calculated with the parameters of table VII, for $Q^2 = 30\ GeV^2$ is given in table VIII. The normalization factor is obviously present in these data. (This comparison is not completely correct, because Ito et al. assume $\bar{s}(x) = \frac{1}{4}(\bar{u}(x) + \bar{d}(x))$ and neglect cnarm. We have corrected the deep-inelastic formulae accordingly and found that these two effects almost cancel each other.)

x	κ
.1	1.89
.2	1.93
.3	1.88
.4	1.78
.5	1.62
.6	1.41
.7	1.13
.8	.76
.9	.33

table VIII: the ratio κ between sea distributions from lepton-pair production data and deep-inelastic scattering data.

The results of table VIII indicate that with some additional work to reduce the uncertainties listed above the explanation of the normalization of the Drell-Yan cross section can become one of the successes of QCD.

Aba 78 J. Abad and B. Humpert, Phys.Lett. 78B, 627 (1978) (Erratum 80B, 433 (1979)).

Aba 79 J. Abad and B. Humpert, Phys.Lett. 80B, 286.

Abb 80a L.F. Abbott, W.B. Atwood and R.M. Barnett, Phys.Rev. D22, 582.

Abb 80b L.F. Abbott and R.M. Barnett, Ann.Phys. (NY) 125, 276.

Abe 73 E.S. Abers and B.W. Lee, Phys.Rep. 9C, 1.

Alt 77 G. Altarelli and G. Parisi, Nucl.Phys. B126, 298.

Alt 78 G. Altarelli, R.K. Ellis and G. Martinelli, Nucl.Phys. B143, 521 (Erratum B146, 544).

Alt 79 G. Altarelli, R.K. Ellis and G. Martinelli, Nucl.Phys. B157, 461.

Ama 78 D. Amati, R. Petronzio and G. Veneziano, Nucl.Phys. B140, 54; B146, 29.

Ash 72 J. Ashmore, Nuov.Cim.Lett. 4, 289.

Atw 73 W.B. Atwood and G.B. West, Phys.Rev. D7, 773.

Bac 78 M. Bacé, Phys.Lett. 78B, 132.

Bad 79 J. Badier et al., Phys.Lett. 89B, 145.

Bar 78 W.A. Bardeen, A.J. Buras, D.W. Duke and T. Muta, Phys.Rev. D18, 3998.

Bar 79 R. Barate et al., Phys.Rev.Lett. 43, 1541.

Bec 75 C. Becchi, A. Rouet and R. Stora, Comm.Math.Phys. 42, 127.

Bia 80 A. Biaℓas and A.J. Buras, Phys.Rev. D21, 1825.

Bjo 69 J.D. Bjõrken, Phys.Rev. 179, 1547.

Bjo 80 J.D. Bjõrken, SLAC-PUB-2372.

Blo 37 F. Bloch and A. Nordsieck, Phys.Rev. 52, 54.

Blo 71 E. Bloom and F. Gilman, Phys.Rev.Lett. 25, 1140.

Bol 72 C.G. Bollini and J.J. Giambiagi, Nuov.Cim. 12B, 20.

Bra 71 R.A. Brandt and G. Preparata, Nucl.Phys. B27, 541.

Bro 73 S.J. Brodsky and G.R. Farrar, Phys.Rev.Lett. 31, 1153.

Bur 77 A.J. Buras, Nucl.Phys. B125, 125.

Bur 78 A.J. Buras and K.J.F. Gaemers, Nucl.Phys. B132, 249.

Bur 80 A.J. Buras, Rev.Mod.Phys. 52, 199.

Cal 70 C.G. Callan, Phys.Rev. D2, 1541.

Cal 77 M. Calvo, Phys.Rev. D15, 730.

Cas 74 W. Caswell, Phys.Rev.Lett. 33, 244.

Cel 80 W. Celmaster and D. Sivers, ANL-HEP-PR-80-28 and -61.

Cha 75 C. Chang et al., Phys.Rev.Lett. 35, 901.

Chr 72 N. Christ, B. Hasslacher and A. Mueller, Phys.Rev. D6, 3543.

Col 73 S. Coleman and D. Gross, Phys.Rev.Lett. 31, 1343.

Col 74 J.C. Collins and A.J. McFarlane, Phys.Rev. D10, 1201.

Con 79a A.P. Contogouris and J. Kripfganz, Phys.Rev. D19, 2207.

Con 79b A.P. Contogouris and J. Kripfganz, Phys.Rev. D20, 2295
(See also [Kri 79]; For a comparison of the results of these papers with those of sections III.3-6 see [Sch 80a]).

Cor 80 M.J. Corden et al., CERN-EP/80-152.

Cur 80a G. Curci and M. Greco, Phys.Lett. 92B, 175.

Cur 80b G. Curci, W. Furmanski and R. Petronzio, Nucl.Phys. B175, 27.

DeG 79 J.G.H. de Groot et al., Zeitschrift für Physik C, vol. 1, 2, 143.

DeR 76 A. DeRújula and H. Georgi, Phys.Rev. D13, 1296.

DeR 77a A. DeRújula, H. Georgi and H.D. Politzer, Ann.Phys. (NY) 103, 315.

DeR 77b A. DeRújula, H. Georgi and H.D. Politzer, Phys.Rev. D15, 2495.

Dok 78 Yu.L. Dokshitser, D.I. Dyakanov and S.I. Troyan, Phys.Lett. 78B, 290 (1978) and Phys.Rep. 58C, 269 (1980).

Dor 80 R. Doria, J. Frenkel and J.C. Taylor, Nucl.Phys. B168, 93 (See also C. DiLieto, S. Gendron, I.G. Halliday and C.T. Sachrajda, ICTP/79-80/47; SHEP 79/80-6).

Dre 70 S. Drell and T.M. Yan, Phys.Rev.Lett. 25, 316.

Duk 79 D.W. Duke and R.G. Roberts, Phys.Lett. 85B, 289 (1979); Nucl.Phys. B166, 243 (1980).

Duk 80 D.W. Duke and M.J. Teper, Nucl.Phys. B166, 84 (See also P. Grassberger, Nucl.Phys. B175, 462).

Ell 78 R.K. Ellis, H. Georgi, M. Machacek, H.D. Politzer and G.G. Ross, Phys.Lett. 78B, 281.

Ell 79 R.K. Ellis, H. Georgi, M. Machacek, H.D. Politzer and G.G. Ross, Nucl.Phys. B152, 285.

Fad 67 L.S. Faddeev and U.N. Popov, Phys.Lett. 25B, 29.

Far 74 G.R. Farrar, Nucl.Phys. B77, 429.

Fey 69 R.P. Feynman, Phys.Rev.Lett. 23, 1415.

Fey 77 R.P. Feynman and R.D. Field, Phys.Rev. D15, 2590.

Fis 79 P.M. Fishbane, C.S. Lam and T.M. Yan, Phys.Rev. D20, 2960.

Flo 77 E.G. Floratos, D.A. Ross and C.T. Sachrajda, Nucl.Phys. B129, 66 (Erratum B139, 545).

Flo 79 E.G. Floratos, D.A. Ross and C.T. Sachrajda, Nucl.Phys. B152, 493.

Fra 80 W.R. Frazer and J.F. Gunion, SLAC-PUB-2489.

Fri 72 H. Fritzsch and M. Gell-Mann in *Proceedings of the 16th International Conference on High Energy Physics, Chicago-Batavia,*

1972, vol. 2, p. 135.

Gab 80 E. Gabathuler, Lectures at the 1980 Scottish Universities Summer School in Physics, St. Andrews, Scotland.

Gel 54 M. Gell-Mann and F.E. Low, Phys.Rev. 95, 1300.

Gel 61 M. Gell-Mann, California Institute of Technology, Synchrotron Report no. CTSL-20.

Gel 62 M. Gell-Mann, Phys.Rev. 125, 1067.

Gel 64 M. Gell-Mann, Phys.Lett. 8, 214.

Gel 72 M. Gell-Mann, Acta Phys.Austr. Suppl. 9, 733.

Geo 74 H. Georgi and H.D. Politzer, Phys.Rev. D9, 416.

Geo 78 H. Georgi, Phys.Rev. D17, 3010.

Gla 61 S.L. Glashow, Nucl.Phys. 22, 579.

Gla 65 S.L. Glashow, Phys.Rev.Lett. 14, 35.

Gon 80 A. Gonzalez-Arroyo and C. Lopez, Nucl.Phys. B166, 429.

Gor 79 B.A. Gordon et al., Phys.Rev. D20, 2645.

Gre 64 O.W. Greenberg, Phys.Rev.Lett. 13, 598.

Gri 72 V.N. Gribov and L.N. Lipatov, Sovjet J. Nucl.Phys. 15, 438; 675.

Gro 50 W. Gröbner and N. Hofreiter, Integraltafel, zweiter teil, p. 71-73 (Springer-Verlag).

Gro 73a D.J. Gross and F. Wilczek, Phys.Rev.Lett. 30, 1323.

Gro 73b D.J. Gross and F. Wilczek, Phys.Rev. D8, 3633.

Gro 74 D.J. Gross and F. Wilczek, Phys.Rev. D9, 980.

Han 65 M.Y. Han and Y. Nambu, Phys.Rev. 139, B1006.

Har 79 K. Harada, T. Kaneko and N. Sakai, Nucl.Phys. B155, 169 (1979) (Erratum B165, 545 (1980)).

Har 80 K. Harada and T. Muta, Phys.Rev. D22, 663.

Hol 74 M.J. Holwerda, W.L. van Neerven and R.P. Van Royen, Nucl.Phys. B75, 303.

Hoo 71 G. 't Hooft, Nucl.Phys. B35, 167.

Hoo 72 G. 't Hooft and M. Veltman, Nucl.Phys. B44, 189.

Hoo 73 G. 't Hooft, Nucl.Phys. B61, 455.

Hum 79a B. Humpert and W.L. van Neerven, Phys.Lett. 84B, 327 (Erratum 85B, 471).

Hum 79b B. Humpert and W.L. van Neerven, Phys.Lett. 89B, 69.

Hum 80 B. Humpert and W.L. van Neerven, CERN-TH-2990.

Ito 80 A.S. Ito et al., FERMILAB-PUB-80/19-EXP.

Jon 74 D.R.T. Jones, Nucl.Phys. B75, 531.

Kin 62 T. Kinoshita, J.Math.Phys. 3, 650.

Kri 79 J. Kripfganz and A.P. Contogouris, Phys.Lett. 84B, 473.

Kub 79 J. Kubar-André and F.E. Paige, Phys.Rev. D19, 221.

Lee 64 T.D. Lee and M. Nauenberg, Phys.Rev. 133, B1549.

Lib 78 S.B. Libby and G. Sterman, Phys.Rev. D18, 3252; 4737.

Mah 80 B.R. Mahapatra, Phys.Lett. 97B, 299.

Mar 78 W. Marciano and H. Pagels, Phys.Rep. 36C, 137.

Mue 78 A.H. Mueller, Phys.Rev. D18, 3705.

Nac 73 O. Nachtmann, Nucl.Phys. B63, 237.

Nee 61 Y. Ne'eman, Nucl.Phys. 26, 222.

Nee 80 W.L. van Neerven, private communication.

Nel 80 C.A. Nelson, FERMILAB-PUB-80/82-THY.

Par 76 G. Parisi, in *Proceedings 11th Rencontre de Moriond* (ed. J. Tran Thanh Van).

Par 80 G. Parisi, Phys.Lett. 90B, 295.

Pag 76 E. Poggio, H. Quinn and S. Weinberg, Phys.Rev. D13, 1958.

Pol 73 H.D. Politzer, Phys.Rev.Lett. 30, 1346.

Pol 74 H.D. Politzer, Phys.Rep. 14C, 129.

Pol 77 H.D. Politzer, Nucl.Phys. B122, 237.

Ros 79 D.A. Ross and C.T. Sachrajda, Nucl.Phys. B149, 497.

Ros 80 G.G. Ross, Lectures at the 1980 Scottish Universities Summer School in Physics, St. Andrews, Scotland.

Sal 64 A. Salam and J.C. Ward, Phys.Lett. 13, 168.

Sal 68 A. Salam in *Elementary Particle Theory* (ed. N. Svartholm) Almqvist and Wiksell, Stockholm, 1968, p. 367.

Sch 79 A.N. Schellekens, Nuov.Cim.Lett. 24, 513.

Sch 80a A.N. Schellekens and W.L. van Neerven, Phys.Rev. D21, 2619.

Sch 80b A.N. Schellekens and W.L. van Neerven, Phys.Rev. D22, 1623.

Sla 75 A.A. Slavnov, Sov.J.Part.Nucl. 5, No. 3, 303.

Ste 80 P.M. Stephenson, University of Wisconsin-Madison preprint DOE-ER/0881-153.

Str 74 H. Strubbe, Comp.Phys.Comm. 8, 1.

Stu 53 E. Stueckelberg and A. Petermann, Helv.Phys.Acta 26, 499.

Sym 70 K. Symanzik, Comm.Math.Phys. 18, 227.

Sym 73 K. Symanzik, Nuov.Cim.Lett. 6, 77.

Tak 57 Y. Takahashi, Nuov.Cim. 6, 370.

Tay 71 J.C. Taylor, Nucl.Phys. B33, 436.

Vel 67 M. Veltman, CERN-preprint, July 1967.

War 50 J. Ward, Phys.Rev. 78, 1824.

Wat 75 Y. Watenabe et al., Phys.Rev.Lett. 35, 898.

Wei 67 S. Weinberg, Phys.Rev.Lett. 19, 1264.

Wil 69 K. Wilson, Phys.Rev. 179, 1499.

Wit 76 E. Witten, Nucl.Phys. B104, 445.

Yan 54 C.N. Yang and R. Mills, Phys.Rev. 96, 191.

Zwe 64 G. Zweig, CERN-reports no. TH-401 and TH-412.

Sinds 1973 beschikt men over een theorie voor de sterke wisselwerkingen die, in dezelfde zin als quantum-electrodynamica (QED), als fundamenteel beschouwd kan worden. Deze theorie vertoont een sterke formele gelijkenis met QED en wordt quantum-chromodynamica (QCD) genoemd. Noch wat betreft de experimentele bevestiging, noch wat betreft de practische toepasbaarheid van QCD is men echter op dit moment zover gevorderd als met QED. De rigoreuze toepassing van QCD is nog beperkt tot hoge-energie processen. Deze blijken een gedrag te vertonen wat volledig in overeenstemming is met QCD, hoewel nog niet geconcludeerd kan worden dat de theorie bevestigd is.

In dit proefschrift worden twee hoge-energie processen bestudeerd, nl. zeer inelastische verstrooiing van leptonen aan hadronen en productie van lepton-paren in hadron-hadron verstrooiingsprocessen. De meeste aandacht gaat daarbij uit naar het laatstgenoemde proces, maar omdat QCD beide processen relateert, is een gelijktijdige en consistente behandeling van beide vereist.

In het eerste hoofdstuk wordt de ontwikkeling van QCD tot ongeveer 1975 beknopt behandeld, waarbij tevens enige begrippen worden geïntroduceerd die in de rest van dit proefschrift gebruikt worden. In eerste instantie was de toepasbaarheid van QCD beperkt tot zeer inelastische verstrooiing (en hadron-productie in e^+e^- annihilatie). In de laatste jaren is de toepassing op andere processen, zoals lepton-paar productie mogelijk geworden. Het hiervoor benodigde formalisme wordt behandeld in hoofdstuk II. Hierbij wordt vooral veel aandacht besteed aan de eenduidigheid van de procedure.

In hoofdstuk III komt lepton-paar productie aan de orde. De beschrijving van dit soort processen is in 1970 gegeven door Drell en Yan. Zij namen aan dat het lepton-paar geproduceerd wordt door annihilatie van een quark en een antiquark uit de twee hadronen. Met behulp van QCD is het mogelijk om de correcties op dit annihilatie-proces te berekenen. Zo lijkt bijvoorbeeld de veronderstelling van Drell en Yan niet gerechtvaardigd voor proton-proton verstrooiing, omdat de kans om in een proton een antiquark aan te treffen vrij klein is. Het Drell-Yan proces zal daarom moeten concurreren met lepton-paar productie in quark-quark verstrooiing, een proces dat mogelijk is in tweede orde in de QCD koppelingsconstante α_s. Om inzicht te krijgen in de relatieve grootte van beide processen wordt het laatste proces berekend.

De nauwe relatie tussen zeer inelastische verstrooiing en lepton-paar productie maakt het mogelijk om op basis van zeer inelastische verstrooiingsdata de werkzame doorsnede voor lepton-paar productie zonder vrije parameters te berekenen. Dit is het onderwerp van hoofdstuk IV. De benodigde parameters worden bepaald door middel van een analyse van de beschikbare zeer inelastische verstrooiingsdata, en vervolgens wordt de grootte van de diverse Drell-Yan correcties berekend, waarbij vanzelfsprekend gezorgd wordt voor de eerder genoemde consistente behandeling van beide processen. Een vergelijking van alle mogelijke eerste en tweede orde processen met het Drell-Yan proces rechtvaardigt de veronderstelling dat quark-antiquark annihilatie de voornaamste bron van lepton-paar productie is. De eerste orde stralingscorrectie op dat annihilatie-proces blijkt echter een zeer grote bijdrage te geven. Hoewel dit enige serieuze theoretische problemen oplevert, lijkt het redelijk om aan te nemen dat de werkzame doorsnede

hierdoor met een factor 1.5 tot 3 verhoogd wordt ten opzichte van het Drell-Yan proces. Een dergelijke factor wordt waargenomen in alle recente lepton-paar productie experimenten, en het is mogelijk dat dit tot de successen van QCD gaat behoren. De in dit proefschrift aangetoonde dominantie van het annihilatie-proces is een noodzakelijke voorwaarde voor de proces-onafhankelijkheid van deze factor.

CURRICULUM VITAE

A.N.J.J. Schellekens

Geboren 04-03-1954 te Nijmegen.

Lagere school van 1960 t/m 1966 te Nijmegen.

Gymnasium β van 1966 t/m 1970 aan de NEBO te Nijmegen

en van 1970 t/m 1972 aan het Dr. Mollercollege te Waalwijk.

Natuurkunde studie aan de Katholieke Universiteit Nijmegen van 1972 t/m 1977

kandidaatsexamen 10-04-1975

doctoraalexamen 13-10-1977.

Vanaf 01-11-1977 wetenschappelijk medewerker in F.O.M.-verband, verbonden aan het Instituut voor Theoretische Fysica, afdeling Hogeenergiefysica, te Nijmegen.

STELLINGEN

I

In een veldentheorie met meerdere koppelingsconstanten $g_1 \ldots g_n$ wordt de transformatie van de β-functies ten gevolge van een set eindige renormalizaties $g_i = g_i(g_1^* \ldots g_n^*)$ gegeven door:

$$\beta_i(g_1(g_1^* \ldots g_n^*), \ldots, g_n(g_1^* \ldots g_n^*)) = \sum_k \beta_k^*(g_1^* \ldots g_n^*) \frac{\partial g_i(g_1^* \ldots g_n^*)}{\partial g_k^*}$$

waarbij g_k^* en β_k^* respectievelijk de nieuwe koppelingsconstanten en β-functies voorstellen. Hieruit kan worden afgeleid dat de tweede coëfficient van de β-functie bij meerdere koppelingsconstanten in het algemeen niet uniek is.

II

Voor de trilog-functie Li_3 (gedefinieerd door formule III.3.17 van dit proefschrift) geldt de volgende relatie (voor $0 < x \leq 1$)

$$Li_3(1-x) + Li_3(1-1/x) + Li_3(x) - Li_3(1) = -\frac{1}{2} \ln^2 x \ln(1-x) + \frac{1}{6} \ln^3 x + \frac{\pi^2}{6} \ln x$$

III

Het is een veelvoorkomende misvatting dat uit de reflectie-invariantie van de electromagnetische stroom zou volgen dat een electron of proton geen electromagnetische γ^5-vormfactoren kan hebben.

IV

Massieve ϕ^4-theorie met normaal geordende interactie-Lagrangiaan is niet renormaliseerbaar.

J. Bjorken en S. Drell, relativistic quantum fields, hst. 17;

E. van Beveren, doctoraalscriptie

V

Door aan te nemen dat de interacties die bijdragen aan de massa's van de laagste baryon-toestanden goed benaderd kunnen worden door een som van tweedeeltjes-interacties kan men vier van de zeven 'equal spacing'-relaties voor het decuplet en de Coleman-Glashow relatie afleiden. *(P. Lederman, H.R. Rubinstein en I. Talmi, Phys.Lett. 22, 208 (1966)).* Om de Gell-Mann-Okubo massaformule en de overige decuplet relaties af te leiden zijn extra veronderstellingen nodig. Wanneer uitsluitend de zwakste van deze veronderstellingen gemaakt wordt, vindt men de volgende massaformule, die binnen de fout klopt met de experimentele waarden:

$$3\Lambda^0 - 3\Lambda^0 + p + n + \Xi^0 + \Xi^- - 2\Sigma^+ - 2\Sigma^-$$
$$= 4\Sigma^{*0} - \Sigma^{*+} - \Sigma^{*-} - 2\Xi^{*-} - 2\Xi^{*0} + 2\Omega^-$$

VI

Indien men veronderstelt dat Higgs-velden samengestelde deeltjes beschrijven met een massa die van de orde van grootte van de effectieve 'cut-off' parameter is, dient men er rekening mee te houden dat hogere orde interactie-termen niet verwaarloosd mogen worden bij de berekening van de vacuum-verwachtingswaarde van het veld.

VII

De SU(3)-flavor octet en singlet toestanden voor isoscalar mesonen - op basis waarvan de Gell-Mann-Okubo massaformule voor mesonen wordt afgeleid en ten opzichte waarvan de vectormesonen ω en ϕ vaak worden beschreven - zijn in geen enkele redelijke benadering eigentoestanden van de massa-matrix, en dragen op geen enkele wijze bij tot verheldering van de discussie van meson-massa's.

VIII

Gezien het feit dat de oververtegenwoordiging van mannen in de fysica niet verklaard kan worden uit een discriminerend benoemingsbeleid is het onjuist om, zoals nu soms openlijk gebeurt, hierin verandering te brengen door voortaan bij benoemingen voorrang te geven aan vrouwen.

IX

De willekeur waarmee in Nederland dienstplichtigen geselecteerd worden, zou met de grondwet van elk beschaafd land in strijd moeten zijn.

12 juni 1981 A.N.J.J. Schellekens